

LEWIS GRANT  
IN-27-CR  
319939  
P. 227

Final Report  
to

NASA-Lewis Research Center  
21000 Brookpark Road  
Cleveland, Ohio 44135

Contract No. NSG 3273 ✓

ION BEAM SPUTTERED COATINGS OF BIOGLASS

Submitted by:

L. L. Hensch, Professor  
J. Wilson, Adjunct Research Assistant  
P. Ruzakowski, Graduate Research Assistant

Department of Materials Science and Engineering  
College of Engineering  
University of Florida  
Gainesville, Florida 32611

March 1, 1982

ION BEAM SPUTTERED COATINGS OF BIOGLASS M.S.  
Thesis Final Report (Florida Univ.) ~~227 p~~ 541170  
CSCL 11C  
434P  
N91-28384  
Unclas  
6/27 0319939

## TABLE OF CONTENTS

	<u>Page</u>
SYNOPSIS.....	iii
CHAPTER ONE: INTRODUCTION.....	1
CHAPTER TWO: EXPERIMENTAL PROCEDURES.....	6
Sample Preparation.....	6
Sputtering and Sputter Coating Process.....	9
Sputter Coating Apparatus and Procedure.....	9
Reaction Analysis.....	13
Analytical Methods.....	14
CHAPTER THREE: PRELIMINARY BIOGLASS COATING STUDIES..	19
Introduction.....	19
Bulk Bioglass Reaction Sequence Data.....	20
Polymer Reaction Sequence Data.....	26
Metal Reaction Sequence Data.....	67
Ceramic Reaction Sequence Data.....	61
<u>In Vivo</u> Analysis.....	83
CHAPTER FOUR: SECOND REACTION SERIES OF BIOGLASS COATED POLYMERS AND COPOLYMERS.....	93
Introduction.....	93
<u>In Vitro</u> Analysis of Bioglass Coated Polymers.	94
ESCA Analysis.....	110
CHAPTER FIVE: SECOND REACTION SERIES OF BIOGLASS COATED 316L STAINLESS STEEL.....	119
Introduction.....	119
<u>In Vitro</u> Analysis of Bioglass Coated Stainless Steel.....	120
AES Analysis.....	138
CHAPTER SIX: SECOND REACTION SERIES OF BIOGLASS COATED ALUMINA.....	153
Introduciton.....	153
<u>In Vitro</u> Analysis of Bioglass Coated Alumina..	154
AES Analysis.....	174
SEM Data.....	186
<u>In Vitro</u> Analysis of a Double Coated Alumina Substrate.....	192
<u>In Vivo</u> Analysis.....	199

PAGE

CHAPTER SEVEN: SUMMARY..... 201

REFERENCES..... 205

## SYNOPSIS

Bioglass is a material which will form a stable bond with living tissue, notably bony tissue, which is stronger than either bone or bioglass.<sup>7,8,26</sup> It has also been shown to form an adhesive bond to the collagen in soft tissues.<sup>36</sup> It is, to date, the only example of an inorganic material which will bond chemically to living tissues, rather than mechanically, and it is unique in this respect.

The bioglass itself is mechanically weak and in situations where loads are applied, as in orthopedic and dental applications, it must be applied as a coating to stronger substrates. Techniques for coating on ceramic and metallic substrates exist but are not entirely satisfactory, particularly for substrates which are complicated in shape.<sup>5,6</sup>

Polymeric materials which will adhere to collagen, as bioglass does, have long been sought but not identified. The flexibility of soft tissue must be matched by any implanted material in order to achieve the bond and if a suitable means of producing a bioglass surface on a flexible substrate can be found there would be many applications in surgery. There are no other techniques available at present for coating polymeric materials with glass.

The ion beam sputtering technique available at the NASA Lewis Center was chosen to apply coatings of bioglass to ceramic, metallic and polymeric substrates. Experiments in vivo and in vitro described in this report investigate the coatings so produced.

Results have shown that the technique may be used to deposit very thin coatings of bioglass on to these substrates, the thickness varying, as expected, with sputter time.

Metallic substrates, so coated, do not show significantly improved coatings over those obtained with existing techniques. No implantations in vivo were done with these samples.

Ceramic substrates, so coated, did not show significantly improved coatings over those obtained with existing techniques. Implantation of these coated samples in bone gave no definite bonding as seen with bulk glass. However, partial and patchy bonding was seen. No data exists as to the minimum coating thickness needed for bonding. It seems likely that the thickest coatings achieved by this technique are approaching the minimum thickness required.

Polymeric substrates, in these studies showed promise of success. The coatings applied were sufficient to mask, although patchily, the underlying reactive test surface. Tissue adhesion of collagen to bioglass was seen. Hydrophilic, hydrophobic, charged and uncharged polymeric surface were successfully coated. It was felt that in some cases there was alteration of the modulus of the polymer during the coating process and the full significance of this change has yet to be assessed. However, it has been shown that the ion beam sputtering technique can successfully produce bioglass-coated polymers. Potential application of such materials are numerous. Any situation where a gap occurs between

implant and host tissue, allows relative movement, scar tissue and infection to interfere with the desired function. A flexible material which bonds, via an active surface layer, to the surrounding tissue could be used as space-filling material, after surgery and tumour removal, and in situations where trans-cutaneous access is needed, such as in dialysis patients and in hydrocephalic shunts. Such materials may derive from the use of this process to coat polymeric substrates.

### Oral Presentations

- May 1980 NASA Review Meeting at Case-Western University, "Possible Applications of Ion Beam Sputter Coatings of Bioglass," L. L. Hench and June Wilson.
- May 1981 7th Annual Meeting of Society for Biomaterials, Troy, NY, "Ion Beam Sputtered Coatings of Bioglass," Pat Ruzakowski, June Wilson, J. Weigand, and L. L. Hench.
- June 1981 NASA Review Meeting at Case Western University, "Ion Beam Sputtered Coatings of Bioglass," L. L. Hench.
- April 1982 8th Annual Meeting of Society for Biomaterials, Orlando, Florida, "Further Studies on Ion Beam Sputtered Coatings of Bioglass," Pat Ruzakowski, June Wilson, J. Weigand, and L. L. Hench

### Papers in Preparation for Submission to the Journal of Biomedical Materials Research

1. "Bioglass Coated Polymers Produced by the Ion Beam Sputtering Technique," Pat Ruzakowski, June Wilson, J. Weigand and L. L. Hench.
2. "Bioglass Coated Alumina and Metals Produced by the Ion Beam Sputtering Technique," Pat Ruzakowski, June Wilson, J. Weigand and L. L. Hench.

Acknowledgment of NASA grant NSG 3273 will appear in these papers.

The text of this report was submitted by Pat Ruzakowski to the Graduate School of the University of Florida for the degree of Master of Science. It has been accepted by the School.

## CHAPTER 1 INTRODUCTION

The possibility of reproducing biological organs improves with both surgical capabilities and biomaterials research. Artificial organs, tissues and prosthetic devices are being investigated all over the world. Historically, the materials that have been most used as prosthetic devices are metals. A variety of alloys such as 316L Stainless Steel, Co-Cr alloys (for example Vitallium), Co-Cr-Mo-Ni alloys and Ti-Al-V alloys have been used for prosthetic devices.

The field of biomaterials contains a wide range of chemical reactivities: nearly inert materials, with minimal reactivity; controlled surface active materials, with controlled reactivity leading to tissue bonding; and totally resorbable materials, which can dissolve into metabolic constituents. Nearly inert materials such as dense alumina ( $\text{Al}_2\text{O}_3$ ) have been used as acetabular cup replacements. Surface reactive materials such as bioglasses, Ceravital, and durapatite have been used due to their ability to bond chemically to bone without adverse tissue reactions. Finally, totally resorbable materials, such as sutures made of polyglycolic and polylactic acids have been used.



Some of the problems associated with implant materials are the result of the specific types of materials being used. In metals the major problem has been metallic corrosion resulting in toxic tissue responses and implant failure. Vitallium and stainless steel (SS) are the least reactive of the alloys mentioned above. In spite of this they cause a fibrous capsule to form around the implant. Metals provide the strength needed for the loads placed on them but may release elements that are toxic to tissue. Dense ceramic materials are capable of resisting degradation in physiological environments but also cause the formation of a fibrous capsule around the implant which in turn can cause loosening of the implant and finally failure of the device. Like metals, polymers may be toxic since chemicals (degradation products) may leach into the physiological environment during use.

To alleviate the above problems the surface of many implant materials can be modified to decrease corrosion, fibrous capsule formation and release of potentially toxic substances. There are various methods that have been investigated to achieve changes in surfaces: composite materials,<sup>1</sup> modification of surface texture,<sup>2</sup> co-polymerization,<sup>3</sup> grafting of one polymer onto another,<sup>4</sup> and the coating of material onto a substrate.

The bioglass bonding concept has alleviated some of the above problems but not all. Specifically, the tensile strength characteristic of bioglass implants is still too

low. For this reason coating of bioglass onto various substrates has been investigated in an effort to combine the physiological compatibility of the surface active bioglass with the strength of the substrate material. The bioglass bonding concept has been proven in previous studies using thick coatings (0.2 to 2.0 mm) applied to surgical alloys<sup>5</sup> and alumina substrates.<sup>6</sup>

The mechanism of bioglass bone bonding has been shown to be due to the formation of a silica ( $\text{SiO}_2$ ) rich layer on the bulk bioglass and a calcium-phosphate (Ca-P) rich layer which forms on the silica rich layer in aqueous environment.<sup>7</sup> There is a similarity between apatite mineral crystals in bone and the Ca-P rich layer formed that results in collagen bonding and bone mineralization at the implant surface. The Ca-P rich layer can be compared with reagent grade hydroxyapatite (HA) using Infrared Reflection Spectroscopy (IRRS) and Auger Electron Spectroscopy (AES). The spectrum formed after reaction of bioglass is similar to the spectrum of HA (compare Figures 3.2 and 3.3). Bone growth from the implant-bone interface results in a chemical bond which is sufficiently strong that the bone or the implant fail before the interface does.<sup>8</sup>

Previous bioglass coating methods<sup>9</sup> investigated in a number of studies include: flame spray coating, enamelling with glass frit, double glaze coating on alumina and immersion coating with a controlled oxide layer on metal alloys. The enamelling methods have problems with diffusion of

metallic ions into the glass coating. Flame spray coating has been unpredictable since at times the coating has broken down during implantation. This was due to porosity at the metal-glass interface caused by the high temperatures used during the coating process. The double glaze coating of alumina has shown the presence of aluminum ions on the surface of the glass coating.<sup>6</sup> The immersion coating process for metals shows minimal diffusion with the additional advantage of controlling the coating composition.<sup>5</sup> Controlling the oxide layer has increased the strength of the metal-to-glass bond in this coating technique.<sup>5</sup>

Some of the problems and limitations associated with the above coating techniques have resulted from the conditions under which the coating was placed on the substrate. These problems have been due mainly to the high temperatures used. For instance high temperatures have caused diffusion of metallic ions into the coating. In addition high temperatures limit the types of materials that can be successfully coated.

A new coating procedure called the ion beam sputtering technique (IBST) is capable of sputter coating materials onto a substrate at low temperatures. Therefore the IBST has the potential for coating various types of materials including flexible substrates to give an implant more closely matched to the mechanical properties of soft tissue.

The objective of this study is to investigate the potential use of an ion beam thruster to sputter-coat medical

or dental implant materials with bioglasses. Our hypothesis is that bioglass coatings can thus be placed on polymeric, metallic and ceramic substrates by the Ion Beam Sputtering Technique to modify the surface properties of implant materials, resulting in desired mechanical properties and physiological compatibility. The sputtering process will be described in Chapter 2.

Chapter 2 will also describe the experimental procedures used on coated samples Chapter 3 will present the preliminary studies on coated samples Chapter 4, 5, and 6 will present the secondary studies with increased coating thickness, and Chapter 7 summarizes the results obtained from preceding chapters.

## CHAPTER 2 EXPERIMENTAL PROCEDURES

### Sample Preparation

Bioglasses of two compositions, both within the bone bonding range, UF 45S5 and OI 52S4.6 (see Table 2.1), were provided to NASA Lewis Research Center as target materials for use in the ion beam thruster. The target materials were in the form of four inch diameter discs provided by the University of Florida. Bulk UF 45S5 bioglass was prepared in the following manner: 83.8 gm  $\text{Na}_2\text{CO}_3$ , 90.0 gm  $\text{SiO}_2$ , 87.4 gm  $\text{CaCO}_3$  and 12.0 gm  $\text{P}_2\text{O}_5$  were mixed for one hour on a roller mill, then melted for 24 hours in covered Pt crucibles at 1350 °C. Samples were poured on to graphite then annealed on alumina setters for six hours at 450 °C. Bulk OI 52S4.6 was prepared at Owens Illinois using a 30 lb batch Pt melter. The glass received was remelted in a Pt crucible for four hours at 1350 °C, then poured on to graphite and annealed for six hours at 450 °C.

The substrate materials to be coated were polymeric, metallic or ceramic. The polymers were of two types: hydrophilic and hydrophobic. The hydrophilic polymers were copolymers of polymethyl methacrylate (PMMA) and one of three other monomers: 1) 10% Hydroxyethyl methacrylate (HEMA)/90% Methyl methacrylate (MMA), 2) 10% Acrylic

Table 2.1  
Bioglass Compositions of  
UF 45S5 and OI 52S4.6

Weight % Glass	SiO <sub>2</sub>	P <sub>2</sub> O <sub>5</sub>	CaO	Na <sub>2</sub> O
UF 45S5	45.0	6.0	24.5	24.5
OI 52S4.6	50.8	6.0	21.6	21.6
Mole % Glass	SiO <sub>2</sub>	P <sub>2</sub> O <sub>5</sub>	CaO	Na <sub>2</sub> O
UF 45S5	46.1	2.6	26.9	29.9
OI 52S4.6	52.1	2.6	23.8	21.5

acid (AA)/90% MMA and 3) 20% dimethylaminoethyl methacrylate (DMAEMA)/80% MMA. The hydrophobic polymers consisted of silicone rubber (SR) and PMMA. For simplicity the hydrophilic polymers were designated as: 1) HEMA/MMA = OH, 2) AA/MMA = A, 3) DMAEMA/MMA = AM. In addition a series of numbers is used to specify each sample. These polymer samples were obtained from Liverpool University - ICI Joint Laboratory courtesy of Drs. D. K. Gilding and J. Wilson. All were of known reactivity and were completely characterized. All polymer samples were approximately 1.0 cm discs of 0.05 cm thickness.

Metal samples coated in this study were of 316L SS obtained from Howmedica, Inc. They measured approximately 3.1 cm in diameter by 0.18 cm in thickness.

The ceramic samples coated in this study were alumina. The samples, obtained from 3M Corporation, were designated as AlSiMag<sup>R</sup> 838 and 850 although both had 99.5% alumina content. The ceramic samples were of three forms: 1) small square chips (4 mm x 4 mm x 1 mm), 2) square plates (12 mm x 12 mm x 0.6 mm) and 3) thick discs with a diameter of approximately 25.3 mm and thickness of 6.4 mm.

The bulk bioglass samples used for comparison purposes were in the shape of square plates measuring approximately 10.6 mm x 2.3 mm.

### Sputtering and Sputter Coating Process

Sputtering is a process by which atoms or ions with energies greater than approximately 30 eV strike a surface, causing material from that surface to be ejected. A sputtering yield is designated as the number of atoms or molecules of material ejected per number of atoms or ions striking the surface. The sputtering yield varies from about  $10^{-4}$  atoms/ion near the minimum threshold to about 10 atoms/ion at optimum bombardment energies of a few thousand volts.<sup>10</sup> Sputtering can be viewed as a momentum transfer from the bombarding particle (atoms or ions) to the target lattice, in this case bulk bioglass, thus energy is lost to atoms in the surface by exciting them vibrationally or electronically. The bombarding particle can dislodge one or more of the lattice atoms in the bioglass from their equilibrium positions giving them sufficient energy to travel a short distance in the lattice. The travelling atoms can then either emerge at the surface as sputtered material or cause a surface atom to be ejected by striking it. Surface bioglass atoms are then directed to a substrate material for sputter coating (see figure 2.1).

### Sputter Coating Apparatus and Procedure

The apparatus and procedure used has been developed by NASA Lewis Research Center, Cleveland, Ohio. The ion beam source is cylindrical in shape, figure 2.2, and comes in a variety of diameters. The eight inch diameter source was



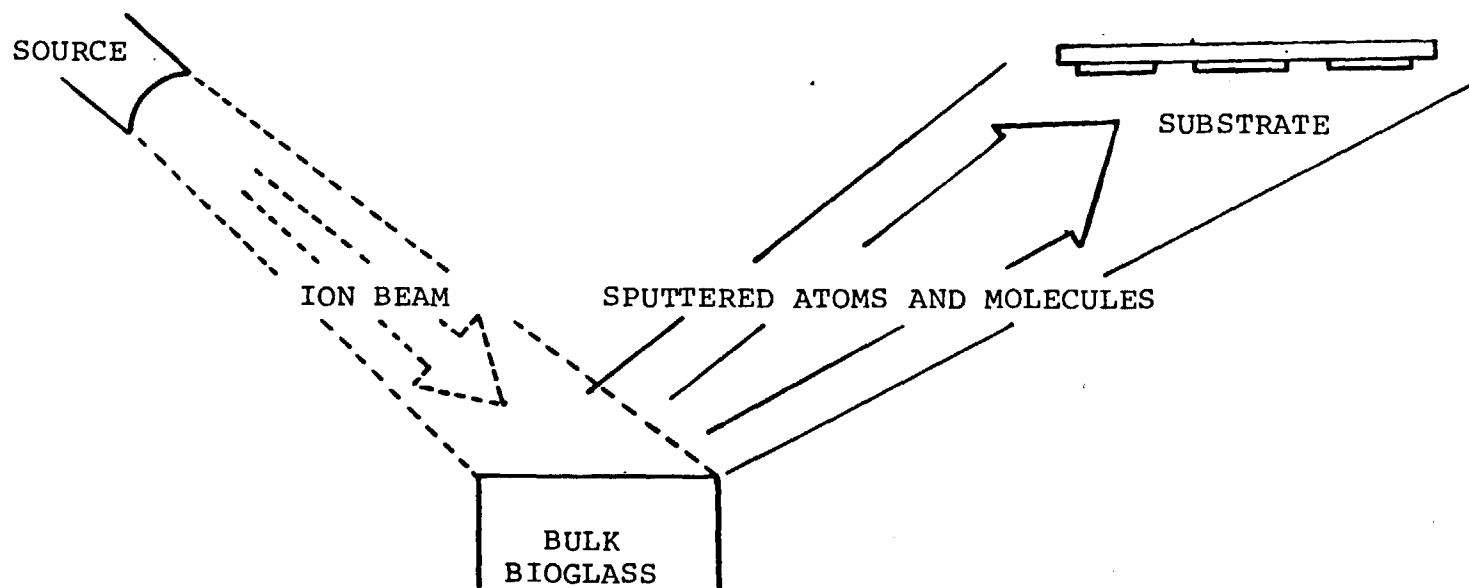


Figure 2.1 Ion Beam Sputter Coating Process

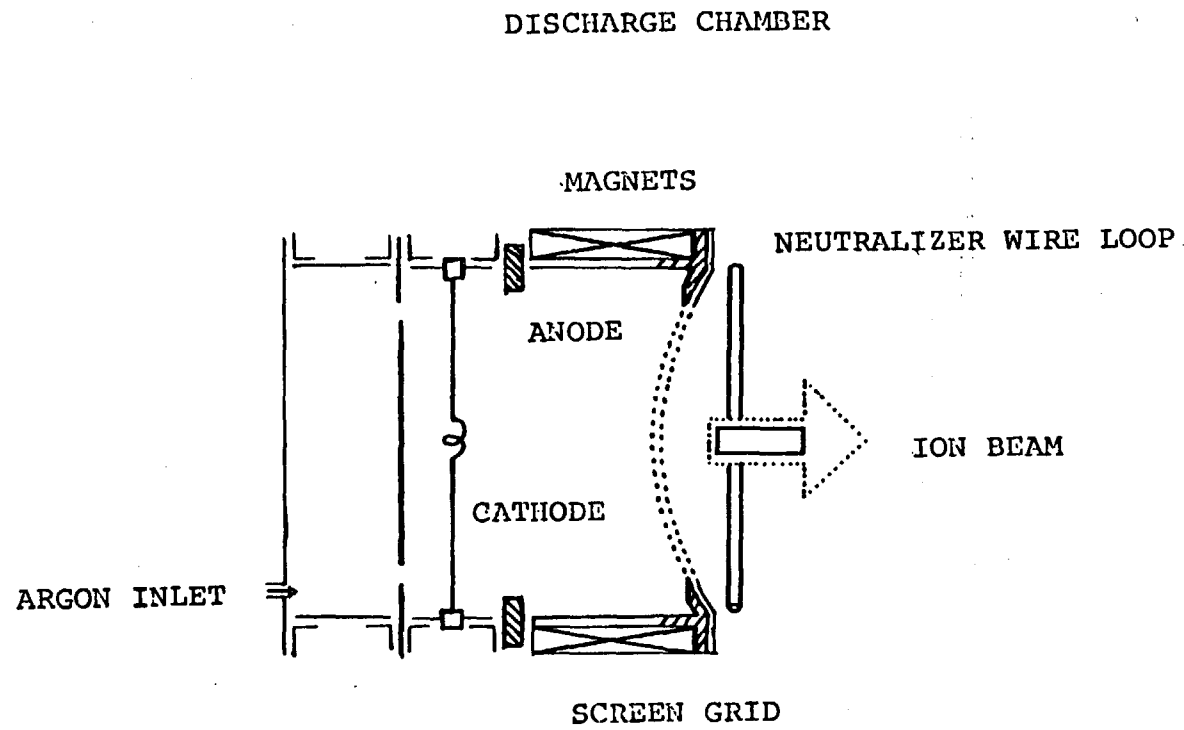


Figure 2.2 Ion Beam Source Schematic

used for sputter coating samples in this study, with Argon as the working gas. There are six major components in the discharge chamber, shown in figure 2.2. These components are as follows: 1) tantalum ribbon cathode, 2) anode, 3) working gas, 4) accelerator grid, 5) screen grid and 6) neutralizer.

Heating the tantalum ribbon cathode creates a source of electrons that can be accelerated to ionize the Argon, thus creating a plasma. A low work function material, Barium oxide ( $\text{BaO}$ ), coats the cathode, aiding in the electron emission process. The amount of power supplied to the cathode filament controls the electron emission rate. The electrons ionize the working gas in the discharge chamber. An anode (+), operating at a positive potential with respect to the cathode (-), is used to attract the electrons. A magnetic field from the magnetic pole pieces increases the electron path through the discharge chamber to the screen grid and through the accelerating grid. The screen grid operates at a negative high voltage while the accelerator grid operates at a positive voltage.

As the ion beam emerges from the accelerator grid it goes through the neutralizer loop, which emits electrons to neutralize the ions. It is this neutralized ion beam that sputter etches the bioglass target and then sputter coats the etched material onto the substrate. The system is at approximately  $100\text{ }^{\circ}\text{C}$  with the bell jar pressure ranging from  $10^{-4}$  to  $10^{-5}$  Torr, and currents and current density between

55-65 mA and 0.1-0.3 mA/cm<sup>2</sup> respectively. The energy of the source was 500 Volts for all samples, unless otherwise specified.

The procedure used to deposit the bioglass onto the substrates was as follows; the source was started and set at 500 Volts at which time oxygen was bled into the system by opening an outside valve to let air into the bell jar. Following this, substrate materials and target are ion beam cleaned for either one and a half minutes at 500 Volts and 60 mA or for five minutes at 500 Volts and 30 mA. After the cleaning procedure is completed the target is sputter etched and the substrates are coated with the sputtered material.<sup>11</sup>

#### Reaction Analysis

Coated samples were placed in containers of various types: 1) Nalgene<sup>R</sup> bottles, 2) plastic vials, 3) polystyrene test tubes or 4) polyethylene test tubes depending on the amount of deionized water required in each case. All containers were sealed prior to use and opened to place coated sample and deionized water in them prior to reaction tests. The containers held sufficient deionized water to yield a surface area to volume of solution ratio of 0.7 cm<sup>-1</sup>. Coated samples were placed in containers as received from NASA. The containers with samples for reaction were placed in large beakers containing deionized water to a half level mark of the beaker. These large beakers were then placed in a

temperature bath maintained at 37 °C. There were three reaction time sequences: 1) 0, 1, 4, 10, 40, 63 and 100 hours, 2) 0, 1, 4, 10, 40, 63, 100, 400 and 1000 hours and 3) 0, 1, 3, 10, 24, 168, 240, 336, 432, 504, 600 and 720 hours.

When samples were removed from the reaction containers their surfaces were air dried. Samples were analyzed after each reaction time with the IRRS technique. In Chapters 4, 5 and 6 pH data were obtained using colorpHast indicator sticks. After the final reaction time samples were stored in desiccators.

#### Analytical Methods

The analytical techniques used to determine the surface morphology and composition of bioglass coated substrates were Infrared Reflection Spectroscopy (IRRS), Auger Electron Spectroscopy (AES), Electron Spectroscopy for Chemical Analysis (ESCA) and the Scanning Electron Microscopy (SEM). IRRS has been used to analyze the surface of glasses by many investigators.<sup>12-16</sup> A Perkin Elmer Model 599 B Infrared Spectrophotometer with a double beam reflection attachment, with a mirror as a reference standard, was used in this study. This technique is a non-destructive technique that produces a spectrum unique to the molecule under investigation. This spectrum is represented as a plot of the reflectance intensity against the frequency of the incident infrared beam. It is known that the detection depth of this

technique is approximately  $0.5 \mu\text{m}$  ( $5000 \text{ \AA}$ ). There is a distinctive spectrum for vitreous silica and for freshly abraded ternary-alkali-silicate glass from  $1300 \text{ cm}^{-1}$  to  $800 \text{ cm}^{-1}$  (see figure 2.3).

In vitreous silica, used as a reference standard throughout, there is a symmetric bridging oxygen peak Si-O-Si at  $1120 \text{ cm}^{-1}$  designated S in figure 2.3. Figure 2.3a compares a vitreous silica spectrum to a ternary silicate glass (10-10-80) where a shift of the S peak to lower wavenumbers is observed. Figure 2.3b compares two glasses 10-20-70 and 20-20-60. The increase in  $\text{Na}_2\text{O}$  and decrease in silica structure causes formation of two peaks in the region  $900 \text{ cm}^{-1}$  and  $1050 \text{ cm}^{-1}$ . Figure 2.3c shows the 20-10-70 spectrum and the 30-10-60 spectrum. There is a decoupling of the peaks upon addition of  $\text{Na}_2\text{O}$  with constant CaO content. A decrease in the S peak is observed as the Si-O-Si bonds are being broken as more alkali is added. Finally by comparing UF 45S5 and OI 52S4.6 in Figure 2.3d we see a decrease in intensity and a shift to lower wavenumbers in the overall spectra. The coupled region is observed as a result of the overlap between the S peak and the Si-O-alkali peak designated as NS.

The peaks occurring at  $450 \text{ cm}^{-1}$  result from the bending or rocking vibrations of the silicon-bridging oxygen bond but are not as sensitive to composition changes as the stretching vibrations. Consequently this study will focus on the changes in the S and NS stretching peaks.

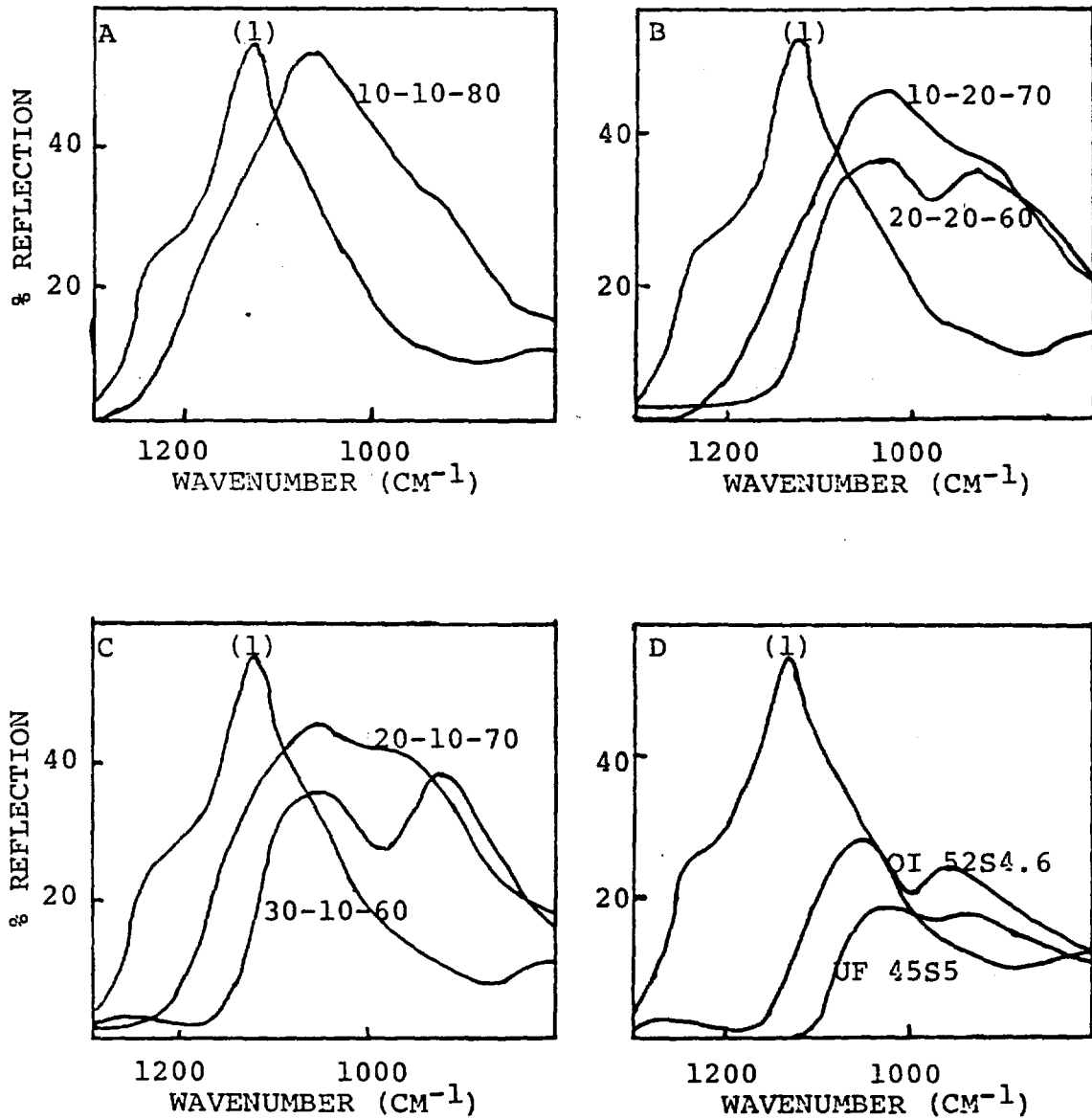


Figure 2.3 Comparison of freshly abraded (f.a.) vitreous  $\text{SiO}_2$  with ternary silicate glasses. The spectra designated by (1) in all graphs are f.a.  $\text{SiO}_2$ .

- A) 10 m%  $\text{Na}_2\text{O}$ - 10 m%  $\text{CaO}$ - 80 m%  $\text{SiO}_2$  (10-10-80)  
 B) 10 m%  $\text{Na}_2\text{O}$ - 20 m%  $\text{CaO}$ - 70 m%  $\text{SiO}_2$  (10-20-70)  
 20 m%  $\text{Na}_2\text{O}$ - 20 m%  $\text{CaO}$ - 60 m%  $\text{SiO}_2$  (20-20-60)  
 C) 20 m%  $\text{Na}_2\text{O}$ - 10 m%  $\text{CaO}$ - 70 m%  $\text{SiO}_2$  (20-10-70)  
 30 m%  $\text{Na}_2\text{O}$ - 10 m%  $\text{CaO}$ - 60 m%  $\text{SiO}_2$  (30-10-60)  
 D) OI 52S4.6: 21.5 m%  $\text{Na}_2\text{O}$ - 23.8 m%  $\text{CaO}$ - 2.6 m%  $\text{P}_2\text{O}_5$   
 52.1 m%  $\text{SiO}_2$   
 UF 45S5 : 24.4 m%  $\text{Na}_2\text{O}$ - 26.9 m%  $\text{CaO}$ - 2.6 m%  $\text{P}_2\text{O}_5$   
 46.1 m%  $\text{SiO}_2$

Aqueous reactions of a glass can be either selective for an alkali ion or can involve network dissolution processes.<sup>17</sup> Selective alkali leaching results in a decoupling of the S and NS peaks. Network dissolution results in a decreased intensity of both peaks but not a change in peak location.

The surface analytical technique used for coated SS and coated alumina samples was AES. This technique is capable of uniquely identifying each element from approximately the top five atom layers. The conditions for analysis varied slightly from sample to sample. In general, vacuum pressure was maintained at about  $10^{-7}$  Torr, beam voltage was either 2 KeV or 3 KeV, beam current was 40 uA and  $P_tP$  (modulation amplitude) was at 5 eV. Individual conditions for specific samples are on the figures in the appropriate chapters. In addition AES coupled with Ar ion milling was done to determine compositional profiles of surface coatings. Before reaction, analyses of coated alumina and coated SS were conducted to compare with bulk bioglass data. After reaction, analyses were also performed to compare results with pre-reaction data.

The surface analytical technique used for coated polymers was ESCA (also known as X-Ray Photoelectron Spectroscopy (XPS)). Chemical shift and compositional information can be determined with this technique. The analysis was performed at the University of South Florida using a GCA McPherson ESCA 36, Model 3103D. The radiation source used



was MgK $\alpha$  radiation at 8 KV, 40 mA and a pumping speed of 260 l/s (liters/second). A CTI cryopump with a 2 hp main pump that is coupled was used during surface analysis of samples to maintain the vacuum. The system was pumped with a turbo-pump with a sample chamber which had its pressure maintained at  $10^{-7}$  Torr.

Surface morphologies were characterized using an SEM, Model JEOL JSM-35C. A vapor deposited film of Au-Pd was applied to all samples in order to eliminate charging. Vacuum pressure during deposition was approximately  $10^{-5}$  Torr with samples maintained at room temperature. SEM conditions were as follows;<sup>18</sup> accelerating voltage was 25 KV for coated metals and ceramics and 15 KV for coated polymers, tilt of sample was at 30 degrees, load current was between 95-100 amps with a vacuum pressure of about  $10^{-5}$  Torr.

CHAPTER 3  
PRELIMINARY BIOGLASS COATING STUDIES

Introduction

Preliminary studies were used to determine if the IBST had the potential to coat polymers, metals and ceramics with thin coatings of bioglass. These coatings were in the range of 0.5  $\mu\text{m}$  to 1.2  $\mu\text{m}$  thick. As mentioned in Chapter 2 the IRRS technique was used to compare uncoated substrates with coated substrates (before and after reaction) and to determine whether the surface had been altered by the coating technique.

A variation in the detected signal could result from at least four effects: 1) the surface could have been damaged by the technique with minimum implantation of ions resulting in a spectrum similar to the uncoated substrate; 2) the coating thickness could be less than the penetration depth of the IRRS technique resulting in a spectrum mostly like the uncoated substrate; 3) the coating could be non-uniform in thickness resulting in a spectrum that partially resembles the substrate and partially resembles a bulk bioglass spectrum; 4) the spectrum resembles bulk bioglass suggesting that the coating is present and masking the substrate.

If a coating was detected by the IRRS technique (see Figures 3.5-3.9) the samples were used for in vitro studies.

All in vitro studies are referenced to bulk bioglass in vitro data. SEM photographs were taken of selected samples after 1000 hours of reaction in vitro and compared with each other. Preliminary in vivo studies used polymer samples coated with approximately 0.5  $\mu\text{m}$  OI 52S4.6 and UF 45S5 bioglasses. Histological sections of coated polymeric samples and adjacent tissues were prepared post-operatively and analyzed for tissue reaction.

#### Bulk Bioglass Reaction Sequence Data

Two bulk bioglass compositions were used in this study: 1) UF 45S5 and 2) OI 52S4.6. Their compositions can be seen in Table 2.1. It was necessary to investigate whether coated samples would react in the same manner as bulk bioglass does in vitro after showing the presence of a glass coating on the substrate material. All in vitro reaction sequence data was compared with the corresponding bulk bioglass in vitro data.

The reaction data of each bulk bioglass seen in Figure 3.1 and Figure 3.2 were obtained using reaction sequence 1 and 3 respectively (see Reaction Analysis in Chapter 2). The IRRS spectrum for UF 45S5 reacted for 100 hours in deionized water at 37 °C is shown in Figure 3.1. The spectrum after four hours of reaction shows a slight decrease in the NS peak resulting from the loss of  $\text{Na}^{+1}$  ions. Between 40 hours and 100 hours there is a decrease in the intensity indicative of surface roughening. Note that 100

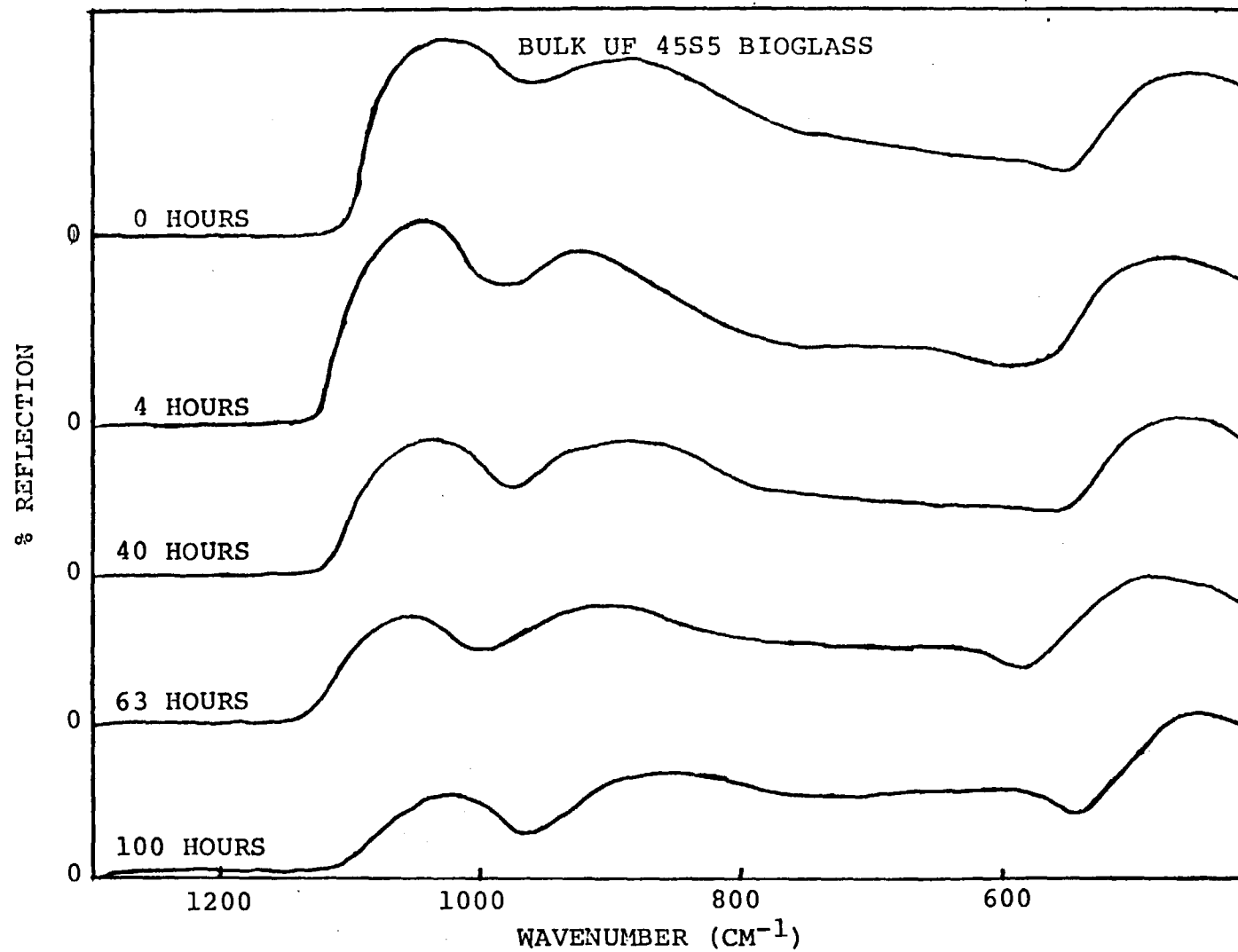


Figure 3.1 IRRS Reaction Sequence Data for UF 45S5 Reacted from 0 to 100 hours.

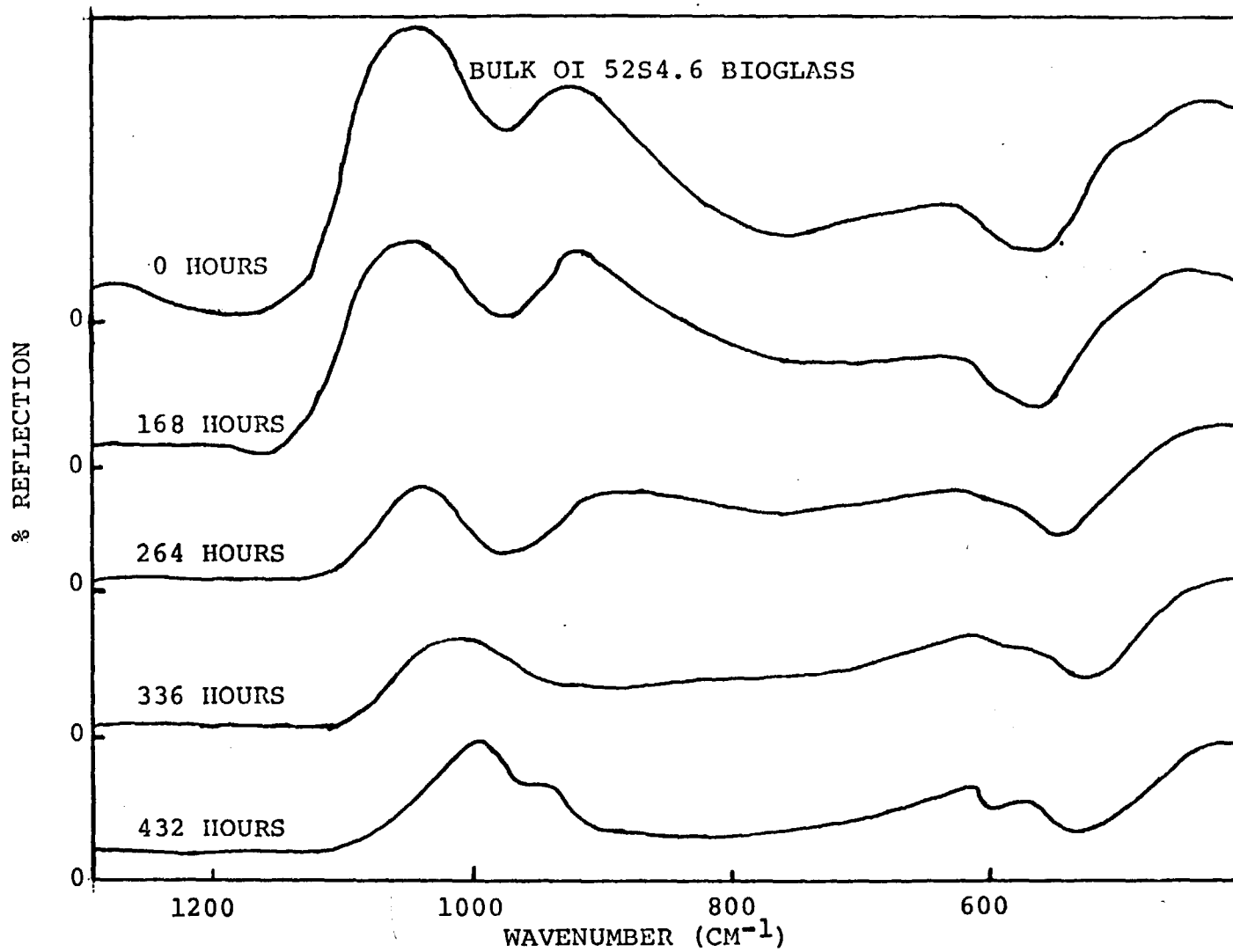


Figure 3.2 IRRS Reaction Sequence Data for OI 52S4.6 Reacted from 0 to 720 hours.

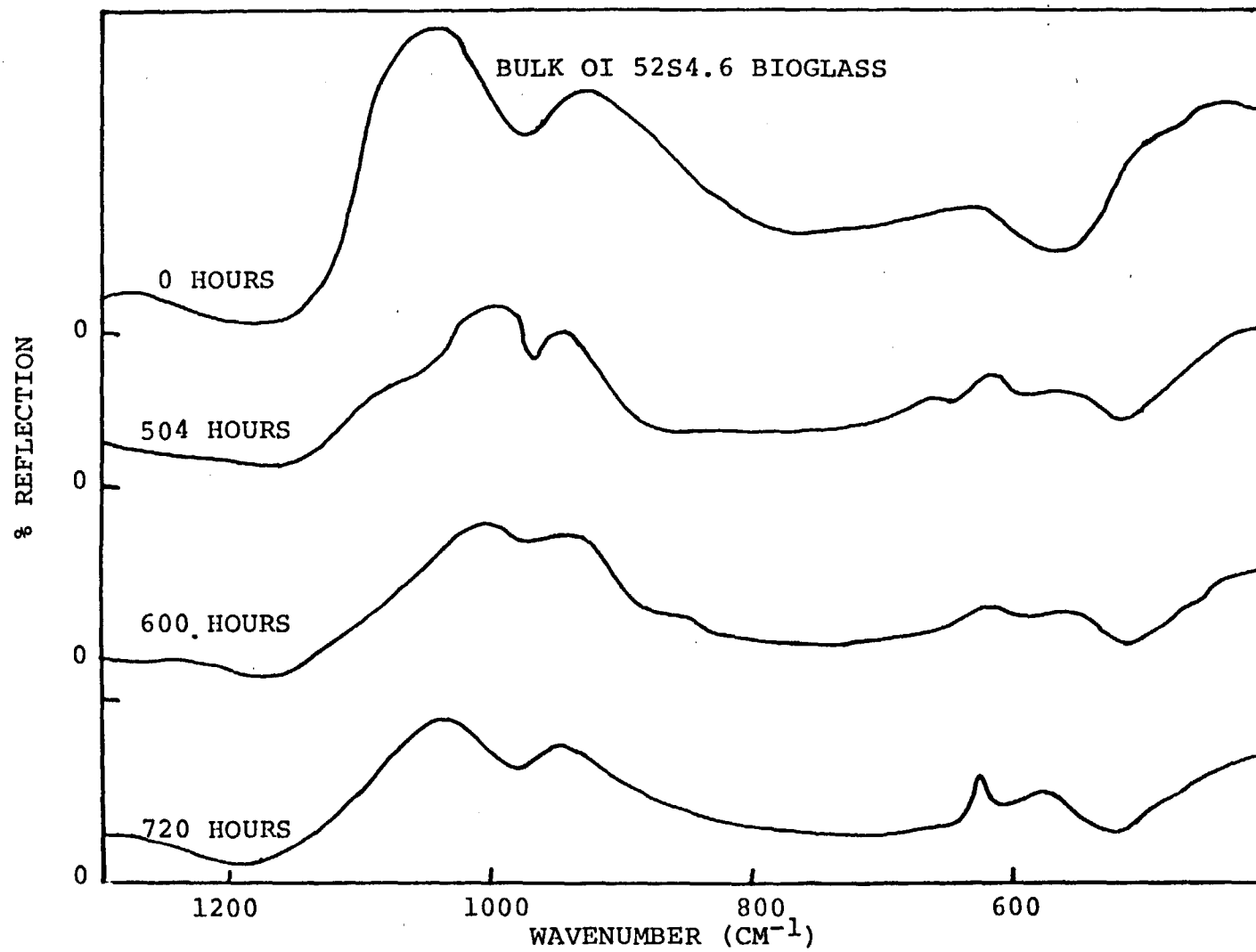


Figure 3.2—continued

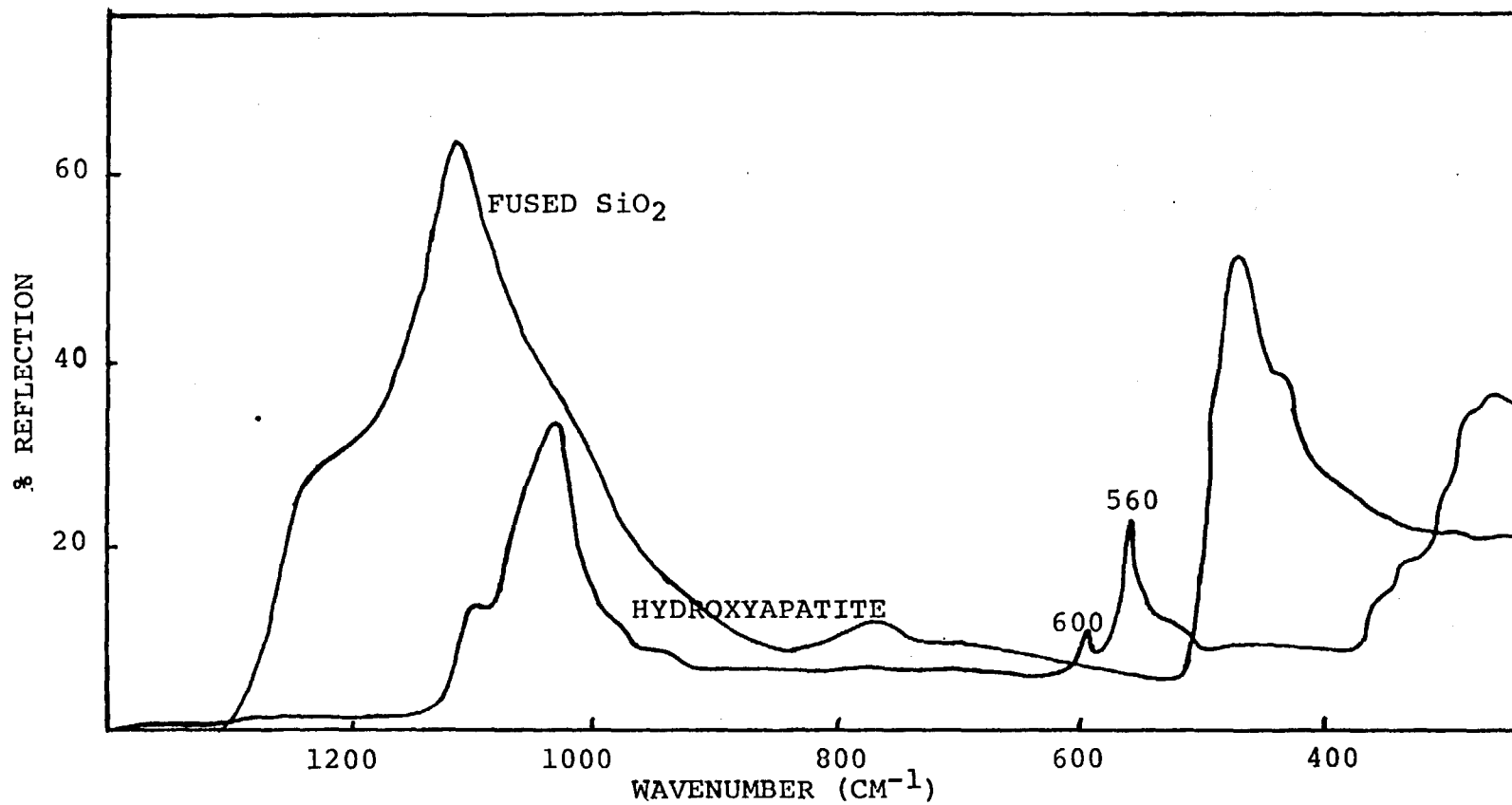


Figure 3.3 IRRS Spectrum of Hydroxyapatite(a bone mineral) compared with Fused SiO<sub>2</sub>.

hours is the maximum reaction time for this sample. Previous work<sup>19</sup> showed that UF 45S5 bioglass reacted in a buffered solution formed a spectrum equivalent to that of hydroxapatite (shown in Figure 3.3). After 100 hours of reaction the spectrum has both S and NS stretching peaks. The reaction sequence data for UF 45S5 bioglass is faster than that of OI 52S4.6 bioglass. For this reason it was decided to use the OI 52S4.6 bioglass composition and analyze its reaction in deionized water from zero to 720 hours. If a Ca-P rich film was observed for OI 52S4.6 bioglass then it was assumed that it would occur for the UF 45S5 bioglass sample but at a faster rate. The idea was to use the slower reacting glass and extrapolate information from these results. Bioglasses UF 45S5 and OI 52S4.6 are both within the bone bonding range and therefore important coating materials.

The reaction sequence data for bulk OI 52S4.6 bioglass are shown in Figure 3.2. After 168 hours there is a slight decrease in the S peak while at 264 hours of reaction the effect of surface roughening is observed with a decrease in overall peak intensity. After 336 hours there is a loss of the NS stretching vibration. Additionally there is growth of two peaks at  $575\text{ cm}^{-1}$  and  $615\text{ cm}^{-1}$ . The intensity of these peaks continues to rise through 720 hours of reaction. After 720 hours of reaction we see a shift between the S and NS peaks toward each other. The spectrum at 720 hours can be compared with Figure 3.3 which shows the spectrum for hydroxyapatite. Thus the bulk OI 52S4.6 bioglass



is showing a spectrum after 720 hours of reaction which is representative of a Ca-P rich film formation on the surface.

#### Polymer Reaction Sequence Data

In the preliminary series of polymers coated with OI 52S4.6 bioglass the samples showing an IRRS spectrum resembling that of bulk bioglass were used for in vitro studies. In vitro tests consisted of exposing the samples to deionized water at a specific ratio of surface area (SA) of sample to volume of solution (V). A SA/V ratio used was  $0.7 \text{ cm}^{-1}$  to compare the present study with previous work.<sup>19</sup> It has been shown that the rate of attack of a glass surface is directly proportional to this ratio.<sup>20</sup>

The original shapes of the five polymers investigated were circular discs, shown in Figure 3.4. Total surface areas were calculated according to the geometry of a thin cylinder. The equation for the total surface area (SA) was;  $SA = D(D/2 + H)$  where D is the diameter of the sample and H is the thickness of the sample being reacted in deionized water at 37 °C. The corresponding values for SA, V, D and H for each coated polymer with approximately 1.2  $\mu\text{m}$  OI 52S4.6 can be seen in Table 3.1.

Polymer samples coated with either UF 45S5 bioglass or OI 52S4.6 bioglass were reacted in deionized water at 37 °C according to reaction sequence 2 as outlined and described in Chapter 2. Control polymers, that is, polymer substrates that are neither reacted nor coated, were analyzed with the

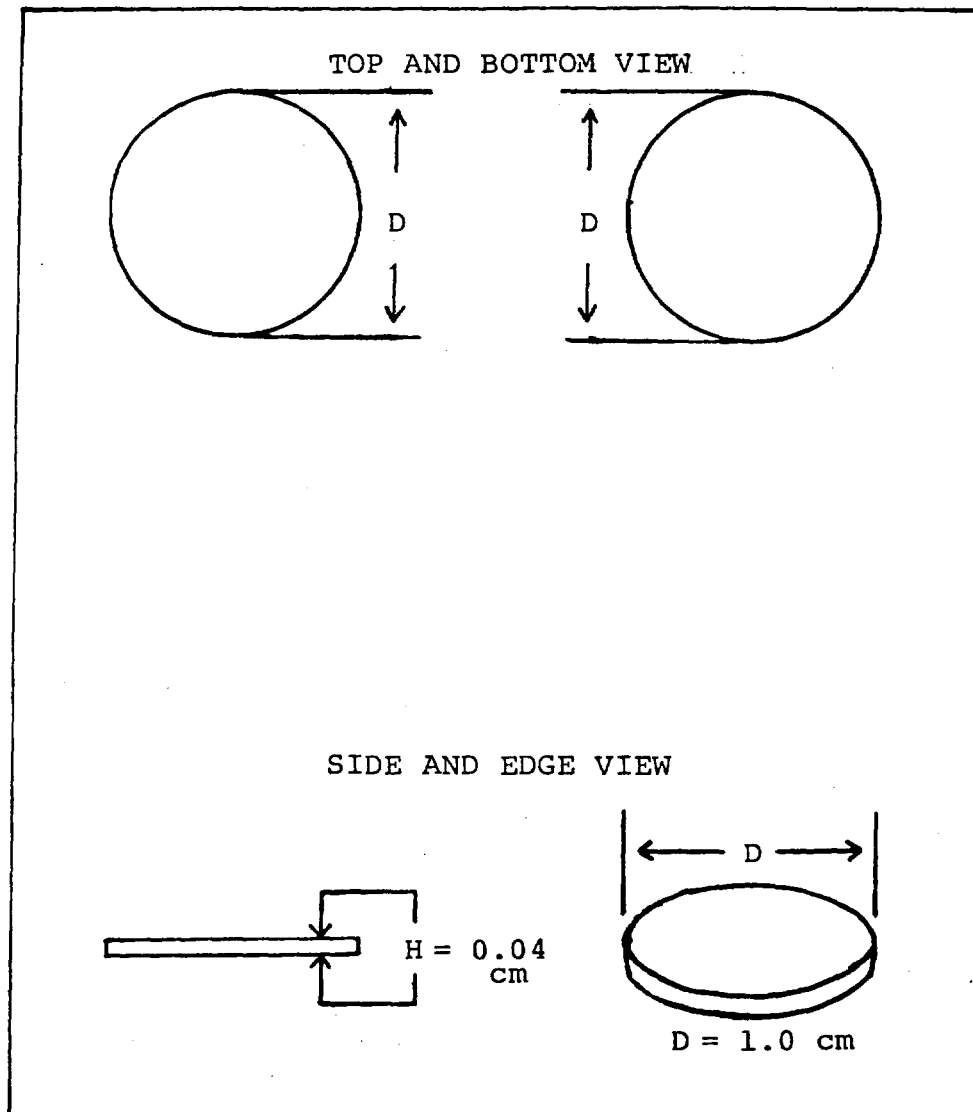


Figure 3.4 Dimensions and geometrics of polymer discs coated with bioglass.

Table 3.1  
Surface Area to Volume of Solution Ratios

Sample	D(cm)	H(cm)	SA(cm <sup>2</sup> )	V(cm <sup>3</sup> )
S-15	1.0	0.05	1.72	2.47
PMMA-8	0.97	0.03	1.56	2.24
OH-11	0.97	0.03	1.56	2.24
A-11	0.97	0.04	1.60	2.28
AM-10	0.97	0.04	1.60	2.28

IRRS technique. From this, characteristic spectra were obtained for each of the five polymer substrates. In addition, each coated polymer was analyzed by the IRRS technique before reaction and compared with the unreacted bulk bioglass spectrum. The initial coating thicknesses on polymers achieved by NASA were approximately 0.5  $\mu\text{m}$  to 2.0  $\mu\text{m}$ .

#### Bioglass Coating Thickness Comparison

Polymer substrates were ion beam sputter cleaned then coated with OI 52S4.6 bioglass as described in Chapter 2. Coating thicknesses ranged from approximately 0.5  $\mu\text{m}$  to 2.0  $\mu\text{m}$ . A comparison of IRRS spectra for each polymer as a function of coating thickness can be seen in Figures 3.5 to 3.9. It was expected that with increasing coating thickness a coated substrate would have properties that resembled that of bulk bioglass in reaction. Consequently increasing coating thickness would show an IRRS spectrum to have features similar to those of the bulk bioglass IRRS spectrum. The presence of S and NS peaks are features which suggested the presence of a coating similar in composition to bulk bioglass. In all cases, except for PMMA-8 (Figure 3.6), the trend observed by the IRRS data was irregular as a function of increasing coating thickness (see Figures 3.5, 3.7, 3.8 and 3.9). The SR coated substrates shown in Figure 3.5 showed the 0.5  $\mu\text{m}$  and 1.95  $\mu\text{m}$  coatings to be similar to the spectrum of amorphous silicate gels not

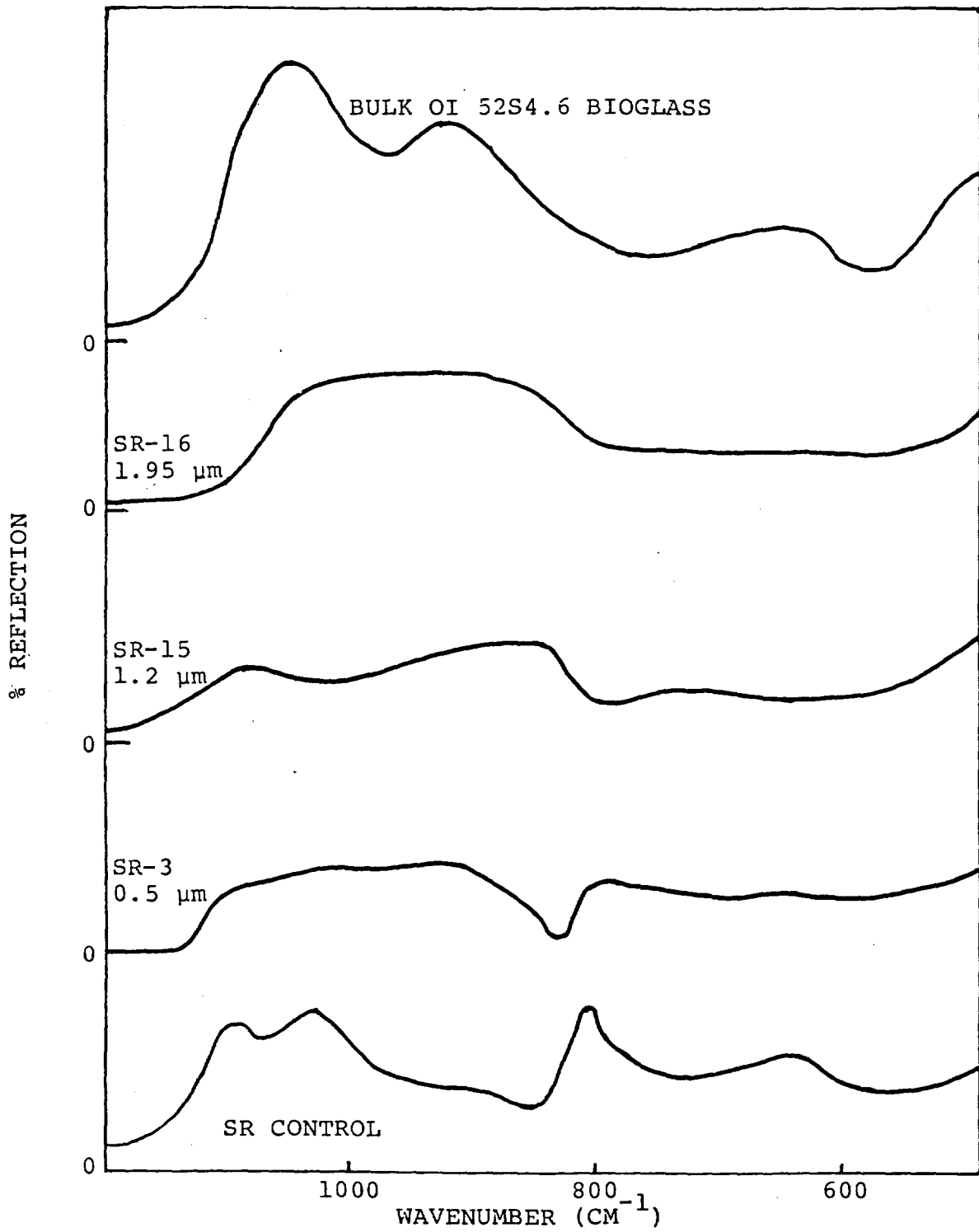


Figure 3.5 IRRS Spectrum: Bulk OI 52S4.6 bioglass vs. coated SR as a function of OI 52S4.6 bioglass coating thickness.

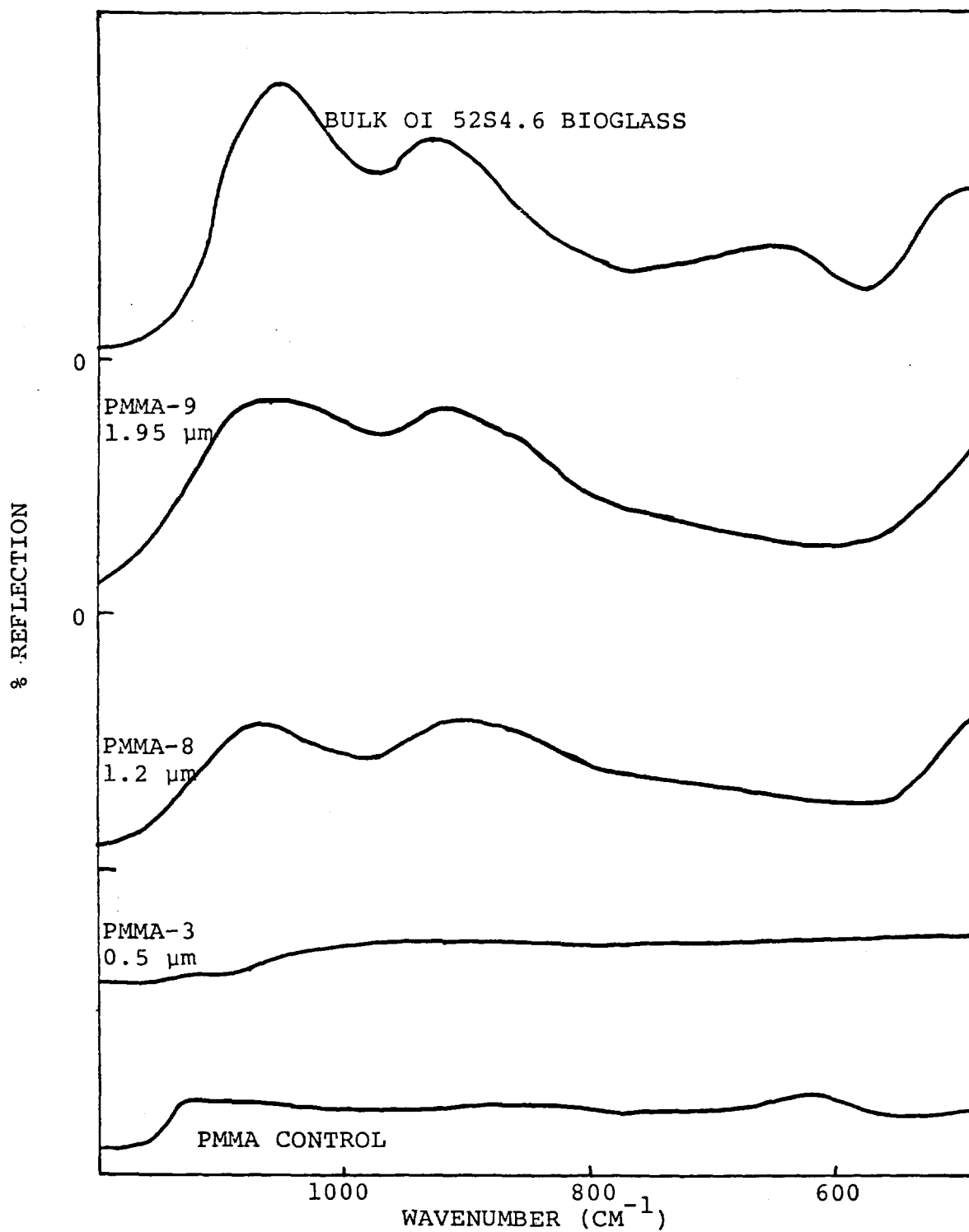


Figure 3.6 IRRS Spectrum: Bulk OI 52S4.6 bioglass vs. coated PMMA as a function of OI 52S4.6 coating thickness.

fully transformed to a glassy network.<sup>21</sup> Another possibility could be loss of resolution by the infrared spectrometer. The 1.2  $\mu\text{m}$  coated SR showed signs of S and NS peaks characteristic of the bulk bioglass.

The AM coated substrates (Figure 3.7) showed the S and NS features characteristic of bioglass at all coating thicknesses. We did not see the trend seen in PMMA-8 (Figure 3.6). In addition AM-3 coated with 0.5  $\mu\text{m}$  showed the most resemblance to bulk bioglass as compared to other 0.5  $\mu\text{m}$  coated polymers. Both PMMA-8 (Figure 3.6) and AM-10 (Figure 3.7) coated with 1.2  $\mu\text{m}$  and PMMA-9 (Figure 3.6) and AM-11 (Figure 3.7) coated with 1.95  $\mu\text{m}$  were very similar in their IRRS features when compared with each other.

The IRRS data from the last two coated polymers (A and OH) shown in Figures 3.8 and 3.9, are very similar to each other and are discussed simultaneously. For both, the 0.5  $\mu\text{m}$  spectra are similar and show a closer resemblance to the control than to the bulk bioglass spectrum. As mentioned previously this could be due to the detection depth of the IRRS technique being larger than the coating thickness. Both the 1.2  $\mu\text{m}$  IRRS spectra of coated A and OH show features representative of a bioglass spectrum while the 1.95  $\mu\text{m}$  spectra are similar to the spectrum of SR coated with 1.95  $\mu\text{m}$  OI 52S4.6 bioglass.

It was unclear from these results whether the spectra obtained for the 0.5  $\mu\text{m}$  bioglass coated polymers were showing damage as a result of the coating process, were a non-uniform

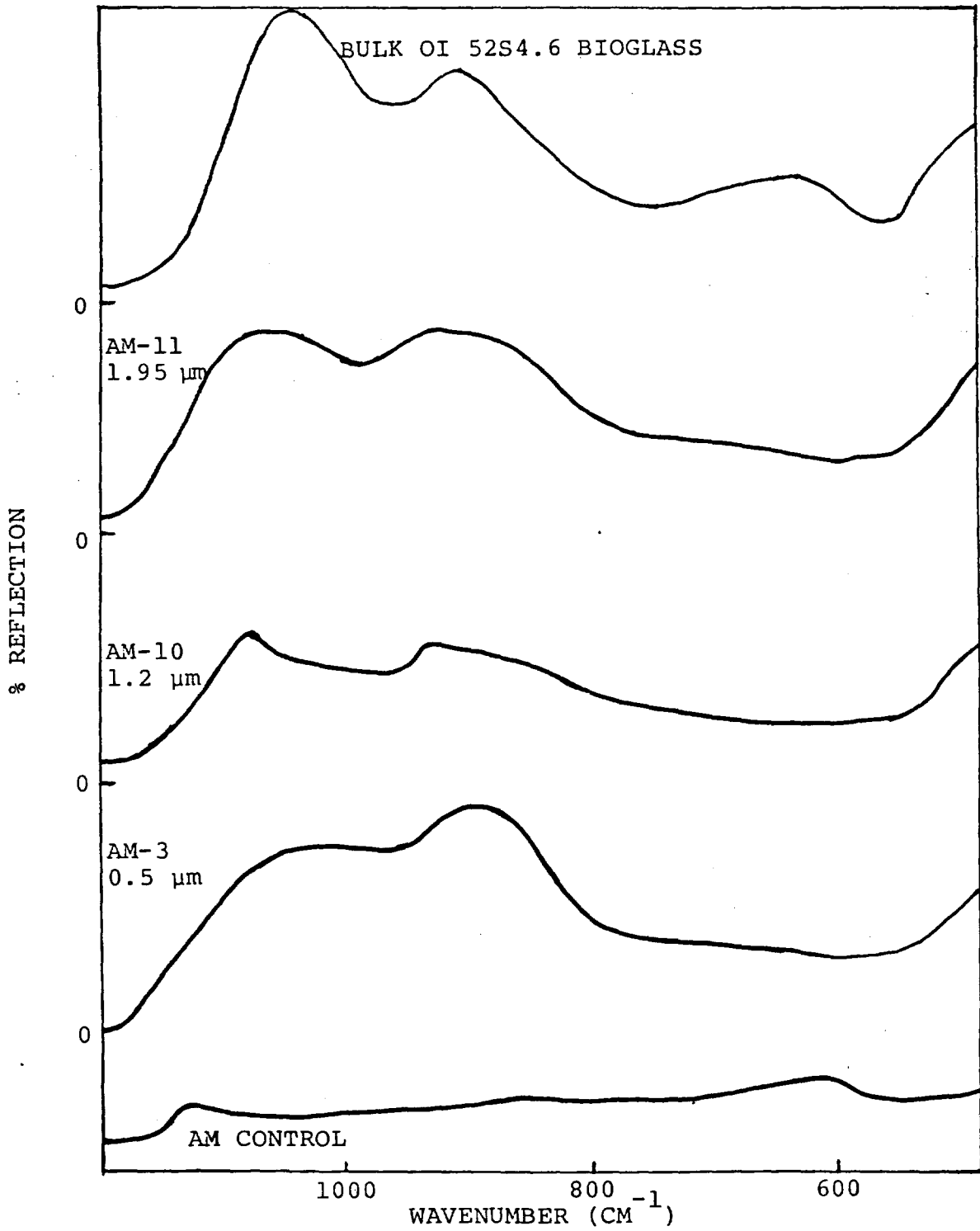


Figure 3.7 IRRS Spectrum: Bulk OI 52S4.6 bioglass vs. coated AM as a function of OI 52S4.6 bioglass coating thickness.



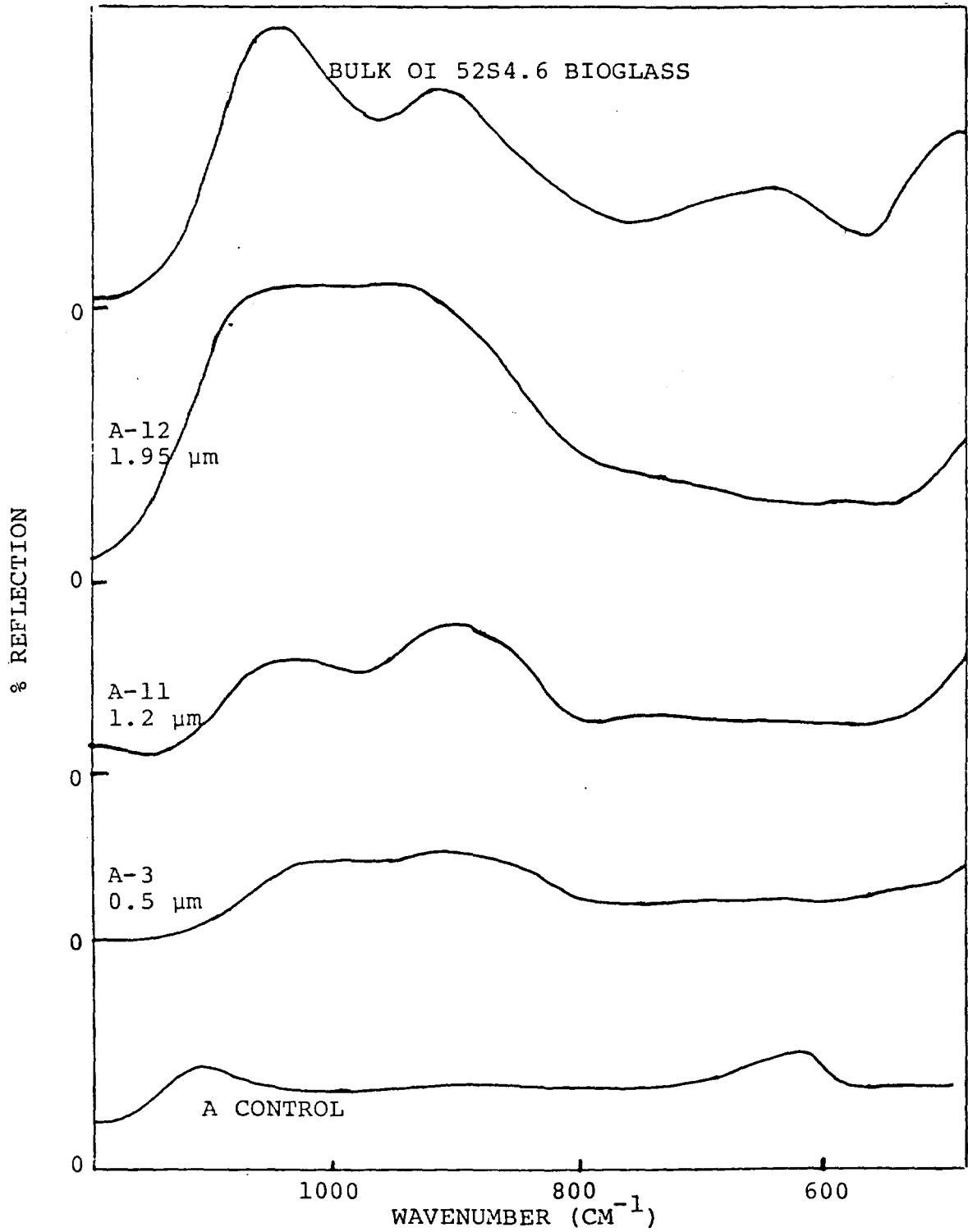


Figure 3.8 IRRS Spectrum: Bulk OI 52S4.6 bioglass vs. coated A as a function of OI 52S4.6 bioglass coating thickness.

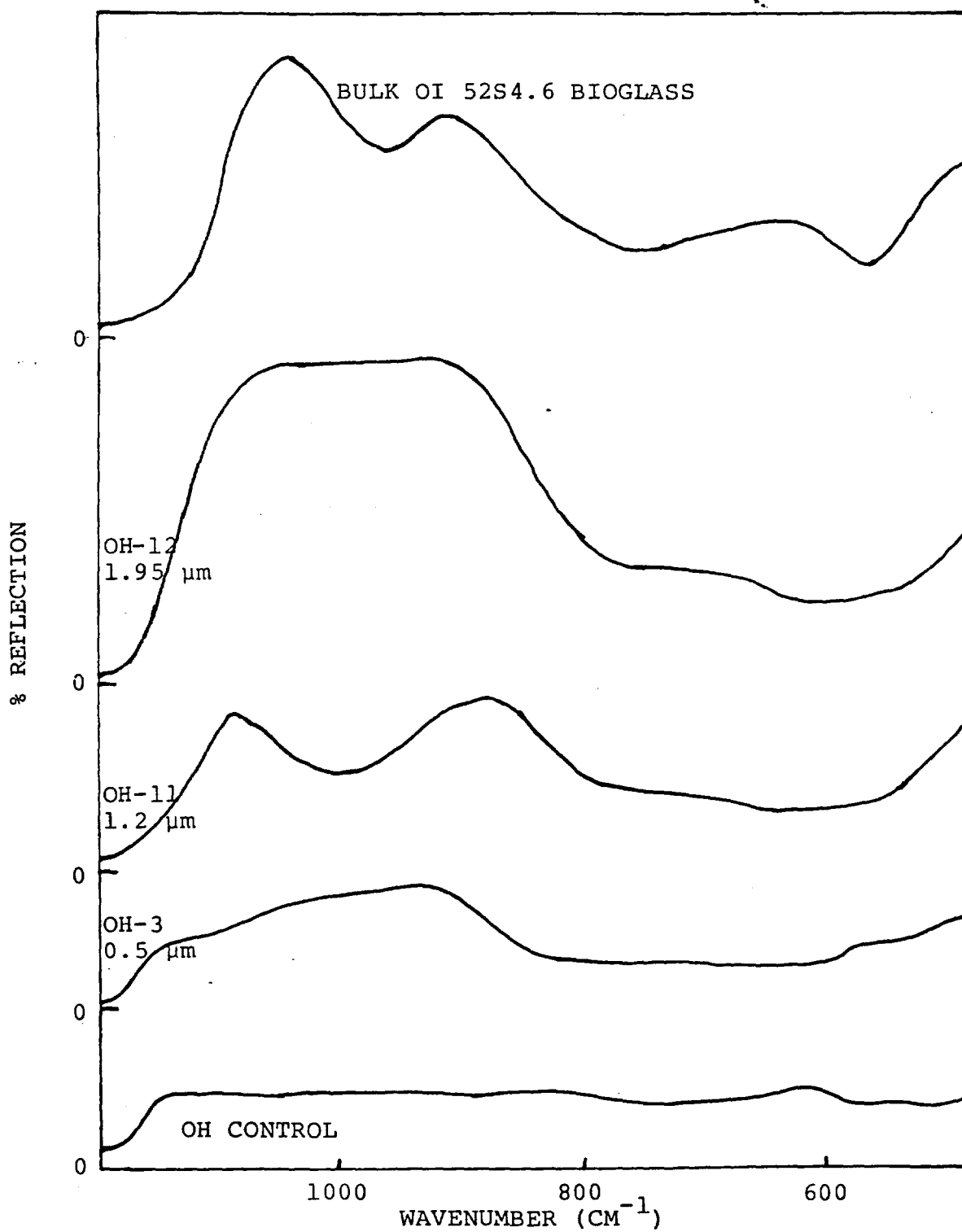


Figure 3.9 IRRS Spectrum: Bulk OI 52S4.6 bioglass vs. coated OH as a function of OI 52S4.6 coating thickness.

coating with respect to composition and/or thickness, or were simply due to the depth limitations of the IRRS technique. The polymers coated with 1.2  $\mu\text{m}$  showed the most consistency.

#### Coated Polymer Reaction Tests

The samples used for the primary reaction sequence were polymeric, coated with 1.2  $\mu\text{m}$  OI 52S4.6 bioglass. In this manner, if the reaction spectra obtained did not resemble either the bulk bioglass or the control, it could more easily be inferred that a non-uniform coating was present, thereby eliminating the problem of the detection depth of the IRRS technique. The formation of a spectrum after 1000 hours that resembles a Ca-P rich spectrum was observed in PMMA-8 (Figure 3.11), AM-10 (Figure 3.12) and OH-11 (Figure 3.14). The SR coated polymer (designated as SR-15) reaction sequence (see Figure 3.10) showed the formation of a silica rich peak and a peak at 1000 hours of reaction characteristic of the control. Finally, sample A-11 (Figure 3.13) showed S and NS peaks as well as a peak at  $600\text{ cm}^{-1}$ . The dotted line in Figures 3.10 to 3.14 is the spectrum for fused silica used as the standard throughout for the identification of the Si-O-Si stretching vibrations. Similarly for comparison purposes the first spectrum in each graph is bulk OI 52S4.6 bioglass while the last spectrum is the uncoated polymer control. The hours of reaction are designated on each spectrum in Figure 3.10 to 3.14.

Figure 3.10 IRRS reaction sequence of SR-15 coated with 1.2  $\mu\text{m}$  OI 52S4.6 bioglass. Coated SR was reacted in deionized water at 37 °C according to reaction sequence 2 as outlined in Chapter 2.

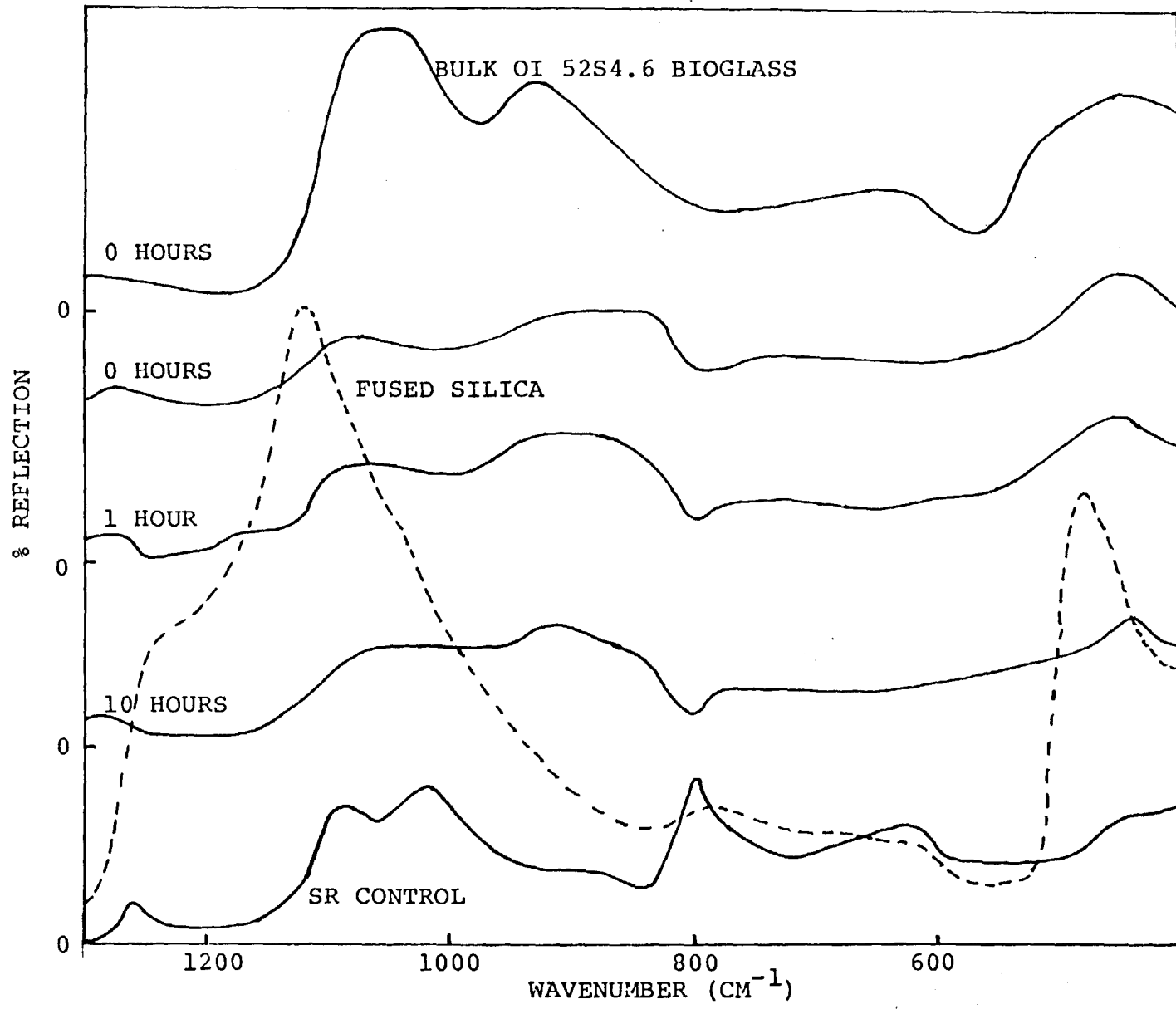


Figure 3.10 Continued

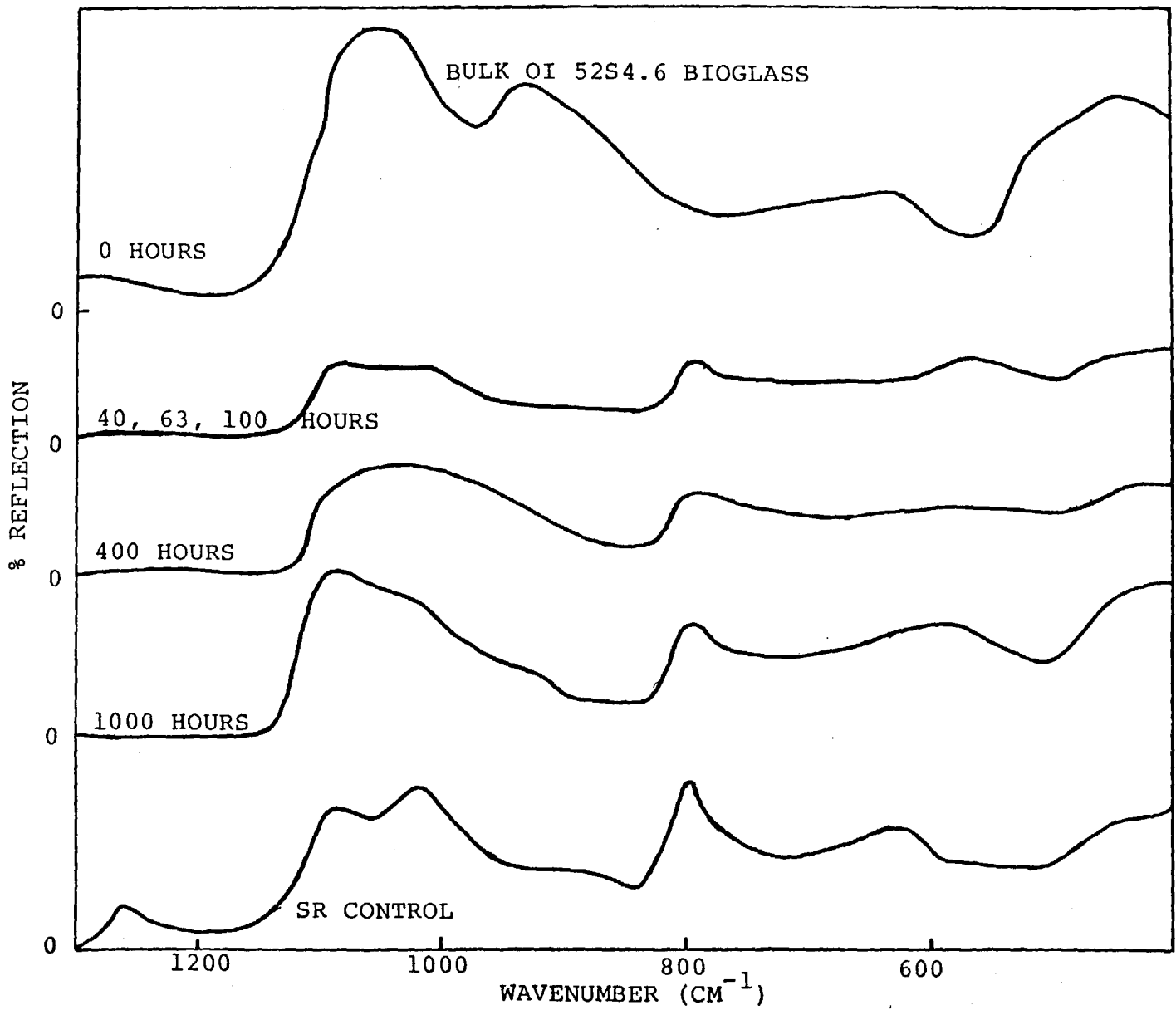


Figure 3.11 IRRS reaction sequence of PMMA-8 coated with 1.2  $\mu\text{m}$  OI 52S4.6 bioglass. Coated PMMA was reacted in deionized water at 37 °C according to reaction sequence 2 as outlined in Chapter 2.



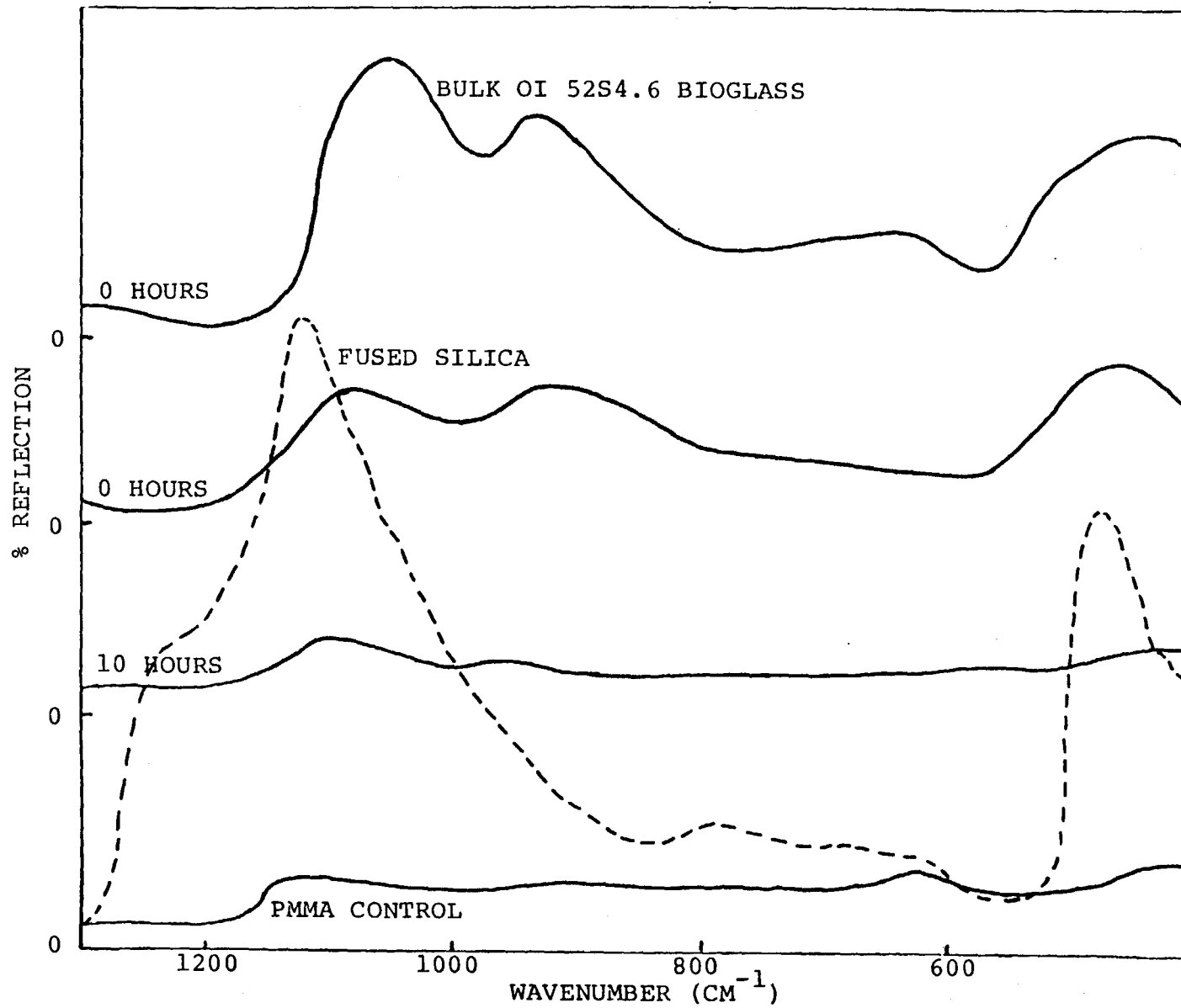


Figure 3.11 Continued

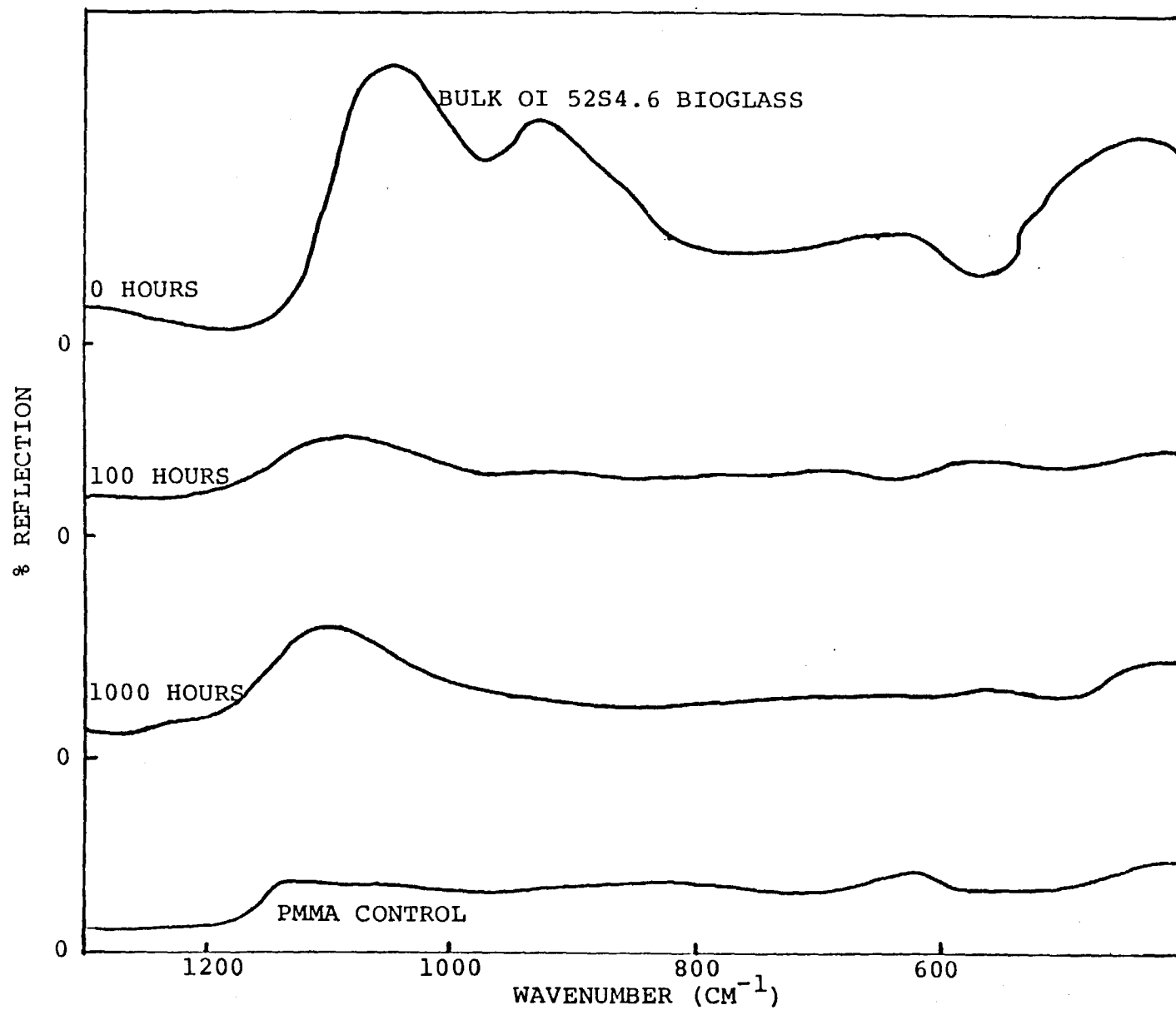


Figure 3.12 IRRS reaction sequence of AM-10 coated with 1.2  $\mu\text{m}$  OI 52S4.6 bioglass. Coated AM was reacted in deionized water at 37 °C according to reaction sequence 2 as outlined in Chapter 2.

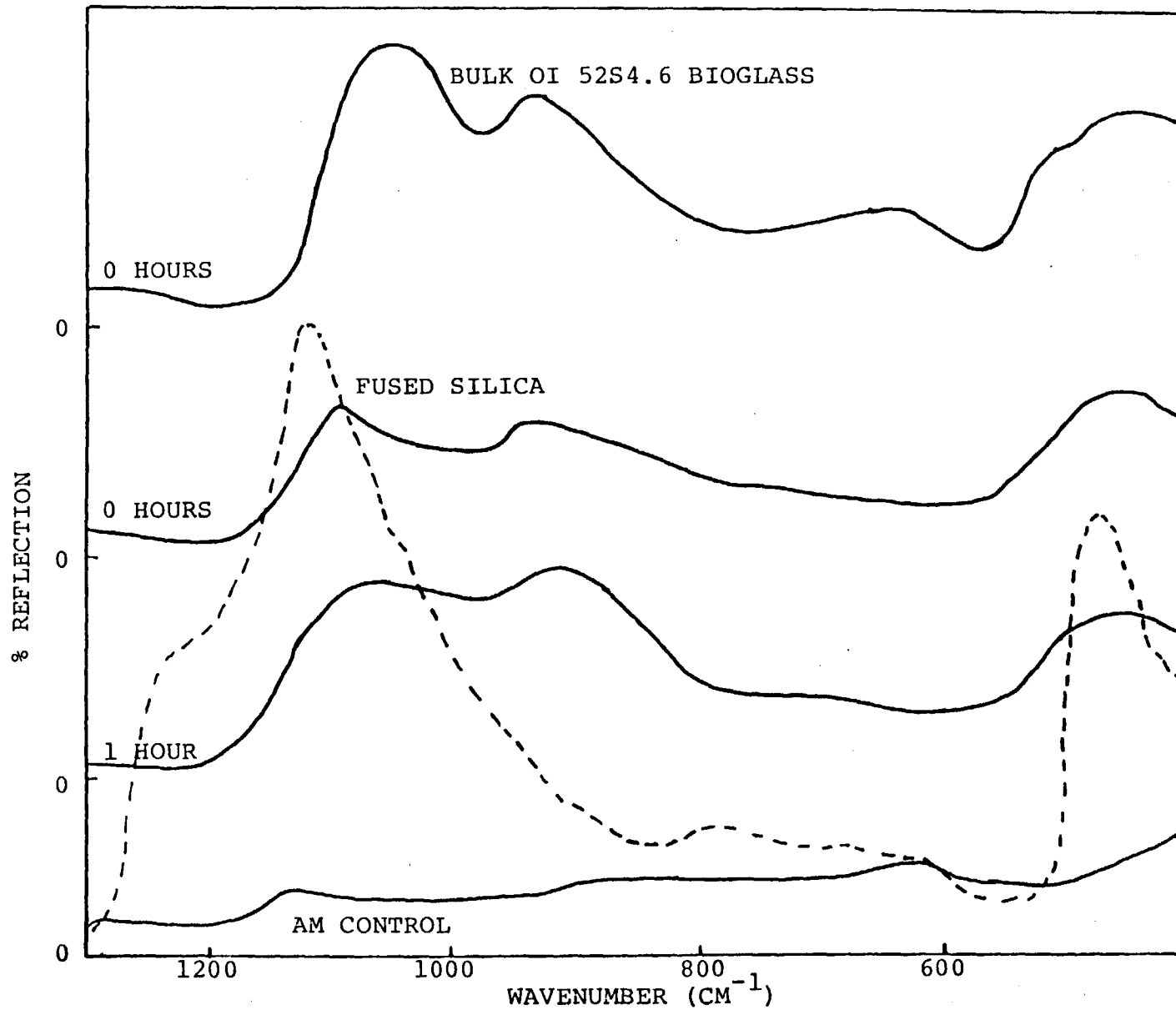


Figure 3.12 Continued

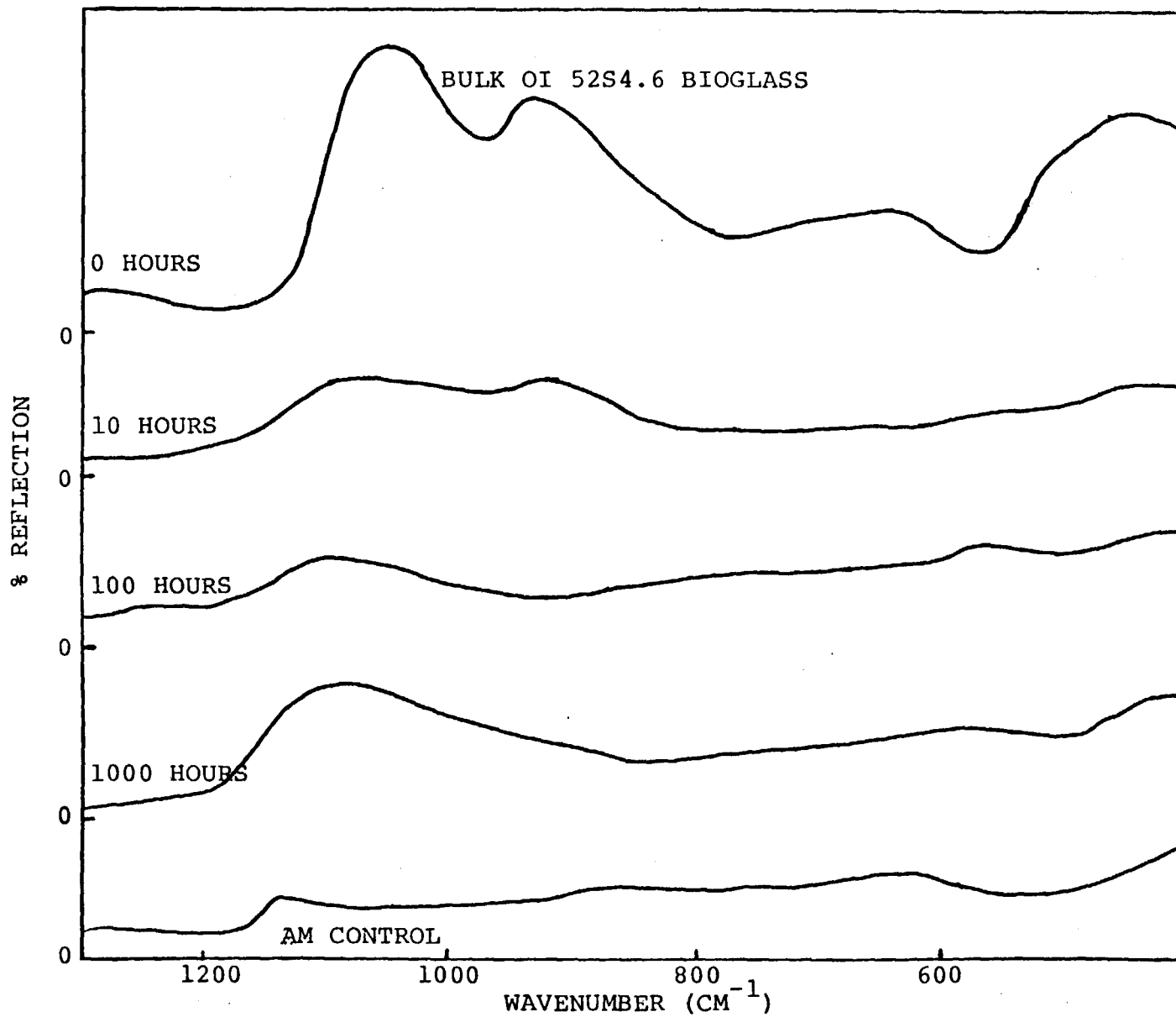


Figure 3.13 IRRS reaction sequence of A-11 coated with 1.2  $\mu\text{m}$  OI 52S4.6 bioglass. Coated A was reacted in deionized water at 37 °C according to reaction sequence 2 as outlined in Chapter 2.



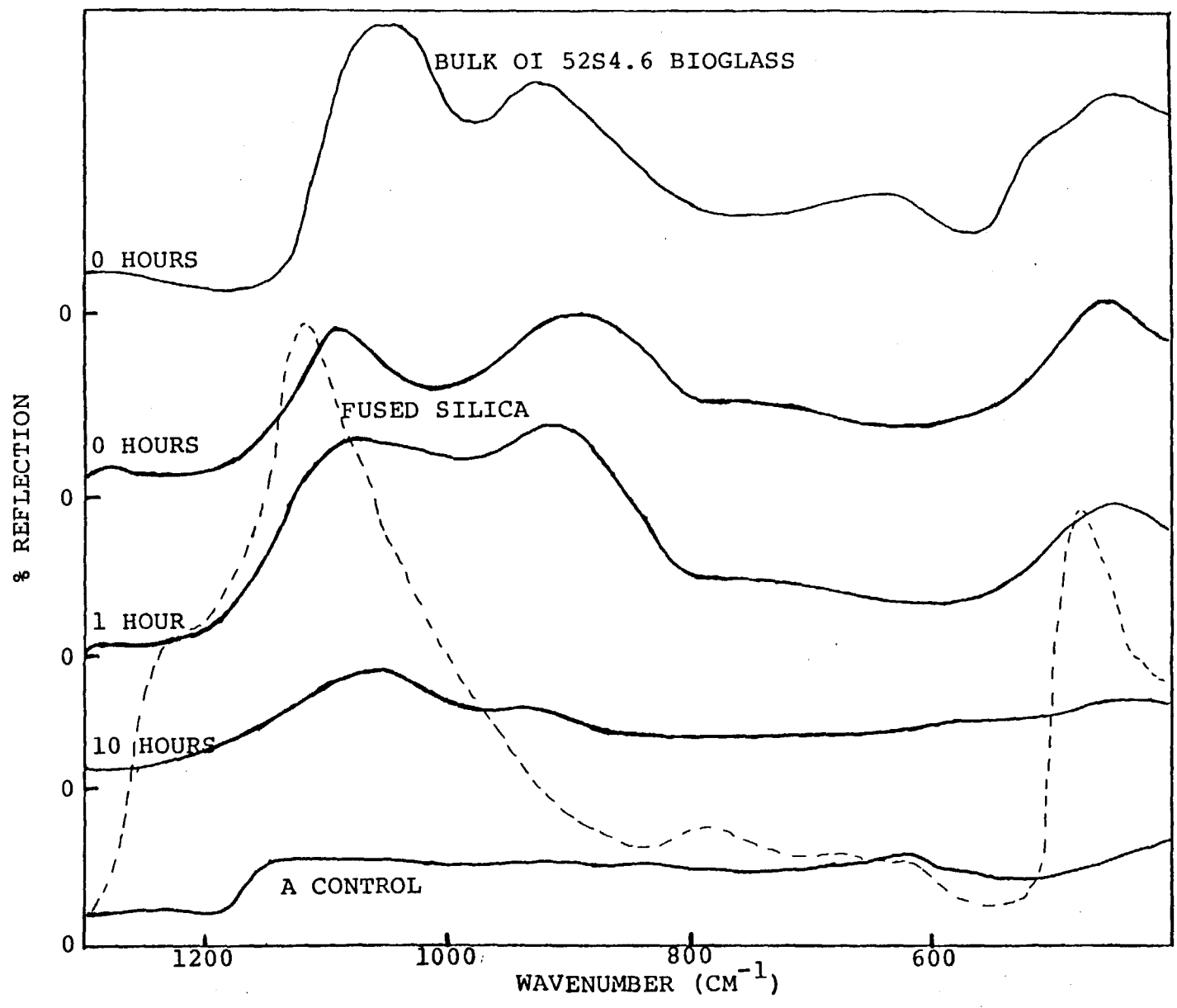


Figure 3.13 Continued

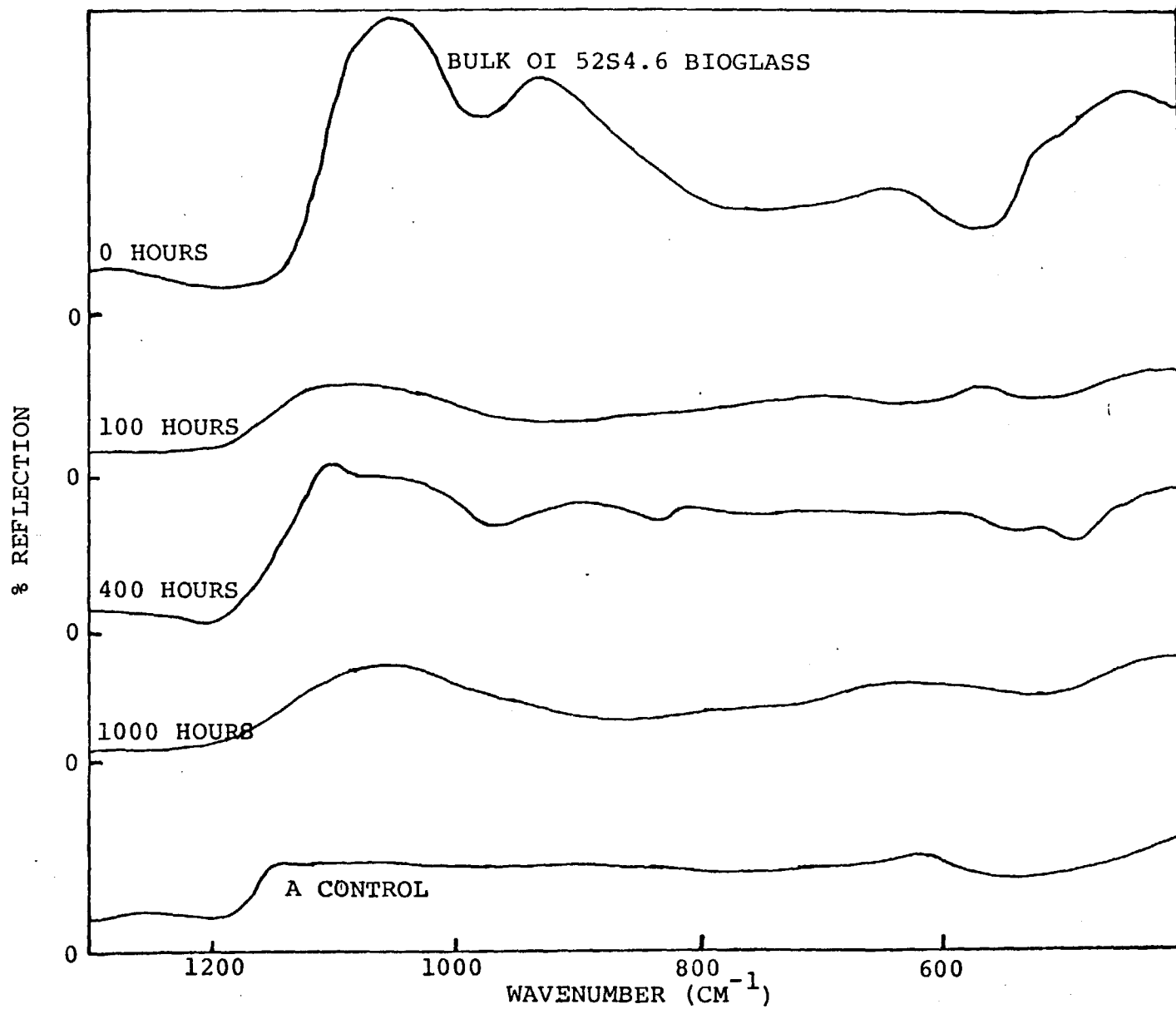


Figure 3.14 IRRS reaction sequence of OH-11 coated with 1.2  $\mu\text{m}$  OI 52S4.6 bioglass. Coated OH was reacted in deionized water at 37 °C according to reaction sequence 2 as outlined in Chapter 2.

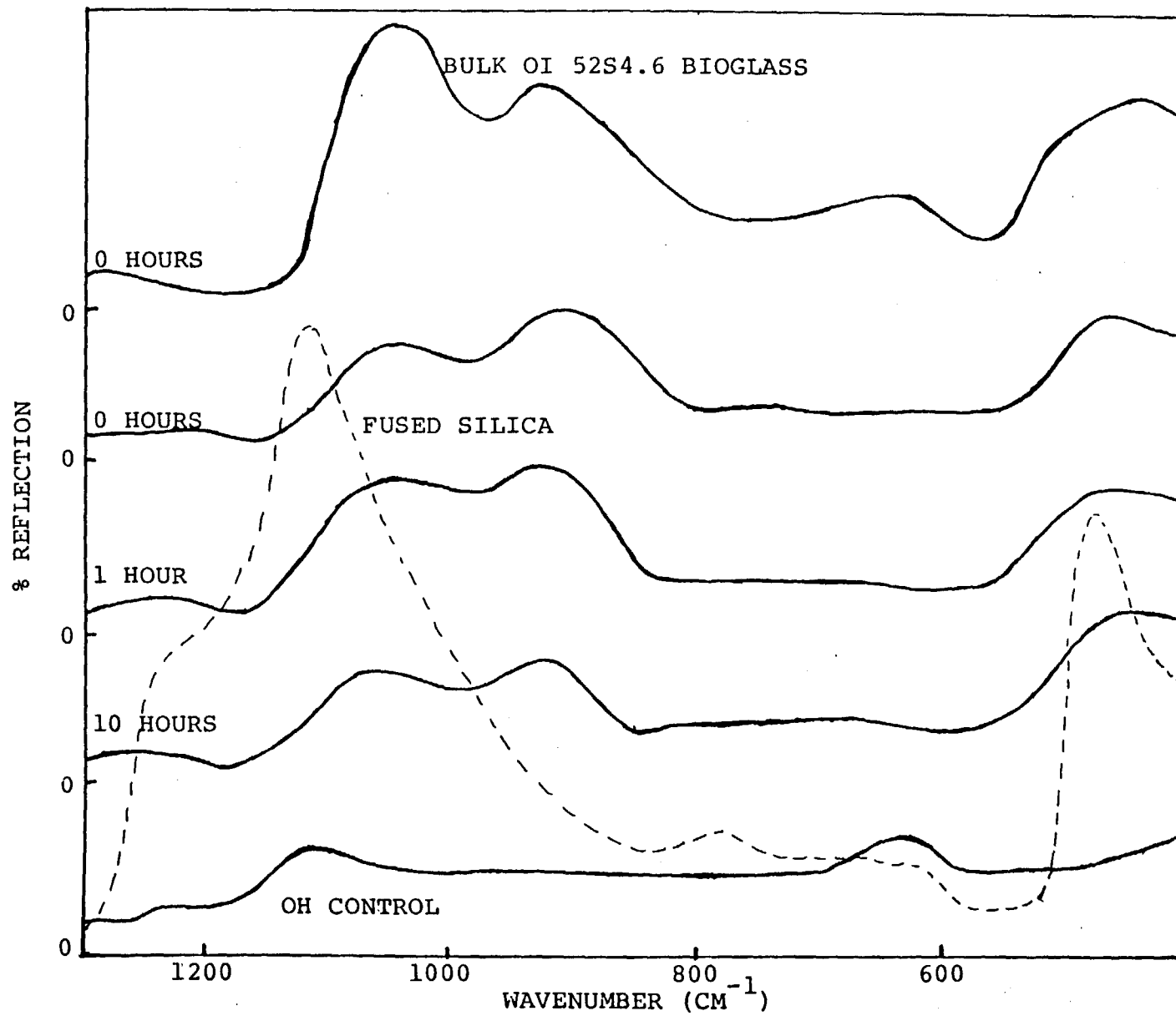
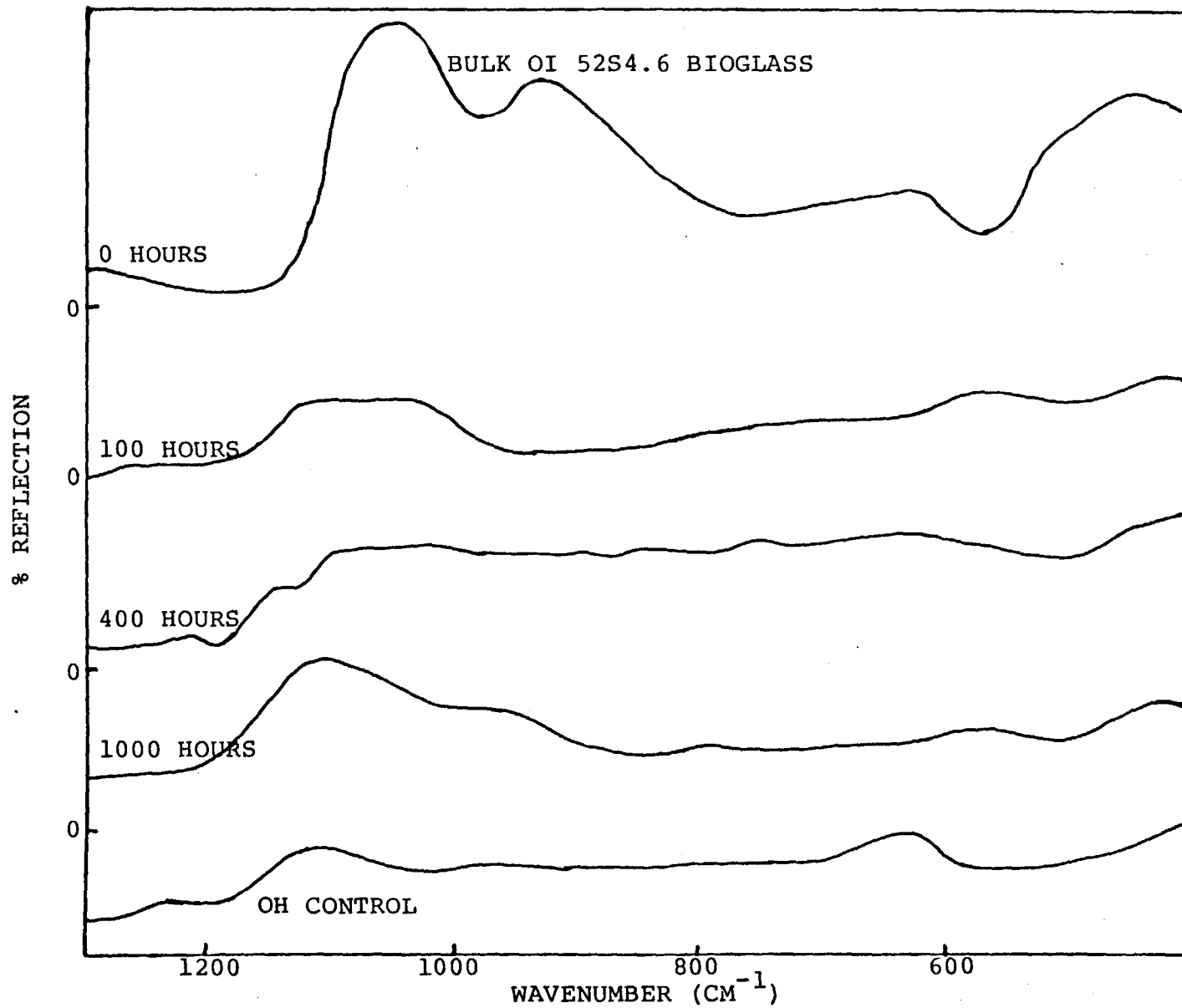


Figure 3.14 Continued



It was observed that the loss of  $\text{Na}^{+1}$  ions for PMMA-8 and AM-10 occurred after 100 hours of reaction while that for OH-11 occurred after 400 hours of reaction. In all cases the spectrum at 1000 hours of reaction resembles a Ca-P rich spectrum, specifically by the broad peak at about  $550 \text{ cm}^{-1}$  which is still present and can be compared with the spectrum in Figure 3.2 at 264 hours. The growth of a peak between  $560 \text{ cm}^{-1}$  and  $590 \text{ cm}^{-1}$  is suggestive of a hydroxyapatite layer on the surface of the bioglass coating during the long term reaction of PMMA-8, AM-10 and OH-11.

In the coated polymer samples of SR and A some anomalies were observed. The SR reaction sequence shown in Figure 3.10 does not show the formation of a spectrum that is characteristic of a Ca-P rich layer. Instead it is seen that the peak at  $800 \text{ cm}^{-1}$ , characteristic of the control, is observed after 40 hours of reaction. At this time it was also noted that the NS peak had disappeared, as is observed in the reaction sequence of bulk OI 52S4.6 bioglass (Figure 3.2). The spectrum after 40 hours was seen to be the same as the spectra for 63 hours and 100 hours. Since some of the characteristics of the control polymer are surfacing it was suspected that the coating was patchy. There was also evidence of a NS peak as well as the formation of a low intensity peak at about  $550 \text{ cm}^{-1}$  both of which are observed in the bulk bioglass spectrum of Figure 3.2. After 400 hours of reaction an increase in the S bridging peak at  $1040 \text{ cm}^{-1}$  has broadened, as well as increased in



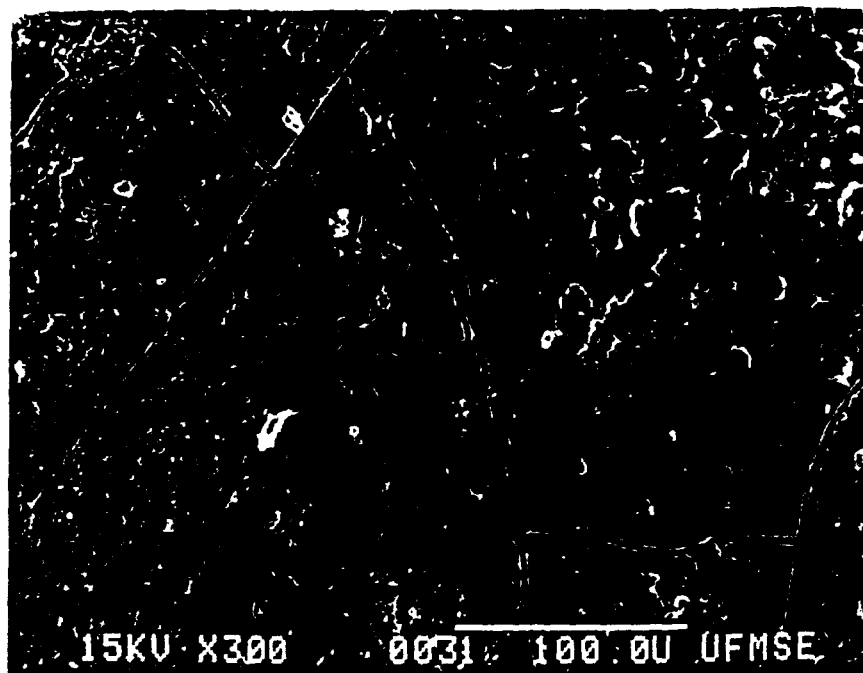
intensity, suggesting the formation of a silica rich film. Finally, the spectrum at 1000 hours of reaction shows an increase and shift to higher wavenumbers in the S bridging peak and an increase and broadening in the peak at about  $550\text{ cm}^{-1}$ . Also observed in the 1000 hour spectrum is an increase in the peak at  $800\text{ cm}^{-1}$ . Sample A-11 (Figure 3.13) shows IRRS data that is different from that of SR-15 (Figure 3.10) but more similar to PMMA-8 (Figure 3.11), AM-10 (Figure 3.12) or OH-11 (Figure 3.14). The control spectrum shows characteristic peaks at  $1120\text{ cm}^{-1}$  and  $630\text{ cm}^{-1}$ . After zero, one and 10 hours of reaction the spectra resembles that of the bulk bioglass. After 100 hours of reaction there is a loss of the S stretching peak and the formation of a broad peak from  $530$  to  $590\text{ cm}^{-1}$ . The spectrum at 400 hours shows surface roughening. After 1000 hours of reaction we see the formation of a silica rich film suggested by an increase in intensity of the S stretching peak and the simultaneous shift to a higher wavenumber. Also present is a NS stretching peak suggesting the presence of alkali on the surface as well as the reoccurrence of a low intensity broad peak in the region  $530$  to  $590\text{ cm}^{-1}$ . It is important to note that the stretching peak at  $625\text{ cm}^{-1}$  of the control spectrum is not seen in the 1000 hours spectrum. An effective coating is still present on the polymer but it reacts slower than those on PMMA-8, AM-10 and OH-11.

SEM data

To obtain preliminary information concerning the microstructure of reacted and coated polymers, SEM photographs were taken of SR-15, OH-11 and PMMA-8 after reaction for 1000 hours. Figure 3.15 shows the SEM photograph of OH-11 (see Figure 3.15 A) and SR-15 (see Figure 3.15 B) at a magnification of 300X. The IRRS data for SR-15 (see Figure 3.10) showed features from the control SR surfacing, as well as the presence of a peak in the S region. The structure of the coating seemed to be patchy from these results. It can be seen that the structure shows signs of cracking, with an overall rough surface and evidence that some flaking has occurred. The areas of flaking are seen as dark grey areas in light grey areas. Additionally, IRRS data for OH-11 (see Figure 3.14) show the presence of a Ca-P rich film with no characteristic peaks of the control present after 1000 hours of reaction. The surface structure of the coating for OH-11 (see Figure 3.14 A) is similar to that of SR-15 (see Figure 3.15 B) at the same magnification (300X). The main difference that can be seen is the larger grain size with wider spacing between grains of OH-11 as compared to grains of SR-15. An area where some flaking has occurred is seen in the top left side of Figure 3.15 A. The surface exposed is that of the polymer.

The SEM photograph of PMMA-8 is shown in Figure 3.16 at a magnification of 300X. This was taken after 1000 hours of reaction. The IRRS reaction data for PMMA-8 suggested

A)



B)

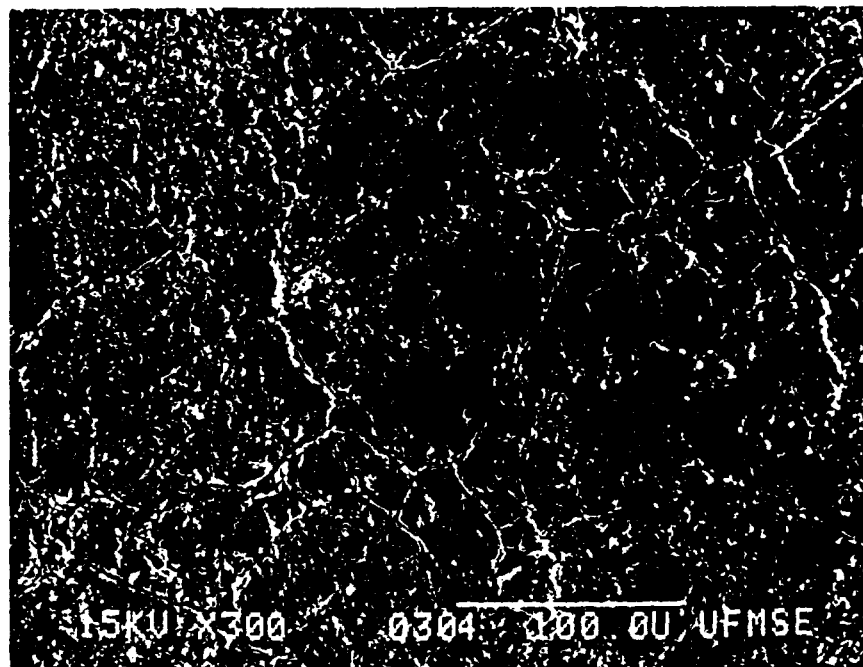


Figure 3.15 SEM photographs of coated and reacted polymers: A) OH-11 (1.2  $\mu\text{m}$  OI 52S4.6 bioglass) and B) SR-15 (1.2  $\mu\text{m}$  OI 52S4.6 bioglass) after 1000 hours of reaction. Original magnification is 300X.

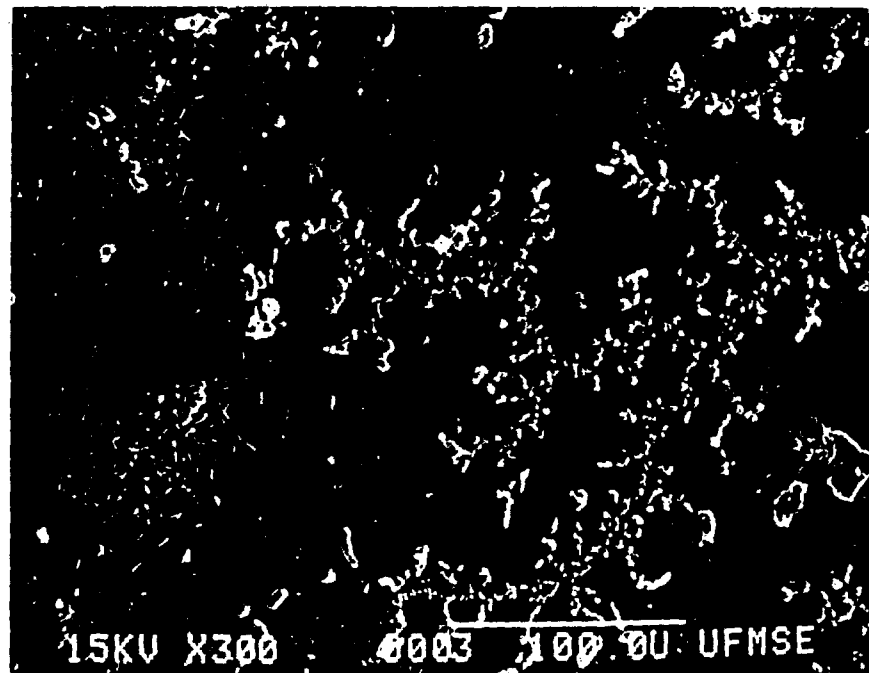


Figure 3.16 SEM photograph of coated and reacted PMMA-8 (1.2  $\mu\text{m}$  OI 52S4.6 bioglass) after 1000 hours of reaction. Original magnification is 300X.

ORIGINAL PAGE IS  
OF POOR QUALITY

that a hydroxyapatite surface layer had formed. The SEM photographs show that the surface is non-uniform with areas of concentrated precipitates, possibly of a Ca-P rich composition.

#### ESCA analysis

Preliminary ESCA analysis was done on substrates coated with approximately 0.5  $\mu\text{m}$  and 1.95  $\mu\text{m}$  OI 52S4.6 bioglass (unreacted) and compared with ESCA analysis of OI 52S4.6 bulk bioglass. Polymers coated with approximately 1.2  $\mu\text{m}$  OI 52S4.6 were analyzed after 1000 hours of reaction. It was shown that in comparing ESCA data of SR-3 (0.5  $\mu\text{m}$ ) and SR-16 (1.95  $\mu\text{m}$ ) both coated with OI 52S4.6, the peaks for C (1s), O (1s), Si (2p) and Ca (2p) were all qualitatively the same as those of the corresponding bioglass peaks. At the same time the ESCA data showed that SR-16 had Na (1s) and P (2p) present while these were not detected on SR-3, possibly due to the limit of detection of the instrument or the difference in composition obtained as a result of the sputtering time. A summary of the atomic compositions of the reacted polymers after 1000 hours is seen in Table 3.2. Calculation of atomic compositions was semi-quantitative and took in to account the photoionization cross-section of each element.<sup>22</sup> A similar qualitative ESCA peak analysis of the 0.5  $\mu\text{m}$  coated polymers and the 1.95  $\mu\text{m}$  coated polymers was compared with the bulk OI 52S4.6 bioglass with similar results to those of the SR coated polymers.

Table 3.2  
ESCA Compositional Analyses of coated polymer substrates  
in atomic %

Sample	<u>Carbon</u>	<u>Oxygen</u>	<u>Silicon</u>	<u>Calcium</u>	<u>Sodium</u>	<u>Phosphorus</u>
Unreacted coated polymer samples (0.5 $\mu\text{m}$ OI 52S4.6)						
SR-3	60.9	17.3	19.4	2.3	ND*	ND*
PMMA-3	84.5	11.3	3.2	0.8	0.3	ND*
OH-3	84.9	12.5	1.53	0.09	0.47	0.48
AM-3	87.5	9.1	2.2	0.94	0.27	ND*
A-3	86.6	10.2	2.2	0.3	0.27	ND*
Unreacted coated polymer samples (1.95 $\mu\text{m}$ OI 52S4.6)						
SR-16	67.3	14.4	15.5	2.0	0.98	0.6
PMMA-9	79.1	14.0	ND*	4.2	0.51	2.2
OH-12	82.1	13.0	0.61	3.2	0.28	0.73
AM-11	84.2	11.4	1.23	2.1	0.42	0.65
A-12	70.2	15.8	6.4	5.9	0.22	1.5
Reacted coated polymer samples (1.2 $\mu\text{m}$ OI 52S4.6-- 1000 hrs)						
SR-15	54.4	16.6	26.0	1.45	ND*	1.46
PMMA-8	71.6	17.3	2.4	5.3	ND*	3.4
OH-11	51.6	25.9	6.2	9.5	ND*	6.7
AM-10	74.0	15.5	1.03	5.5	ND*	3.7
A-11	38.0	34.0	2.0	15.9	ND*	9.7

\*ND: NOT DETECTED

The quantitative data were obtained by using the peak height to approximate the area under the curve in question. This approximation is valid for comparison between two samples of different coating thickness for each element as long as the peaks are similar in shape. This peak similarity was observed for the 0.5  $\mu\text{m}$  and 1.95  $\mu\text{m}$  coated polymers. A problem in this semi-quantitative procedure is that contamination is present as carbon and silicon as well as the carbon and silicon characteristic of specific polymers. This can especially be seen for SR-3 and SR-16 which shows that most of the surface composition is carbon, while ESCA data from an SR control shows silicon to be present as the major component. One can also compare this with the atomic composition of bulk bioglass which has no carbon in its structure yet shows carbon to be a major surface constituent from ESCA analysis. The presence of silicon contamination can be seen by analyzing the ESCA data from the control polymers which show silicon to be present in a range from 3-9 % in those polymers that contain no silicon in their chemical structure (see Table 3.3)

Information that can be obtained from this technique is the presence or absence of the bioglass components in the outer 50 A. Phosphorus is detected in only one 0.5  $\mu\text{m}$  coated polymer sample and at an atomic percentage much less than that detected in the 1.95  $\mu\text{m}$  coated polymers. The lack of silicon contamination in PMMA-9 (1.95  $\mu\text{m}$ ) is anomalous, possibly due to only one sample size, experimental error or

Table 3.3  
 ESCA Compositional Analyses of Polymer Control Samples  
 and Bulk Bioglass in Atomic %

Bulk Bioglasses						
Sample	Carbon	Oxygen	Silicon	Calcium	Sodium	Phosphorus
OI 52S4.6	75.5	13.3	6.6	3.5	0.15	0.90
UF 45S5	80.4	14.4	1.1	3.5	0.15	0.43
Polymer control samples						
Sample	Carbon	Oxygen	Silicon	Calcium	Sodium	Phosphorus
A	80.2	13.8	5.99	ND*	ND*	ND*
SR	29.8	7.2	63.0	ND*	ND*	ND*
OH	81.4	12.8	5.9	ND*	ND*	ND*
AM	78.9	12.8	5.9	ND*	ND*	ND*
PMMA	82.6	14.5	2.9	ND*	ND*	ND*

\*ND: NOT DETECTED



sample variability. IRRS data in Figure 3.6 show an S peak present for PMMA-9 indicating the presence of silicon. This is in direct conflict with ESCA data. This same discrepancy is seen between the IRRS spectrum for SR-3 in Figure 3.5 showing an NS peak (note: this peak could simply be a Si-O-Ca peak) suggesting the presence of Na while ESCA data (Table 3.2) show Na is not detected. The above anomalies could result from sampling depth effects. In general more Ca and P has been deposited for the 1.95  $\mu\text{m}$  coated polymers while the amount of Na deposited is about the same as for the 0.5  $\mu\text{m}$  coated polymers.

After 1000 hours of reaction the ESCA data of all the 1.2  $\mu\text{m}$  coated polymers showed no detectable Na (see Table 3.2). The silicon content of all polymers except SR show silicon to be present between 1 and 7%. SR was expected to be higher due to its chemical structure (see Table 3.3). In all cases of 1.2  $\mu\text{m}$  coated and reacted polymers except SR-15 Ca and P were present in a greater percentage than the corresponding Ca and P in each of the 1.95  $\mu\text{m}$  coated and unreacted polymers. This suggests a Ca-P rich film has formed since more Ca and P is detected after reaction than on corresponding samples with thicker coatings before reaction. These findings additionally support all the preliminary IRRS data and are consistent with previous work in the area of reacted bulk bioglass.<sup>23, 24, 25, 26</sup>

It was noted that in all of the reacted samples after 1000 hours of reaction the carbon peak at 284.6 eV showed

a different curve when compared with either the carbon peaks in 0.5  $\mu\text{m}$ , 1.95  $\mu\text{m}$  coated polymers or bulk bioglass peaks. The carbon peaks for coated polymers and bulk bioglass suggested the carbon to be in an oxidized state, possibly as a carboxylic acid, thus the presence of the peak at approximately 288.6 eV (see Figure 3.17).<sup>27, 28, 29, 30, 31</sup> This implies that the chemical state of carbon initially observed in all coated and unreacted polymer samples was oxidized as compared after reaction where carbon was unoxidized as suggested by absence of a peak at approximately 288.6 eV for samples A-11, OH-11, AM-10, PMMA-8 and SR-15 (see Table 3.4). Additional work would be required to identify the reasons for changes in surface chemical species resulting in a change in the carbon peak before and after reaction. One possibility is carbon contamination from the air.

#### Metal Reaction Sequence Data

In the preliminary series of 316L SS coated with either bulk OI 52S4.6 or UF 45S5 bioglass it was seen that spectra for approximately 0.5  $\mu\text{m}$  OI 52S4.6 bioglass coatings were inconsistent. In vitro reaction studies were done in the same manner as for the bioglass coated polymer samples. The metal substrates were discs 3.1 cm in diameter. The approximate surface area was calculated according to the equation  $SA = D(D/2 + H)$  previously used for polymers. The corresponding values for SA, V, D and H for each coated SS sample are seen in Table 3.5.

Table 3.4  
Relative Intensity of ESCA peaks  
for C (1s) (284.6 = 1.00)

	Peak Position (eV)		
	284.6	288 $\pm$ 1 <sup>a</sup>	290 $\pm$ 1 <sup>b</sup>
OI 52S4.6	1.00	0.09	ND*
A	1.00	0.19	ND*
A-3	1.00	0.13	ND*
A-12	1.00	0.15	ND*
A-11	1.00	ND*	ND*
A-10	1.00	ND*	ND*
OH	1.00	0.16	ND*
OH-3	1.00	0.13	ND*
OH-12	1.00	0.13	ND*
OH-11	1.00	ND*	ND*
OH-10	1.00	ND*	ND*
AM	1.00	0.13	ND*
AM-3	1.00	0.12	ND*
AM-11	1.00	0.14	ND*
AM-10	1.00	ND*	ND*
AM-9	1.00	ND*	ND*
PMMA	1.00	0.20	ND*
PMMA-3	1.00	0.13	ND*
PMMA-9	1.00	0.12	ND*
PMMA-8	1.00	ND*	ND*
PMMA-7	1.00	1.65	0.19
SR	1.00	ND*	ND*
SR-3	1.00	0.07	ND*
SR-16	1.00	0.07	ND*
SR-15	1.00	ND*	ND*
SR-14	1.00	0.14	ND*

\*ND: NOT DETECTED

a: OXIDIZED CARBON, PROBABLY CARBOXYLIC ACID OR ESTER

b: OXIDIZED CARBON, PROBABLY CARBONATE

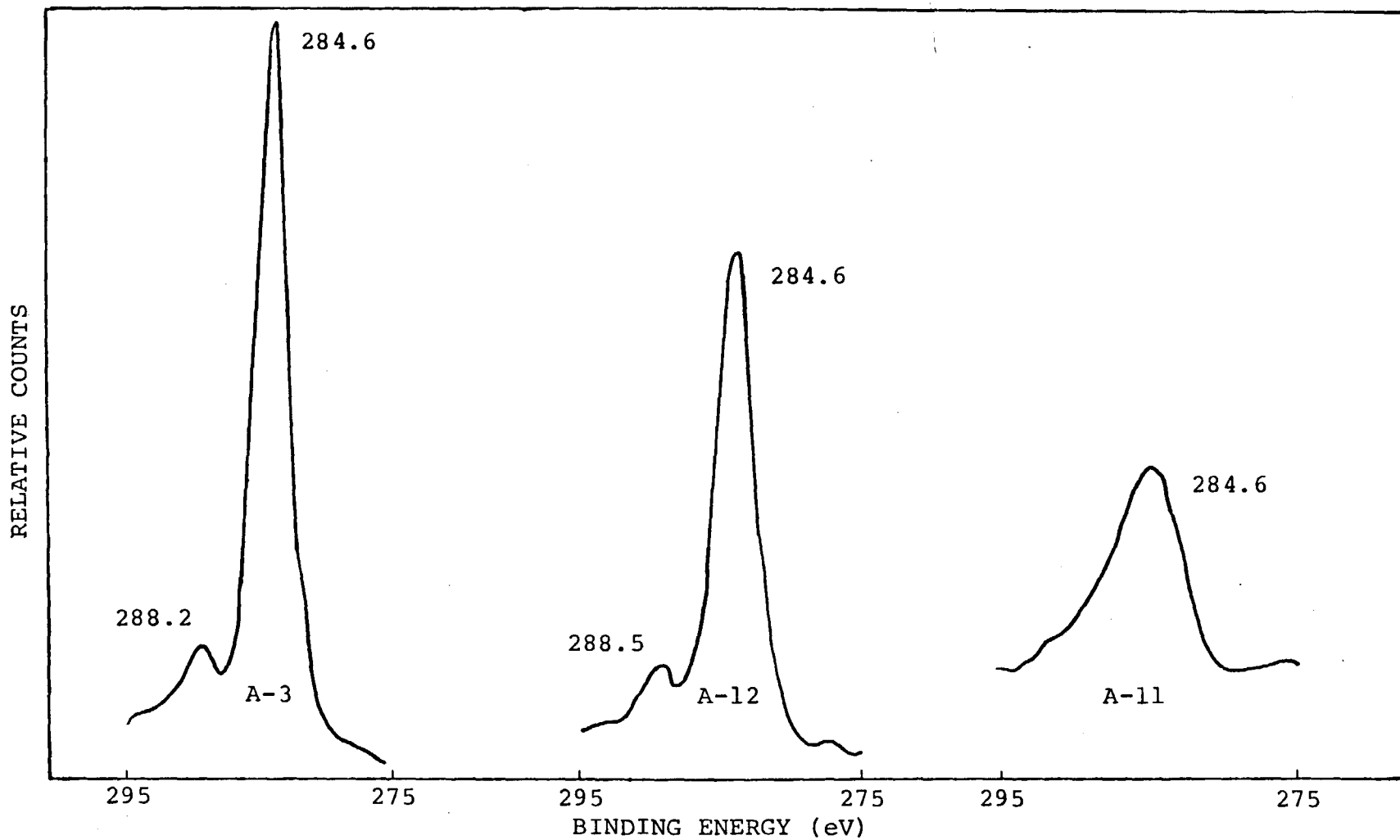


Figure 3.17 ESCA comparison of C(1s) peaks for reacted and unreacted A polymers coated with OI 52S4.6 bio-glass.

Figure 3.18 shows the inconsistency of two SS substrates coated with 0.5  $\mu\text{m}$  OI 52S4.6 bioglass (compare SS(a) and SS(b) in Figure 3.18). In addition it is observed that the 1.2  $\mu\text{m}$  UF 45S5 bioglass coated SS (designated SS(d) in Figure 3.18) does not show a spectrum like bulk bioglass.

The IRRS spectra for reacted SS(a) and SS(d) are shown in Figures 3.19 and 3.20 respectively. For comparison purposes the first spectrum in each graph is of the bulk bioglass deposited onto the SS substrate while the last spectrum is the control SS. After 10 hours of reaction SS(a) forms a sharp peak at  $1050\text{ cm}^{-1}$  similar to the control SS. There is also a broad peak formed between  $550\text{ cm}^{-1}$  and  $380\text{ cm}^{-1}$  that partially resembles the bulk OI 52S4.6 bioglass. After 100 hours of reaction the spectra seen partially resembles the SS control but is not equivalent to it.

At zero hours of reaction for SS(d) shown in Figure 3.20 there is a peak at  $670\text{ cm}^{-1}$  that is seen in the SS control spectrum. This peak disappears for the next 63 hours of reaction suggesting the surface composition and structure are changing. Nevertheless, the spectrum at 100 hours of reaction is equivalent to the control SS spectrum. It was interesting to note that a thicker coating, namely, 1.2  $\mu\text{m}$  bulk UF 45S5 bioglass seemed to be removed from the surface during the reaction or at a thickness less than 0.5  $\mu\text{m}$  while the SS(a) sample retained some masking from the 0.5  $\mu\text{m}$  bulk OI 52S4.6 bioglass coating placed on it after 100 hours of reaction.

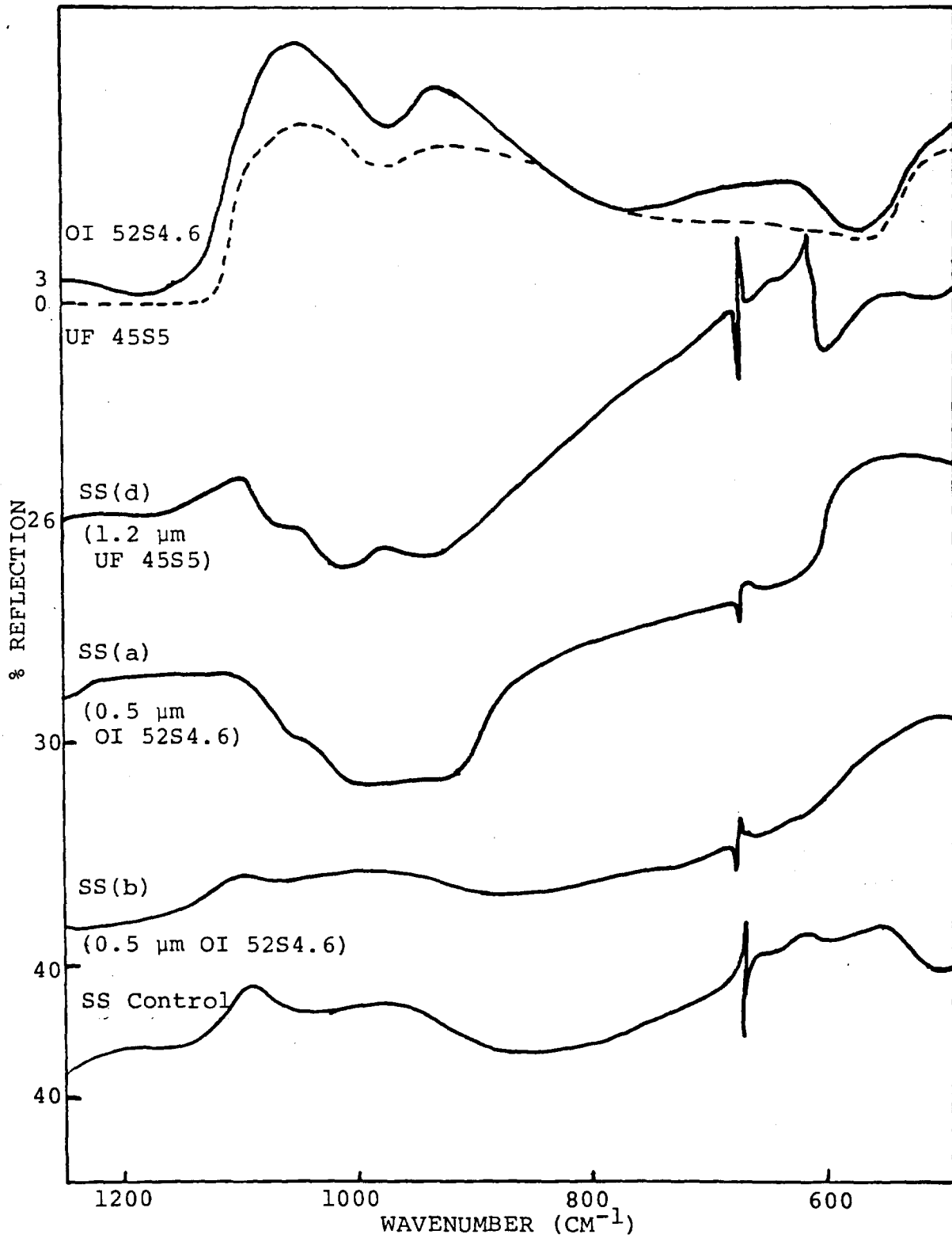


Figure 3.18 IRRS Spectrum: Bulk bio glasses vs. coated SS as a function of coating thickness.

Table 3.5  
Surface Area to Volume of Solution Ratios

Sample	D(cm)	H(cm)	SA(cm <sup>2</sup> )	V(cm <sup>3</sup> )
SS(a)	3.18	0.18	17.68	25.26
SS(d)	3.17	0.19	17.68	25.25

Figure 3.19 IRRS reaction sequence of SS(a) coated with 0.5  $\mu\text{m}$  OI 52S4.6 bioglass. Coated SS was reacted in deionized water at 37 °C according to reaction sequence 1 as outlined in Chapter 2.



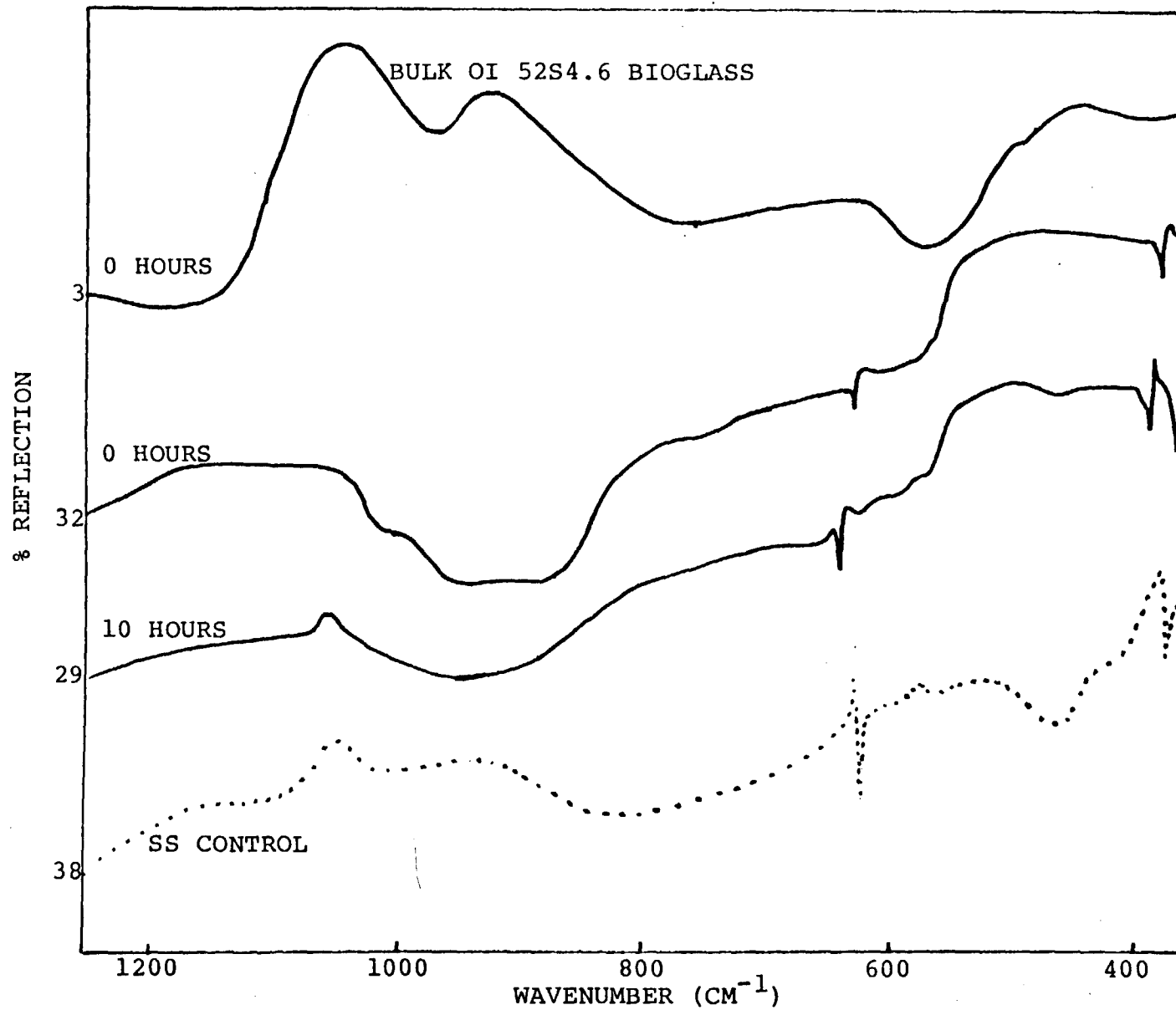


Figure 3.19 Continued

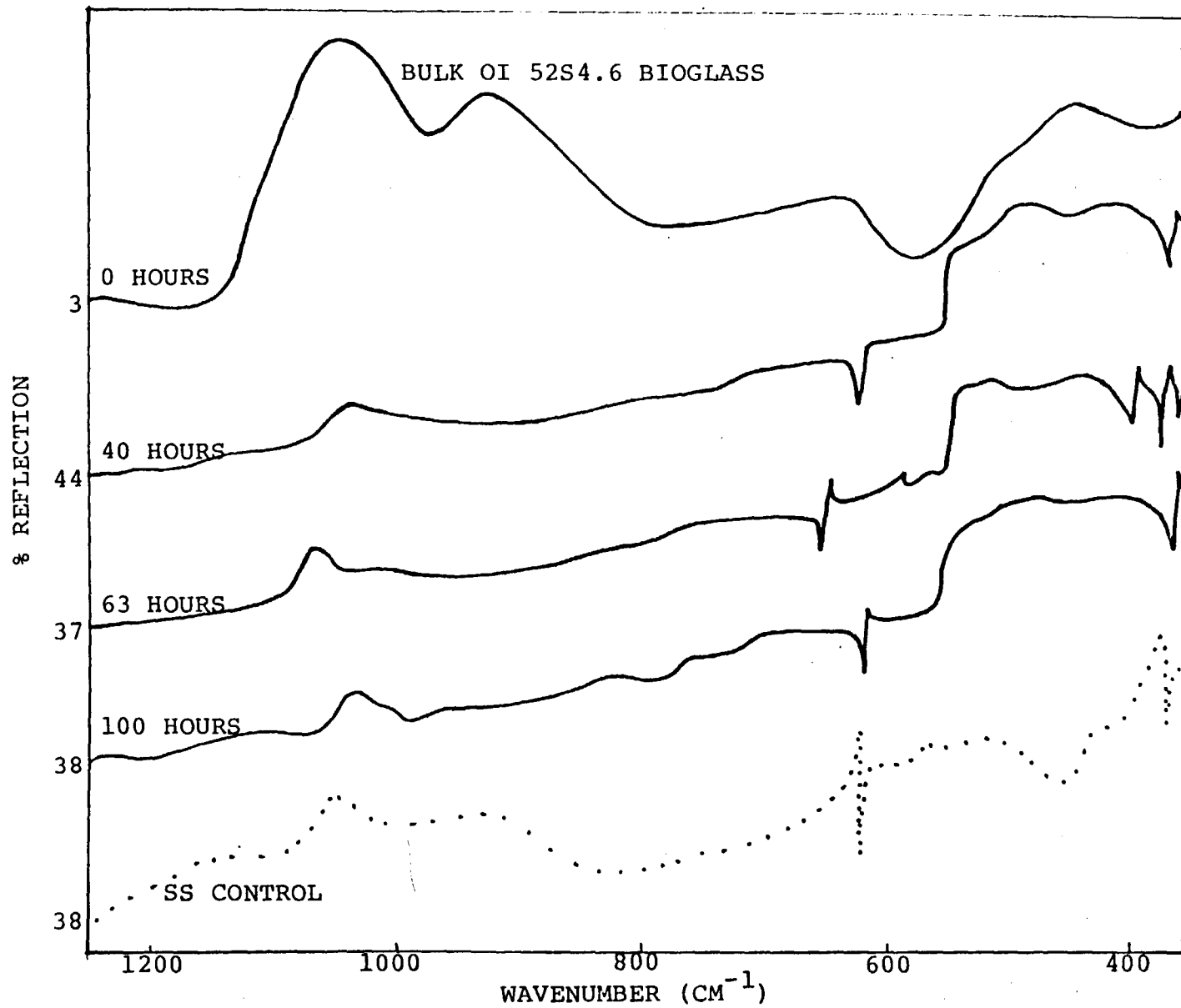


Figure 3.20 IRRS reaction sequence of SS(d) coated with 1.2  $\mu\text{m}$  OI 52S4.6 bioglass. Coated SS was reacted in deionized water at 37 °C according to reaction sequence 1 as outlined in Chapter 2.

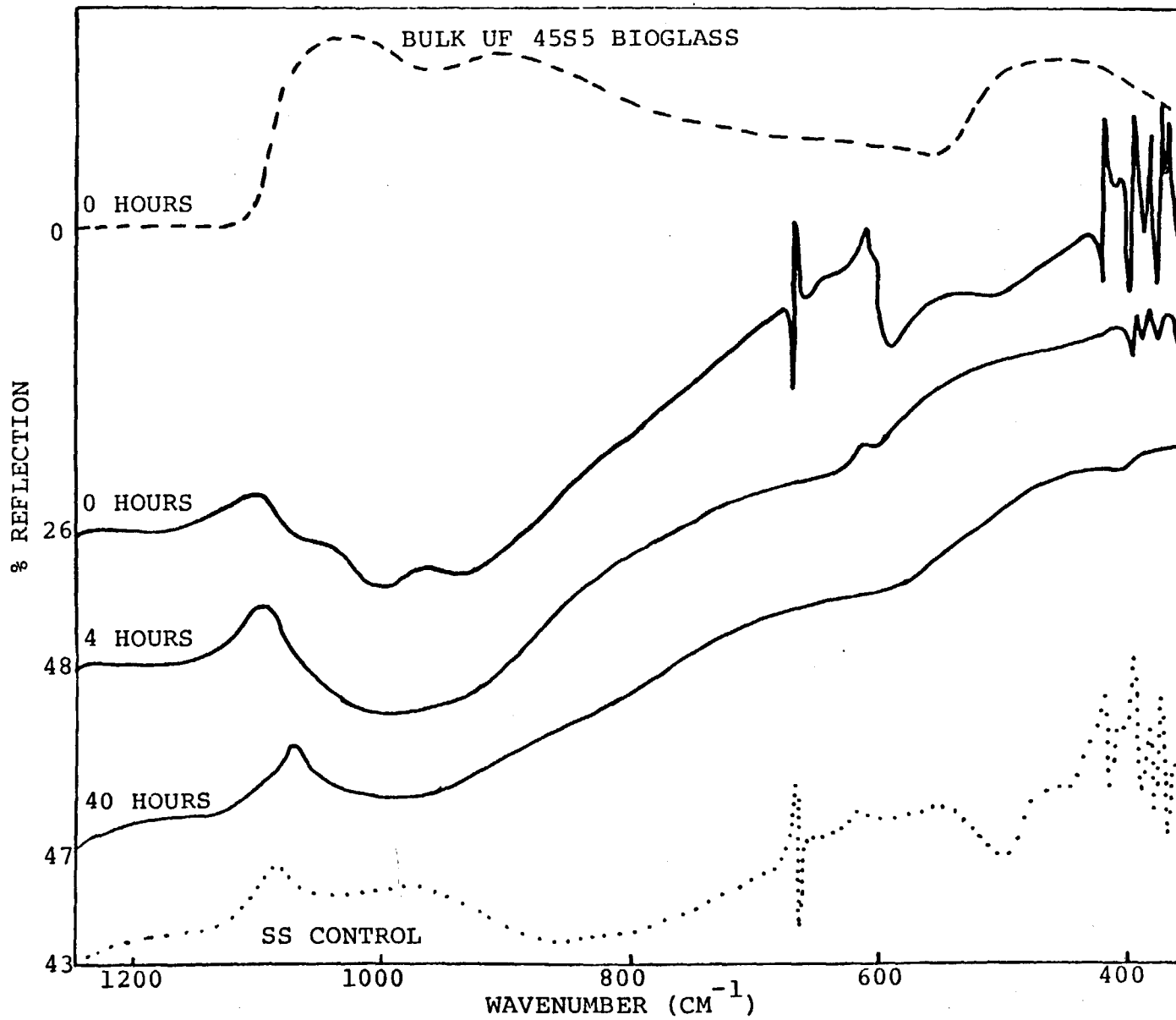
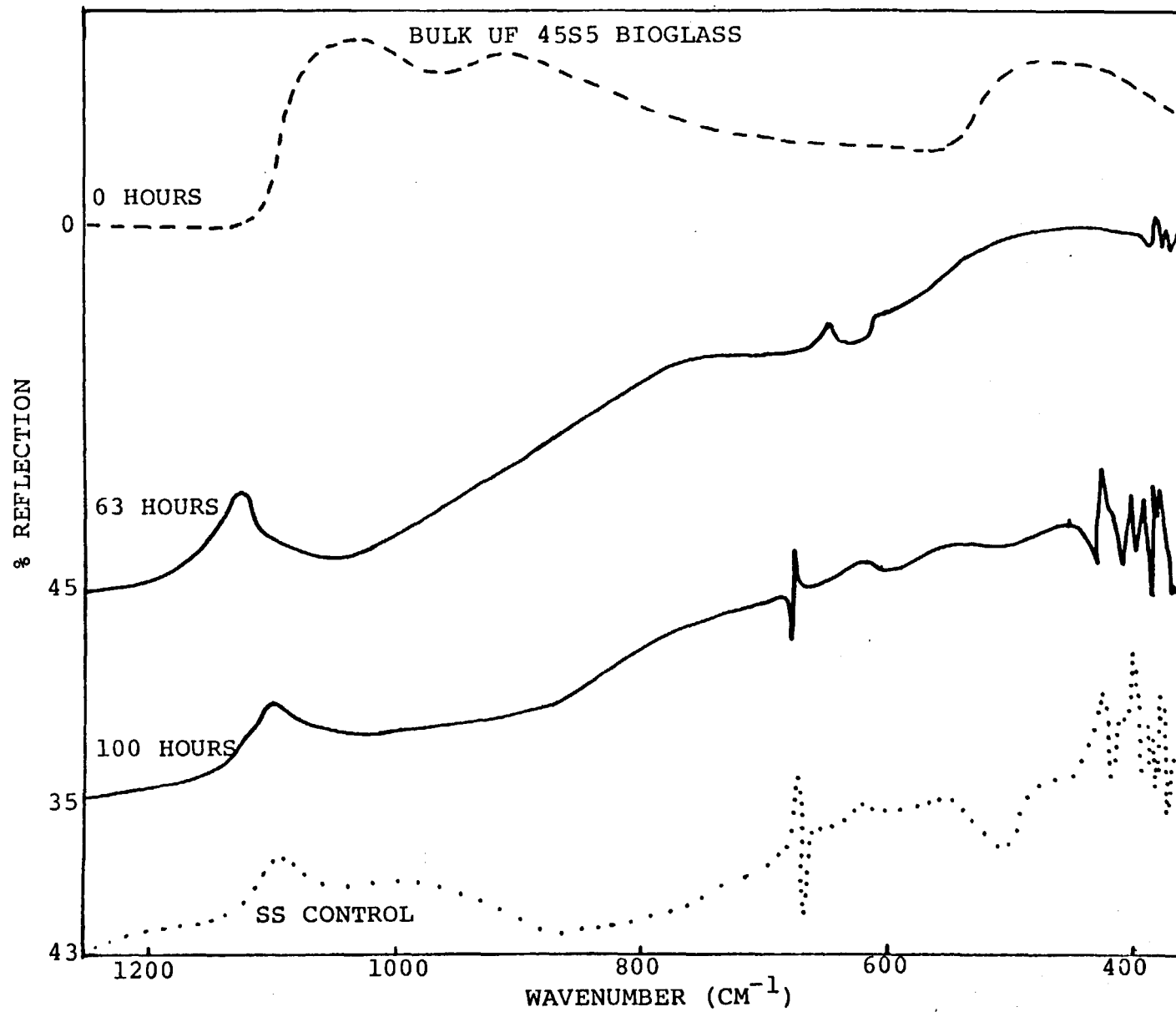


Figure 3.20 Continued



AES Data

AES ion milling was performed on SS(b) to determine the compositional profile from the outer surface of the coating to the interface of the coating and the bulk SS. The results of this analysis are shown in Figure 3.21. Peak heights were identified by comparing peaks with reference peaks.<sup>32</sup> All peak heights were measured and recorded for each element for plotting purposes. The time in minutes of ion milling is proportional to the depth of the surface being analyzed. As ion milling goes from the surface to the bulk SS the elements Si, Ca and O characteristic of the bioglass are seen. After 30 minutes of ion milling (approximately 900 Å) Fe is seen. Soon after Ca, O and Si decrease while Fe steadily increases suggesting the glass-metal interface and the beginning of the bulk SS. Thus, the 0.5 µm bioglass coated SS shows evidence of a good coating even though the IRRS spectral evidence was inconclusive.

Ceramic Reaction Sequence Data

As mentioned in Chapter 2 there were three shapes that were coated with either UF 45S5 or OI 52S4.6 bioglass:

1) thick discs; 2) square plates and 3) small square chips.

In vitro analysis was done as described in Chapter 2. The surface area was calculated according to the geometry of the sample, from which the volume of solution necessary for reaction was obtained ( $SA/V = 0.7 \text{ cm}^{-1}$ ).



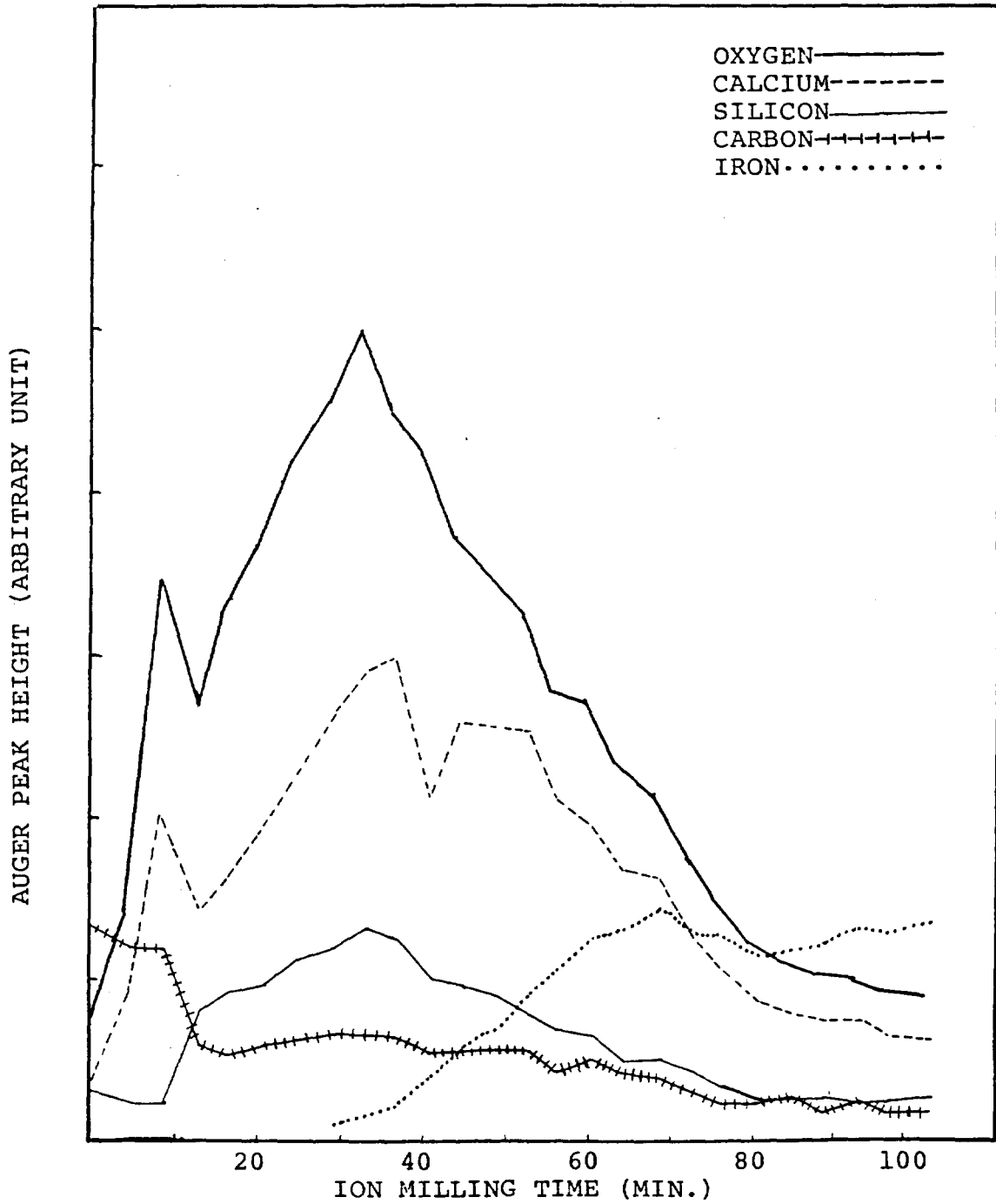


Figure 3.21 AES analysis of unreacted SS(b) coated with 0.5  $\mu\text{m}$  OI 52S4.6 Bioglass.

Figure 3.22 shows the comparison between a 1.2  $\mu\text{m}$  bulk UF 45S5 bioglass coated thick disc of alumina (A-1.2) and a 0.5  $\mu\text{m}$  bulk OI 52S4.6 bioglass coated thick disc alumina (A-0.5). In both cases there is evidence of a glass coating present. However, preliminary IRRS reaction data has shown that the thinly coated thick disc alumina substrates have lost their coatings after 10 and 40 hours of reaction. Figure 3.23 is an example of the reaction sequence data of a thinly coated thick disc alumina A-0.5. The zero hours IRRS spectrum shows the presence of an S peak and a decrease in the intensity of the alumina control spectrum. After one and four hours of reaction there is still evidence of a glass coating. Finally, it is seen that after 100 hours of reaction the spectrum is much like that of the alumina control. Thus, the in vitro reactions show that thin coatings on the order of 0.5  $\mu\text{m}$  are not stable. They either dissolve, come off the substrate, or are too thin to be detected.

#### In Vivo Analysis

Preliminary in vivo studies were done because of the encouraging data obtained from the in vitro studies on bioglass coated polymers. When a thin bioglass coating (on the order of 1.2  $\mu\text{m}$  thickness) was placed on the polymers, initial IRRS spectra showed the coatings to be present even after 1000 hours of reaction and in a form that showed signs of forming a Ca-P rich film (see Figures 3.10 to 3.14). Supporting this data was the ESCA data from coated polymers

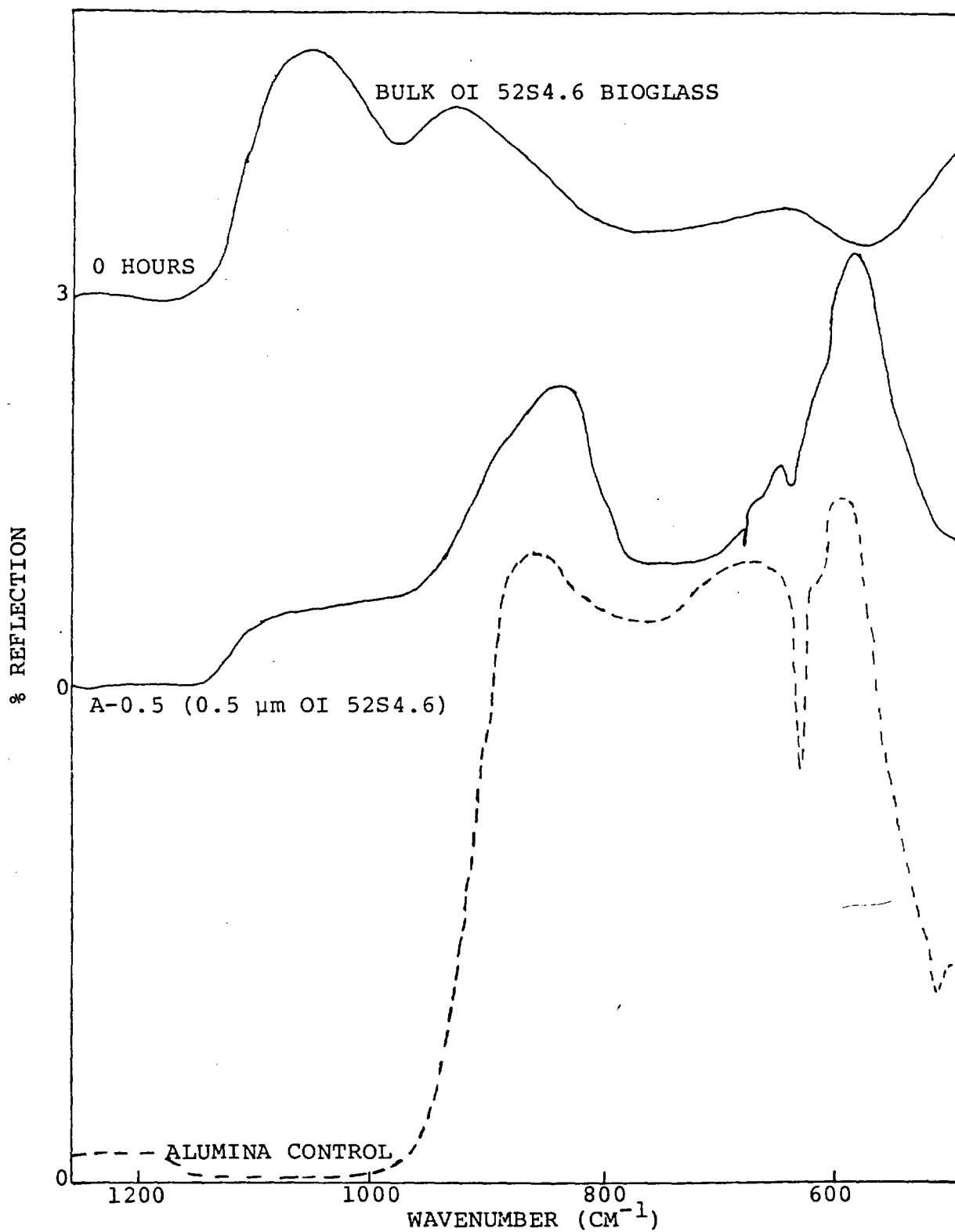


Figure 3.22 IRRS Spectrum: Bulk bioglasses OI 52S4.6 and UF 45S5 vs. coated aluminas A-0.5 and A-1.2 respectively as a function of coating thickness.

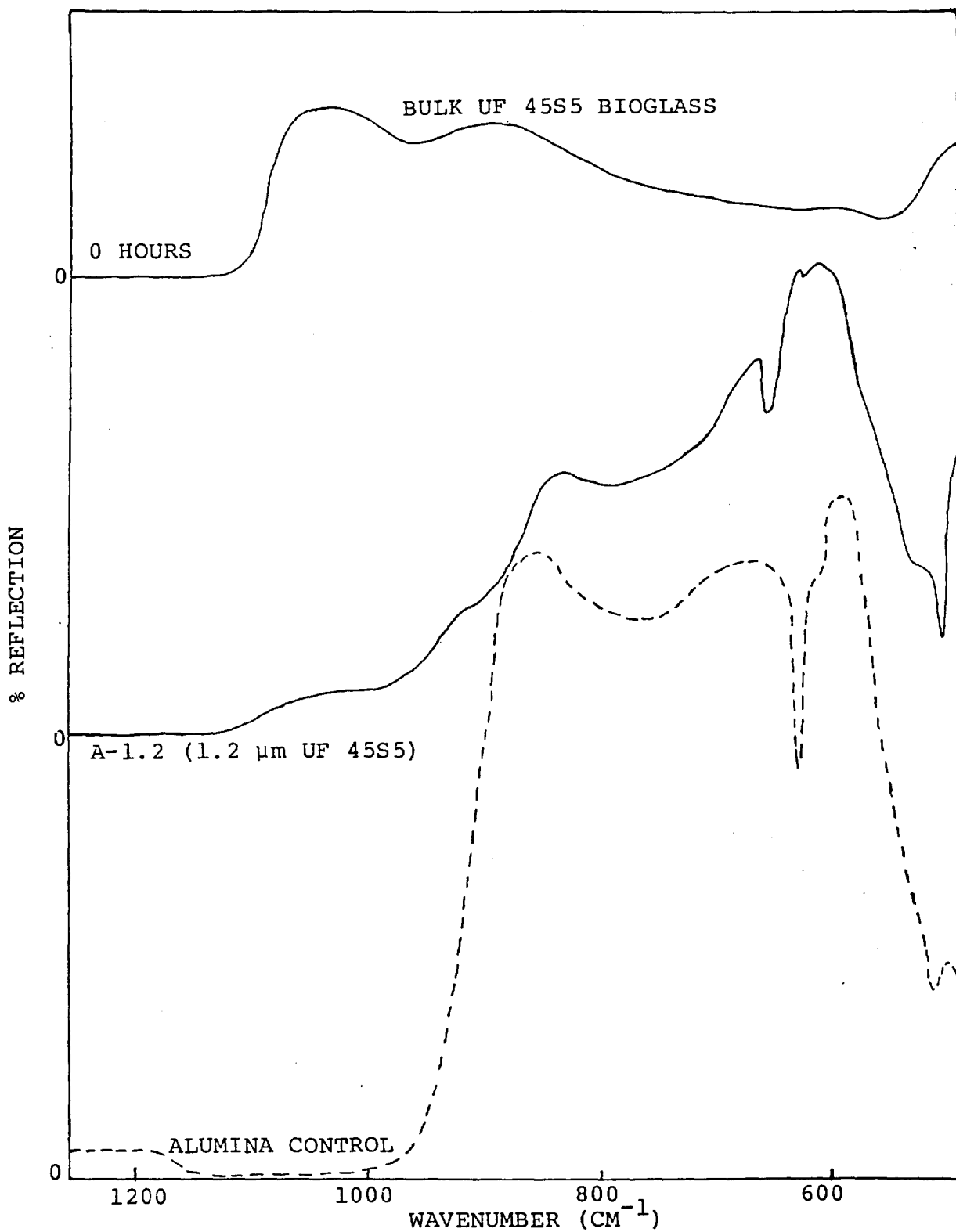


Figure 3.22 Continued.

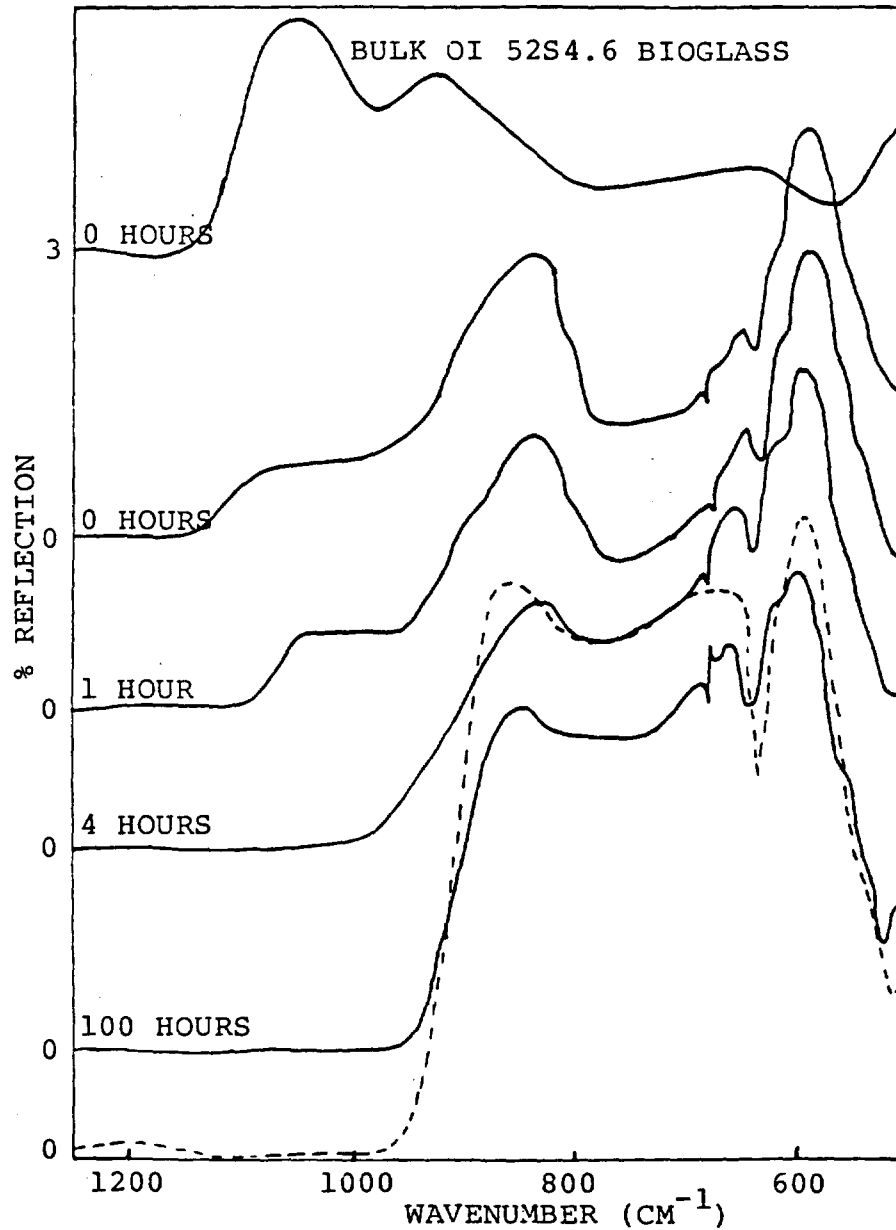


Figure 3.23 IRRS reaction sequence of A-0.5 coated with 0.5  $\mu\text{m}$  OI 52S4.6 bioglass. Coated alumina was reacted in deionized water at 37  $^{\circ}\text{C}$  according to reaction sequence 1 as outlined in Chapter 2.

after 1000 hours of reaction (Table 3.2). From this it was concluded that a Ca-P rich layer was present on the bioglass coated polymer after 1000 hours of reaction.

Encouraging results such as these justified the in vivo studies. Certain of the test polymers are known to be very reactive in vivo. Since bioglass produces little reaction in tissues, both hard and soft, it should be possible to determine if the coating was producing the desired effect, firstly by masking the reaction of the polymers and secondly by adhering to tissue.

It has been shown by previous workers that PMMA, SR (silicone rubber) and OH (10 HEMA/90 MMA) show very similar in vivo responses, that is, they are almost inert, non toxic and stable.<sup>33</sup> On the other hand the hydrophilic charged polymers showed the most response, a severe inflammatory response. The positively charged AM (20 DMAEMA/80 MMA) polymer was reactive and produced a cellular capsule rather less than the negatively charged polymer but still greater than those associated with the hydrophobic materials.

Sprague-Dawley rats were used for the subcutaneous implantation of coated polymers. The animals were anesthetized with sodium pentobarbital given intraperitoneally. The back was shaved and swabbed with alcoholic betadine solution (povidone iodine). An incision was made parallel to the spine on either side of the spine, approximately 2-3 cm long. A pocket was made in the subcutaneous tissue using blunt dissection. The implants were placed in the



Figure 3.24 Histological Section of bulk bioglass implanted subcutaneously into rat tissue for eight weeks. Original magnification is 100X.

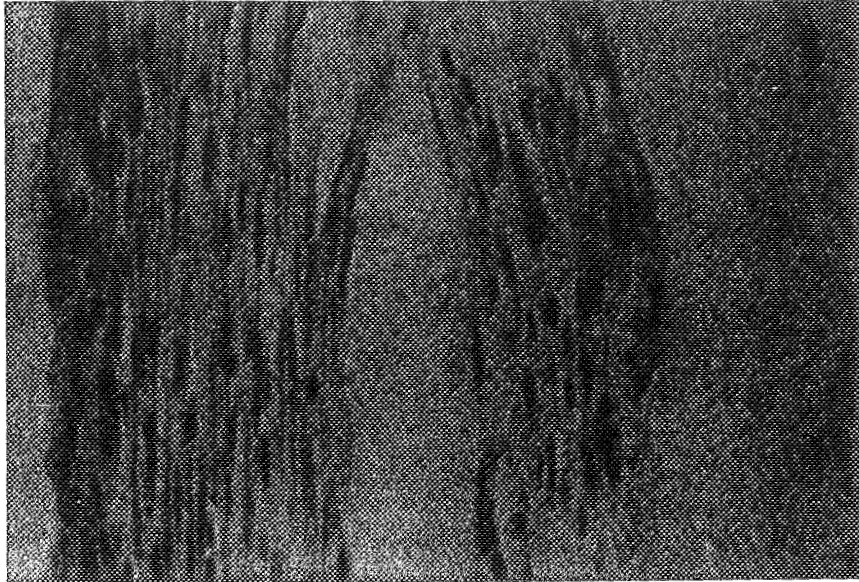


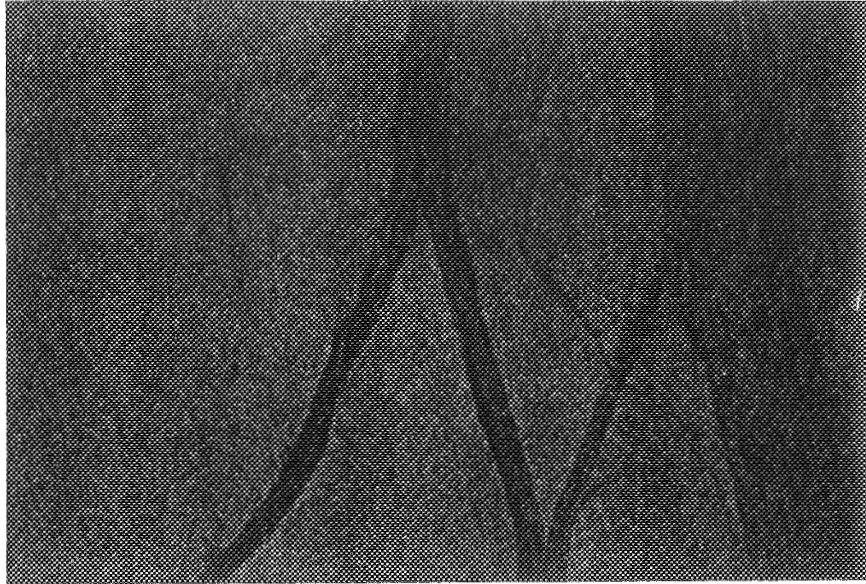
Figure 3.25 Histological Section of an active coated polymer A coated with  $0.5 \mu\text{m}$  OI 52S4.6 bioglass and implanted subcutaneously into rat tissue for eight weeks. Original magnification is 250X.

NOTICE TO READER:  
This material may be protected by  
copyright law (Title 17 U.S. Code)

ORIGINAL PAGE IS  
OF POOR QUALITY



A)



B)

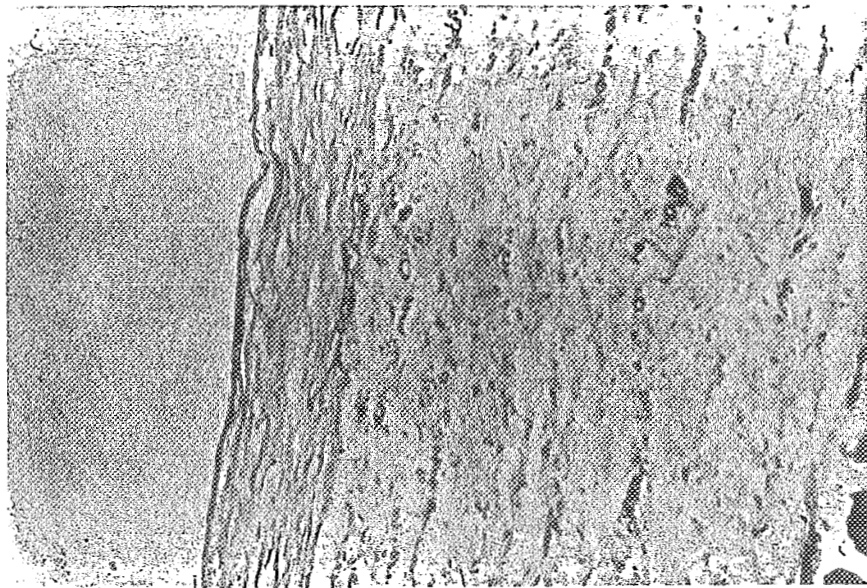


Figure 3.26 Histological Section Comparison of A) SR coated with  $0.5 \mu\text{m}$  OI 52S4.6 (original magnification is 100X) and B) SR uncoated (original magnification is 100X), both implanted subcutaneously into rat tissue for eight weeks.

pocket so formed, distant from the incision. The incision was closed with stitches using silk or other suitable sutures.

The implants were removed after one, four and eight week periods. The animals were killed with an overdose of ether. Implants were removed and prepared by standard techniques for histological study.

The histological sections were examined for tissue adherence and evidence of toxicity. These were compared with the histological sections of bulk bioglass implanted subcutaneously. Figure 3.24 shows a microscope section of tissue surrounding an implant of bioglass in place for eight weeks in the subcutaneous tissues. It is very difficult to retain the interface between a hard material such as this and the softer connective tissue when section are cut. Decalcification of the glass makes the process easier but there is no entirely satisfactory solution. The fragments of residual glass are seen attached to collagen fibers of the capsule and the fibers of the capsule have separated during sectioning, suggesting that the adhesive bond of glass to collagen is greater than the cohesive bond between collagen fibers in the capsule. The capsule formed is thin and acellular showing no signs of inflammation. The implant is to the left in the figure.

Histological sections from all implants removed were examined. It was found that most showed indication of the reactivity of the polymer present. There was some evidence

suggesting tissue adhesion of thinly coated ( $0.5 \mu\text{m}$  OI 52S4.6 bioglass) polymers. Figure 3.25 shows the in vivo histological section of a coated active polymer designated A (10 AA/90 MMA). The implant was on the left side of the figure. A thick capsule is observed which is cellular in nature. Inflammation can also be seen. The activity seen is due to the polymer and not the bioglass coating. A comparison of an uncoated silicone rubber subcutaneously implanted with a  $0.5 \mu\text{m}$  OI 52S4.6 bioglass coated silicone rubber after eight weeks reaction in vivo is seen in Figure 3.26. A thin fibrous capsule is present in Figure 3.26A as compared to Figures 3.25 and 3.26B. There are no signs of inflammation in Figure 3.26A. In addition there are areas of tearing which suggest that possible tissue adhesion has occurred.

By comparing the in vivo histology sections it is seen that the coatings on these polymers were not uniform. In some cases we see masking of the polymer and in others we see the activity of the control polymer surfacing.

CHAPTER 4  
SECOND REACTION SERIES OF BIOGLASS  
COATED POLYMERS AND COPOLYMERS

Introduction

Thus far it has been shown that thin bioglass coatings can be placed on polymeric, metallic and ceramic substrates. The preliminary studies have suggested that the coatings are patchy (nonuniform). Substrates coated with the same glass show a variety of IRRS spectra for approximately the same coating thickness ( $0.5 \mu\text{m}$ ) on the same substrate. However, the substrates coated with approximately  $1.2 \mu\text{m}$  bulk bioglass showed much improvement in their resemblance to bulk bioglass spectra. In addition, the in vitro data was encouraging enough to justify the in vivo studies which showed that some polymer coatings behaved similar to bulk bioglass. These encouraging results led to development of a second series of samples coated to a thickness of approximately  $4.0 \mu\text{m}$  with bulk OI 52S4.6 bioglass.

In this chapter, the in vitro and in vivo data for  $4.0 \mu\text{m}$  coated polymer substrates are reported. These data will be used to determine if increased sputtering time and the resulting thicker coatings will produce a bioglass coated polymer with surface reactivity equivalent to bulk bioglass. By comparing data from  $4.0 \mu\text{m}$  coated and reacted

polymers with that from 1.2  $\mu\text{m}$  coated and reacted polymers (Chapter 3) the observed improvement in thicker coated polymer substrates is seen.

#### In Vitro Analysis of Bioglass Coated Polymers

Polymers were coated and reacted by the same procedures as described in Chapter 2. We expected that by increasing the coating thickness from 1.2  $\mu\text{m}$  to 4.0  $\mu\text{m}$  we would increase the detectable bioglass composition gradient from the polymer substrate to the surface of the coating.

With this in mind it is of interest to analyze the in vitro data of coated polymers from this second series. The in vitro solution method was used in the same manner as described in Chapter 2. The values for SA, V, D and H are shown in Table 4.1. The first polymer to be discussed is SR-14 coated with approximately 4.0  $\mu\text{m}$  OI 52S4.6. Shown in Figure 4.1 is the IRRS reaction sequence. For comparison purposes the first spectrum in Figures 4.1 to 4.5 are from bulk OI 52S4.6, while the last spectrum in each figure is from the control polymer. Once again the dashed spectrum is from fused silica. The initial spectrum from zero hours shows characteristic S and NS stretching peaks. There is a slight shift and increase in the S peak after one hour of reaction. The decrease in the spectrum after four hours of reaction is the result of surface roughening. After 63 hours of reaction there is an enhancement of the S peak and formation of a peak at about  $500\text{ cm}^{-1}$ . The spectrum at

Table 4.1  
Surface Area to Volume of Solution Ratios

Sample	D(cm)	H(cm)	SA(cm <sup>2</sup> )	V(cm <sup>3</sup> )
S-14	1.01	0.05	1.76	2.51
PMMA-7	0.98	0.03	1.60	2.29
AM-9	0.99	0.04	1.66	2.37
A-10	0.99	0.04	1.59	2.28
OH-10	0.98	0.04	1.63	2.33

Figure 4.1 IRRS spectra from reaction sequence for SR-14 (4.0  $\mu\text{m}$  coating of OI 52S4.6 bioglass). SR-14 was reacted in deionized water at 37 °C according to reaction sequence 2 as outlined in Chapter 2.

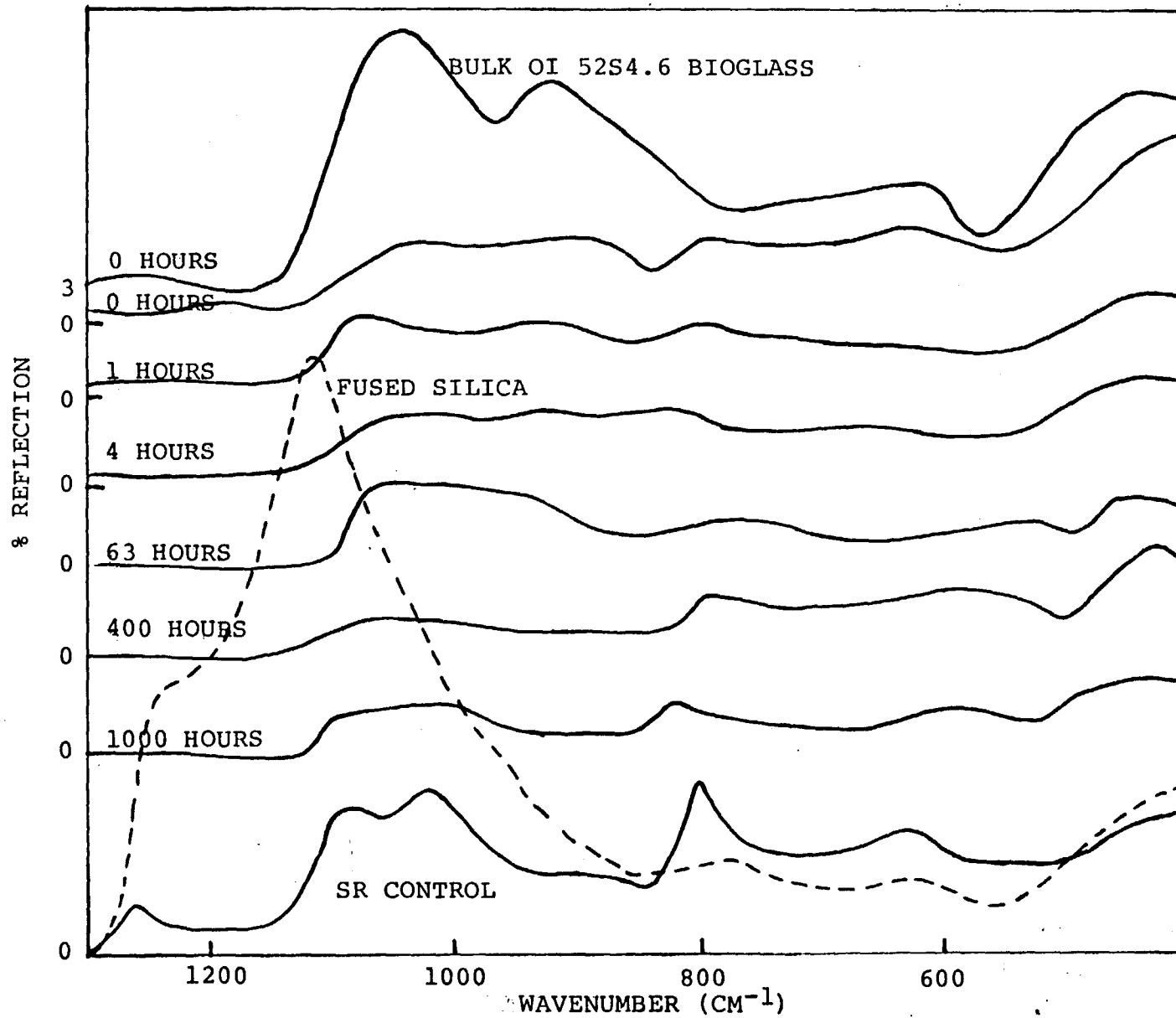




Figure 4.2 IRRS spectra from reaction sequence for PMMA-7 (4.0  $\mu\text{m}$  coating OI 52S4.6 bioglass). PMMA-7 was reacted in deionized water at 37 °C according to reaction sequence 2 as outlined in Chapter 2.

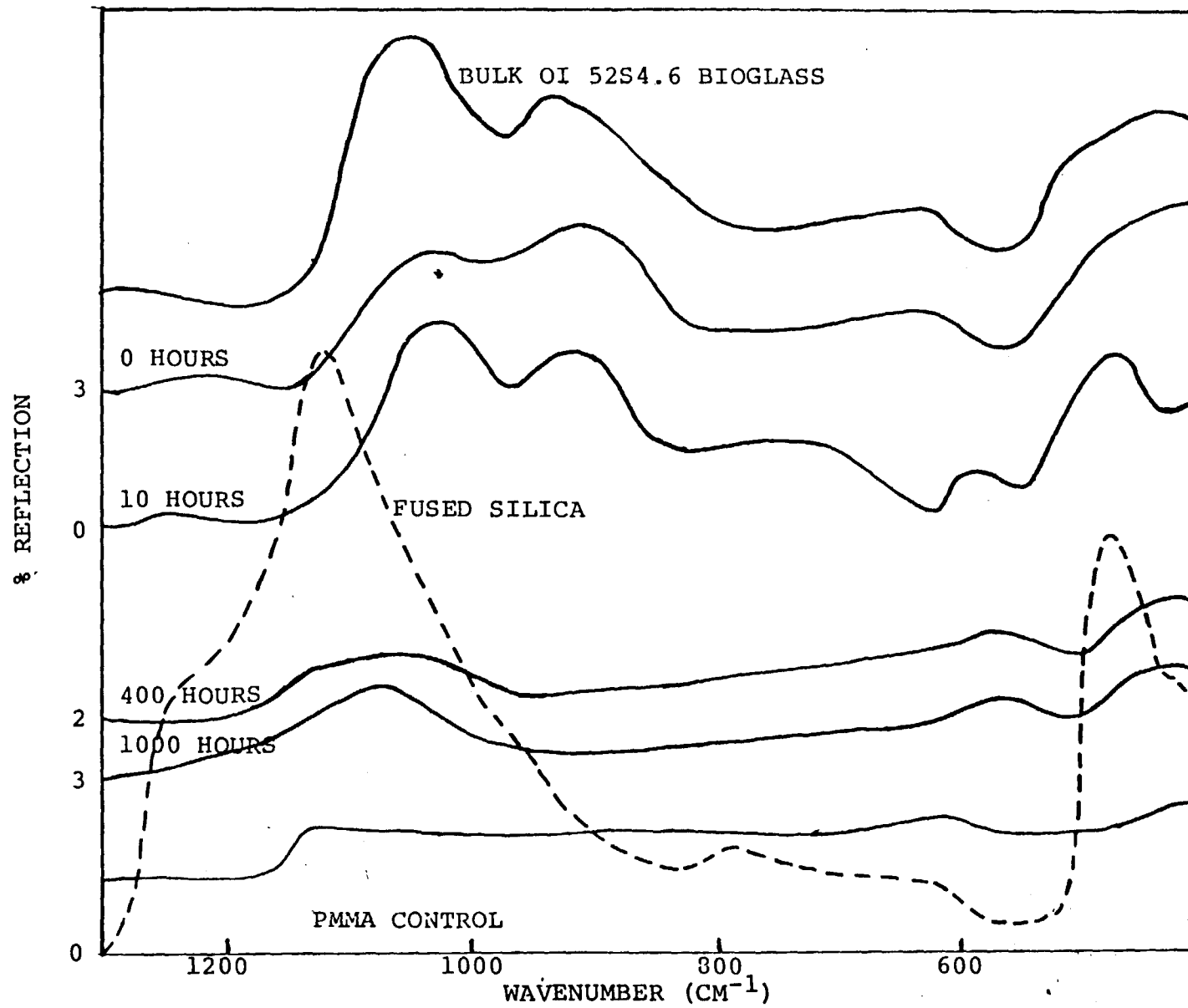


Figure 4.3 IRRS spectra from reaction sequence AM-9 (4.0  $\mu\text{m}$  coating OI 52S4.6 bioglass). AM-9 was reacted in deionized water at 37  $^{\circ}\text{C}$  according to reaction sequence 2 as outlined in Chapter 2.

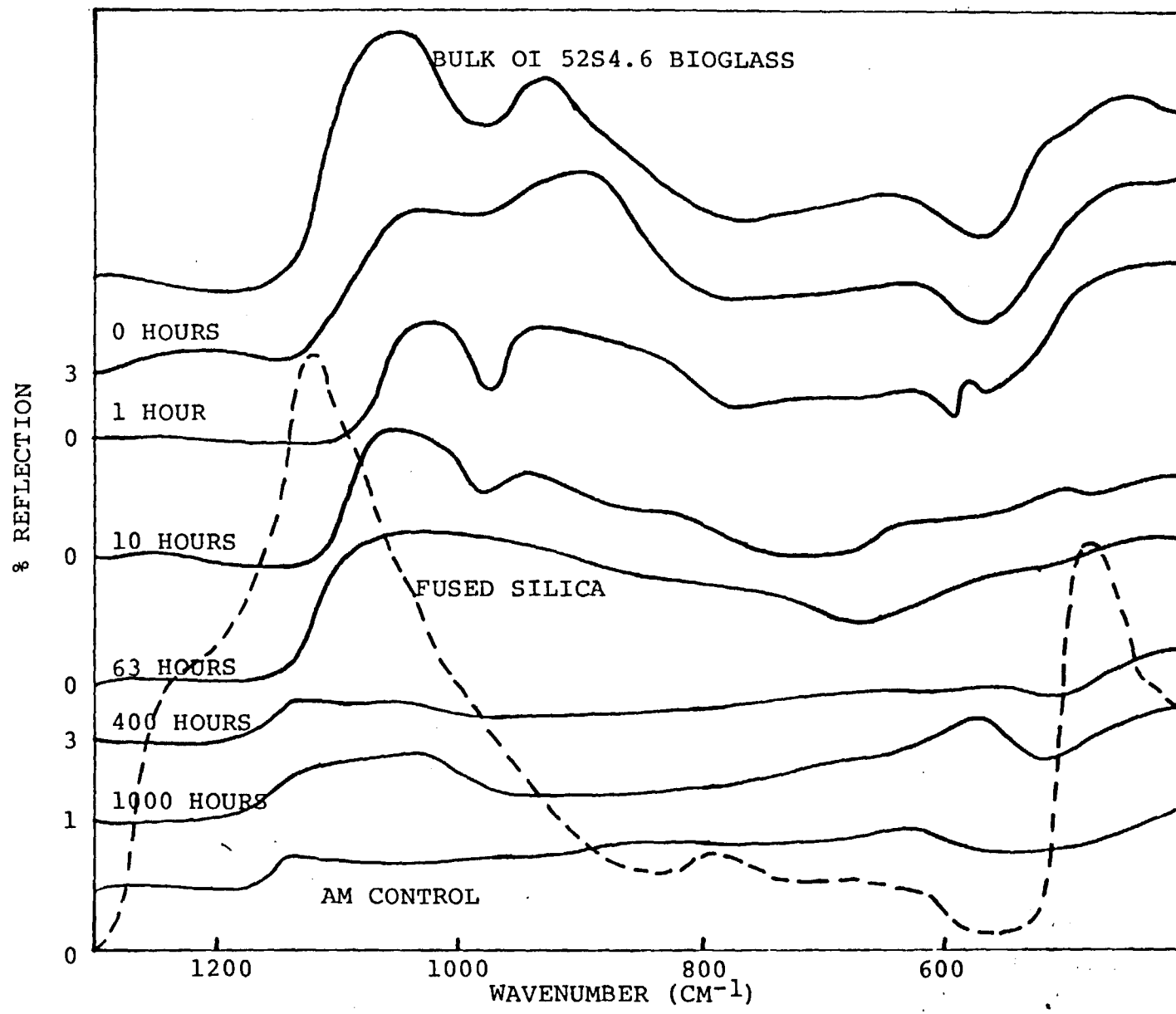


Figure 4.4 IRRS spectra from reaction sequence A-10 (4.0  $\mu\text{m}$  coating OI 52S4.6 bioglass). A-10 was reacted in deionized water at 37 °C according to reaction sequence 2 as outlined in Chapter 2.

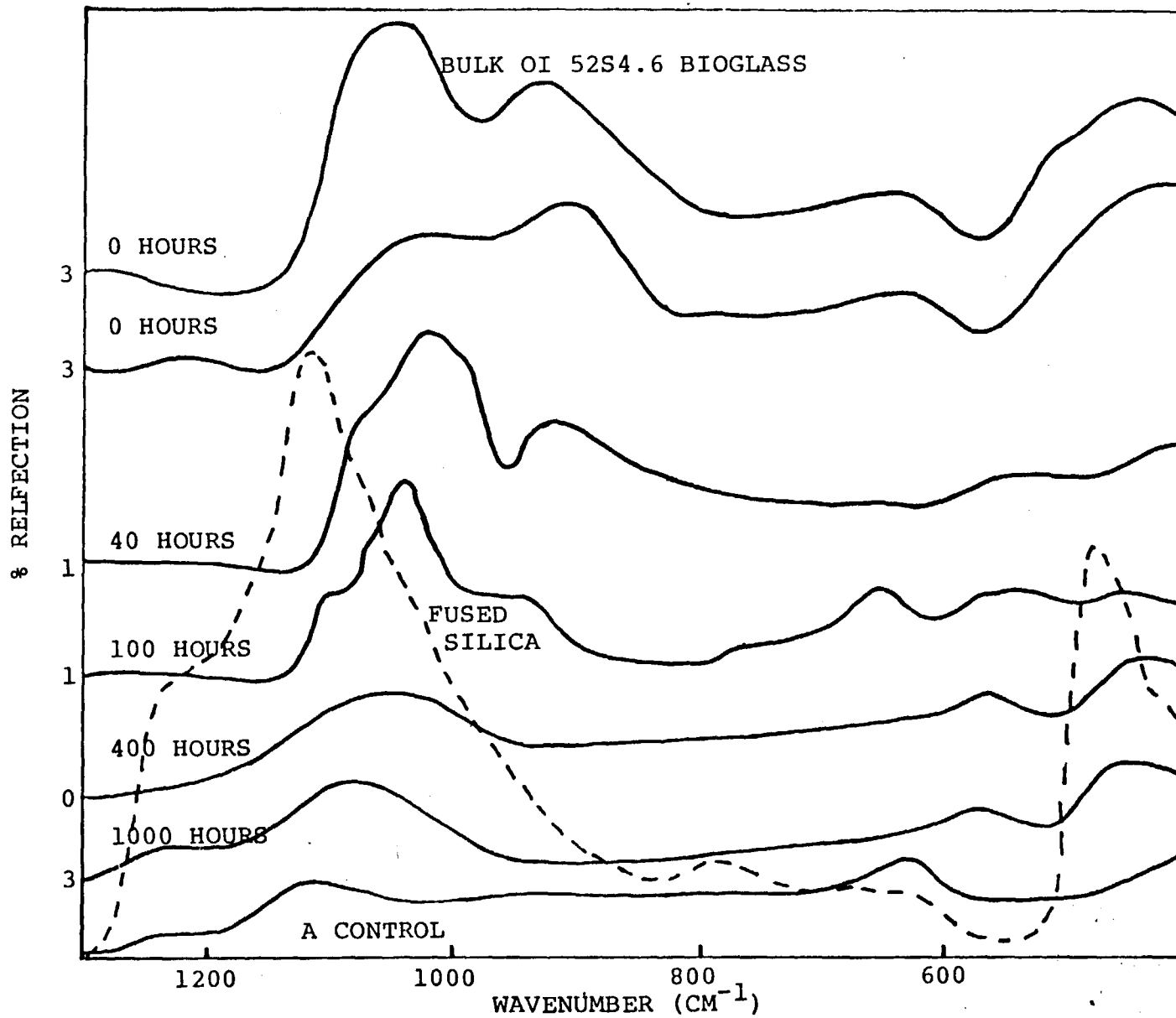
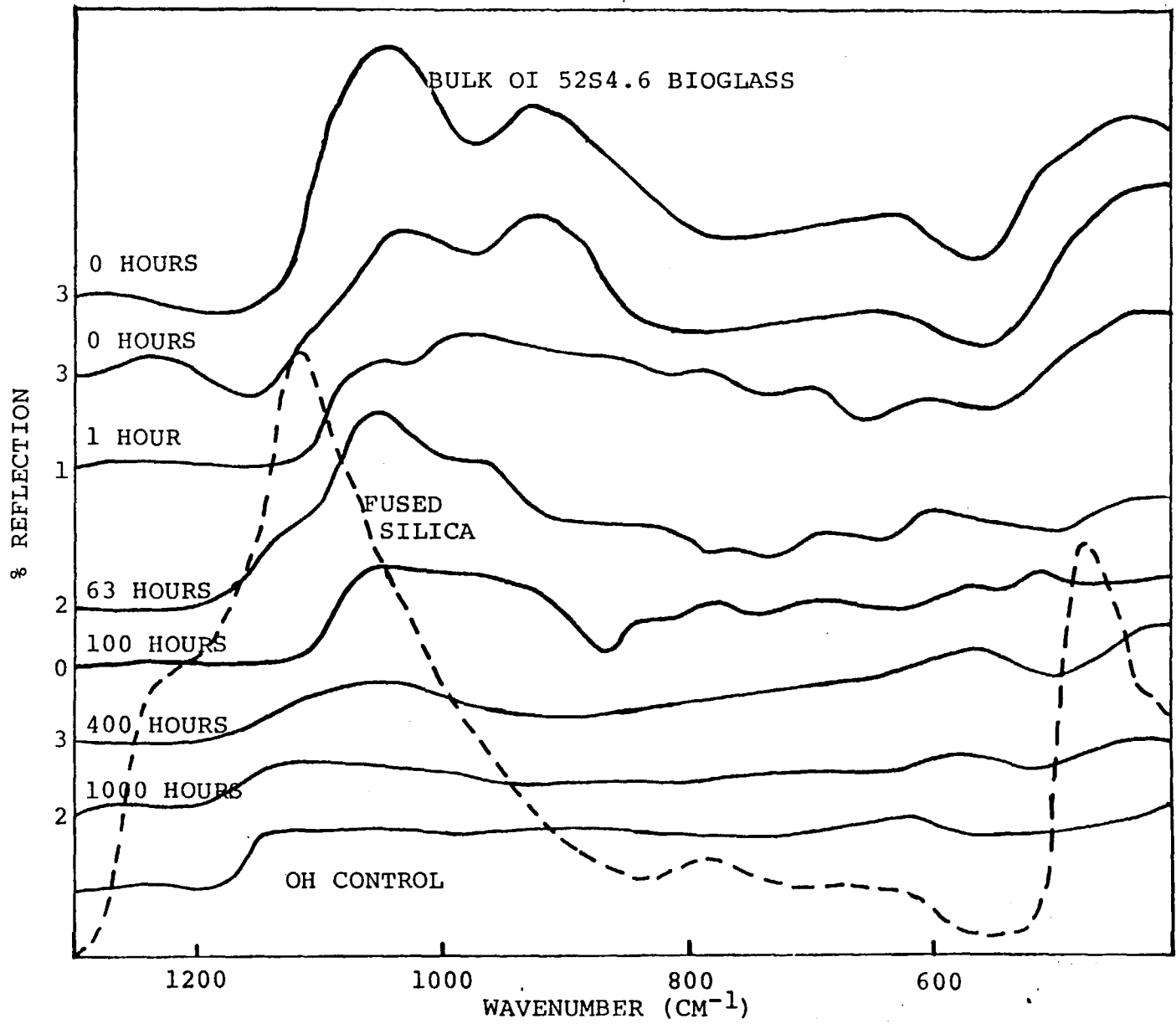


Figure 4.5 IRRS spectra from reaction sequence OH-10 (4.0  $\mu\text{m}$  coating OI 52S4.6 bioglass). OH-10 was reacted in deionized water at 37 °C according to reaction sequence 2 as outlined in Chapter 2.





1000 hours of reaction is masking the control spectrum through two peaks, the first being the S peak and the second being a peak at  $590\text{ cm}^{-1}$ . The combination of these peaks suggests that a Ca-P rich film is forming. This reaction series can be compared with Figure 3.10 which, after 1000 hours of reaction, showed a spectrum very similar to that of the silicone rubber (SR) control. Thus, the thicker coating on SR is stable and produces a Ca-P rich film during 1000 hours of reaction whereas the thinner coating did not (Figure 3.10).

Figure 4.2 shows the IRRS spectra of PMMA-7 which has a  $4.0\text{ }\mu\text{m}$  coating of bulk OI 52S4.6 bioglass and was reacted for up to 1000 hours. The initial spectrum at zero hours of reaction is similar to that of a ternary silicate glass of composition 30-10-60 (see Figure 2.3c). Comparison with the zero hours spectrum of PMMA-8 ( $1.2\text{ }\mu\text{m}$  coating, Figure 3.11) shows this to be of a composition closer to 20-20-60 (see Figure 2.3b). This implies that the longer sputtering time has deposited a higher ratio of  $\text{Na}_2\text{O}$  to  $\text{CaO}$  in the coating. After 10 hours of reaction the spectrum more closely resembles the bulk OI 52S4.6 bioglass than in the initial spectrum at zero hours. This indicates the excess  $\text{Na}_2\text{O}$  is depleted quickly from the coating. Also observed at 10 hours is the formation of a peak at  $585\text{ cm}^{-1}$  which is similar to the peak in the spectrum of hydroxyapatite shown in Figure 3.3. This peak is seen throughout the reaction sequence with a shift to  $570\text{ cm}^{-1}$  at 1000 hours of reaction.

Finally, 1000 hours of reaction shows enhancement of the S stretching peak. Sample PMMA-7 shows more of an increase in the masking of the PMMA substrate than did sample PMMA-8 shown in Figure 3.11. This also indicates that the 4.0  $\mu\text{m}$  coating is much more effective than the thinner 1.2  $\mu\text{m}$  coating.

The hydrophilic copolymers; AM-9 (positively charged), A-10 (negatively charged) and OH-10 (neutral) were each coated with 4.0  $\mu\text{m}$  bulk OI 52S4.6 bioglass and reacted for up to 1000 hours. These are discussed next and compared with preliminary data from Chapter 3. It can be generalized that all three copolymers show an initial spectrum at zero hours that is similar to that of PMMA-7 (see Figure 4.2, 4.0  $\mu\text{m}$  coating). That is, a composition slightly richer in  $\text{Na}_2\text{O}$  as compared to  $\text{CaO}$ . At 10 hours of reaction (Figure 4.2) a slight loss in the NS stretching peak is observed, with a complete loss occurring after 400 hours of reaction. Finally, 1000 hours of reaction shows the formation of a peak at  $575\text{ cm}^{-1}$  similar to that of Figure 3.3, suggesting formation of a Ca-P rich film. In comparing AM-9 (Figure 4.3) with AM-10 shown in Figure 3.12 the thicker coating results in the appearance of a sharper peak in the region of  $575\text{ cm}^{-1}$  and is probably due to the formation of a thicker layer of hydroxyapatite.

Figure 4.4 is the IRRS spectra from the reaction series for A-10. After 40 hours of reaction there is a decrease in the NS stretching peak and an increase in the S stretching

peak. Loss of the NS peak is observed after 400 hours of reaction with the formation of a peak at  $565\text{ cm}^{-1}$ . Both the 400 hour and 1000 hour spectra suggest the formation of a Ca-P rich film. Once again, comparing A-10 with A-11 (see Figure 3.13) there is a peak at  $570\text{ cm}^{-1}$  that is sharper in peak width as well as higher in intensity than its counterpart in Figure 3.13.

The third and last copolymer is OH-10, its IRRS spectra reaction sequence is seen in Figure 4.5. After 63 hours of reaction we see depletion in the Na ion content as evidenced by a decrease in NS stretching peak. By 100 hours there is a loss in the S peak but no simultaneous loss in the NS stretching peak. A peak formed at  $560\text{ cm}^{-1}$  which increased at 400 hours but then decreased after 1000 hours of reaction. Loss of the NS peak is observed at 400 hours while at 1000 hours the peak formed is similar to that of the OH control spectrum. The peak at  $565\text{ cm}^{-1}$  suggests that masking is still occurring even after 1000 hours. However, comparison with OH-11 ( $1.2\text{ }\mu\text{m}$  coating), Figure 3.14, the OH-10 spectrum is not as representative of a Ca-P rich film after 1000 hours of reaction as is the thinner coating.

It is concluded that the in vitro reactions of the above coated polymers ( $4.0\text{ }\mu\text{m}$  OI 52S4.6) is due to an ion exchange mechanism similar to bulk bioglasses. This conclusion is based on the IRRS spectra compared with bulk bioglass and the pH data shown in Table 4.2. The high pH values in the 10 to 100 hours time period are probably due

Table 4.2  
pH Data for Reaction Analysis of 4.0  $\mu\text{m}$  coated Polymers

Sample	----- Reaction time (hrs) -----								
	0	1	4	10	40	63	100	400	1000
S-14	5.7	6.5	7.2	7.6	9.5	8.8	8.9	6.7	7.6
PMMA-7	5.7	7.2	7.6	8.4	8.9	8.9	8.9	7.4	7.2
AM-9	5.7	7.0	7.2	8.6	9.2	9.2	9.2	8.4	7.8
A-10	5.7	7.0	7.0	8.4	9.2	9.2	9.2	7.8	7.6
OH-10	5.7	7.2	7.6	7.8	8.9	8.9	8.9	8.9	7.6
OI									
52S4.6	5.7	7.0	7.6	8.4	8.6	9.0	9.2	9.5	9.5

to preferential loss of Na ions from the surface of the bioglass coating, as noted above in the IRRS results. At longer times, formation of the hydroxyapatite film on the glass results in a solution buffering reaction.

#### ESCA Analysis

Coated polymer samples reacted for 1000 hours in de-ionized water at 37 °C were analyzed with ESCA. Data from these polymers will be compared with that from coated polymers as reported in Chapter 3. Specifically, the semi-quantitative data shown in Table 3.2 will be compared with the data in Table 4.3. The semi-quantitative data obtained was calculated using the same procedure as in Chapter 3.<sup>22</sup>

Peak shapes for C (1s), O (1s), Si (2p), Ca (2p), Na (1s) and P (2p) in ESCA studies were found to be qualitatively similar between coated and reacted polymers of 1.2  $\mu\text{m}$  and 4.0  $\mu\text{m}$  thicknesses. There were two peaks observed, one at 284.6 and another at  $288.0 \pm 1$  eV. The first is for an unoxidized carbon while the second is for an oxidized carbon, possibly a carboxylic acid or ester. A carboxylic acid is present in the MMA portion of all polymers except SR (see Table 3.4, Figure 4.6 and 4.7 for peak comparisons).

After 1000 hours of reaction A-10, OH-10 and AM-9 showed a peak for C (1s) at 284.6 eV with no detection of a peak at 288.6 eV. Thus, these coated and reacted polymers do not show carbon to be in an equivalent state as bulk

Table 4.3  
ESCA compositional Analysis of coated polymer substrates in  
atomic % for reacted coated polymer samples (4.0  $\mu\text{m}$  OI 52S4.6).

Sample	<u>Carbon</u>	<u>Oxygen</u>	<u>Silicon</u>	<u>Calcium</u>	<u>Sodium</u>	<u>Phosphorus</u>
S <sup>R</sup> -14	51.9	18.2	23.8	3.7	ND*	2.4
PMMA-7	27.7	30.5	31.0	5.9	ND*	4.8
OH-10	47.5	25.2	18.2	5.4	ND*	3.7
AM-9	58.1	24.8	4.7	7.3	ND*	5.0
A-10	29.8	29.4	26.1	8.8	ND*	5.9

\*ND: NOT DETECTED

Figure 4.6 Comparison of ESCA C (1s) peaks for SR and A polymers without a bioglass coating, and bulk OI 52S4.6 bioglass with reacted and coated polymers SR-14 and A-10. Data for SR-14 and A-10 are shown after 1000 hours of reaction in deionized water at 37 °C according to reaction sequence 2 as outlined in Chapter 2. Unoxidized carbon peak is at 284.6 eV with oxidized peaks labelled in the figure.

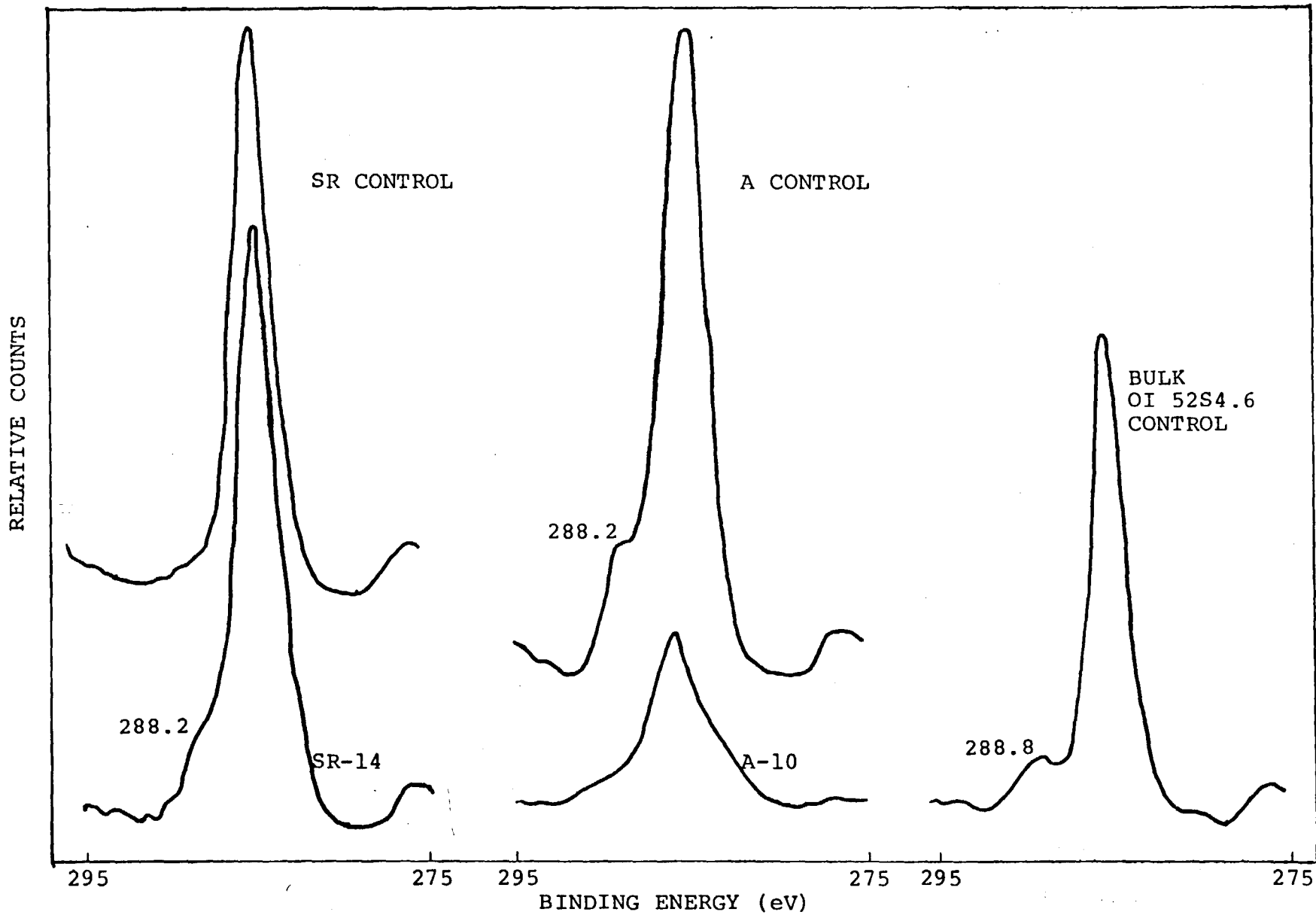
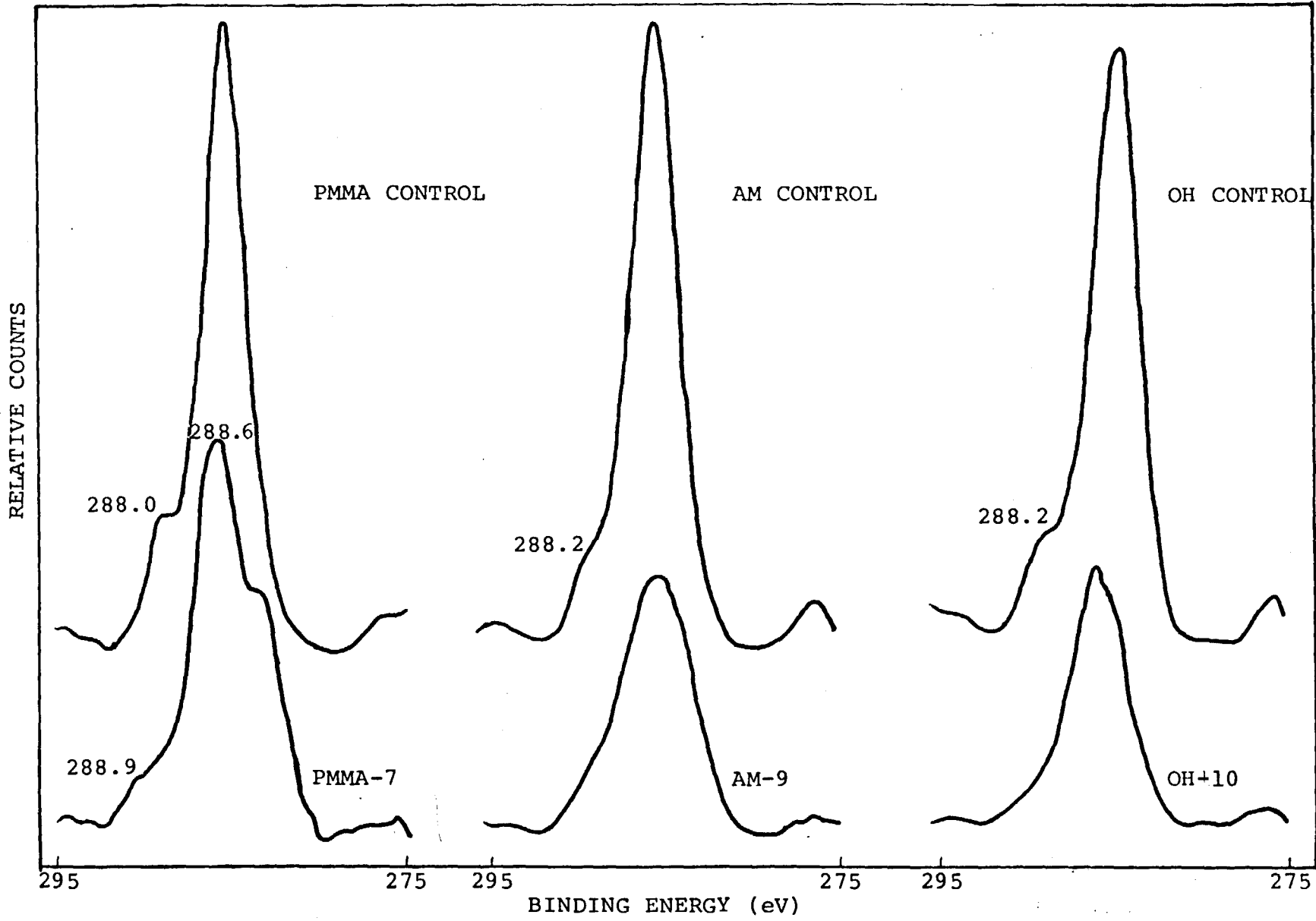




Figure 4.7 Comparison of ESCA C (1s) peaks for PMMA, AM and OH polymers without bioglass coatings with coated and reacted PMMA-7, AM-9 and OH-10 after reaction. Data for PMMA-7, AM-9 and OH-10 are shown after 1000 hours of reaction in deionized water at 37 °C according to reaction sequence 2 as outlined in Chapter 2. Unoxidized carbon peak is at 284.6 eV with oxidized peaks labelled in the figure.



bioglass or the control polymer (compare Figures 4.6 and 4.7). Moreover, these were similar to their counterparts in Chapter 3 for the 1.2  $\mu\text{m}$  coated and reacted polymers which also showed no detection of a peak at 288.6 eV.

However, PMMA-7 showed three peaks for C (1s) at 284.6, 286.6 and 288.9 eV after 1000 hours of reaction (see Figure 4.7). This suggested the surface of PMMA-7 to be in a more oxidized carbon state as compared to PMMA-8 which showed no peak at 288.6 eV. ESCA data for SR-14 showed detection of a peak at 288.2 eV representative of a carboxylate, thus suggesting a more oxidized carbon for thicker coated and reacted SR. Discrepancies between the thinner coated and reacted (1.2  $\mu\text{m}$  OI 52S4.6) samples could be due to experimental error, small sample size or a consequence of the longer sputtering time in combination with the specific polymer. Only one sample of each condition was measured.

It was observed that all the thicker coated and reacted polymer samples showed a Ca-P rich film while Na was absent after 1000 hours of reaction (see Table 4.3). This correlated well with the ESCA analysis obtained for the 1.2  $\mu\text{m}$  coated and reacted polymers (Table 3.2). To illustrate this point, ratios of Ca to P from the atomic % calculation in Tables 3.2 and 4.3 were compared between polymers. This comparison is shown in Table 4.4. After 1000 hours of reaction in vitro the polymers have a range of surface Ca/P ratio from 1.23 to  $\frac{1.64}{4.6}$ .

Table 4.4  
ESCA Comparison of Ca/P ratios

Sample	Ca/P ratios
Unreacted coated polymer samples (1.95 $\mu\text{m}$ OI 52S4.6)	
S-16	3.32
PMMA-9	1.91
AM-11	3.23
OH-12	4.60
A-12	3.93
Unreacted Bulk bioglass	
OI 52S4.6	3.89
Reacted coated polymer samples (1.2 $\mu\text{m}$ OI 52S4.6-- 1000 hrs)	
S-15	1.33
PMMA-8	1.56
AM-10	1.41
OH-11	1.50
A-11	1.64
Reacted coated polymer samples (4.0 $\mu\text{m}$ OI 52S4.6-- 1000 hrs)	
S-14	1.54
PMMA-7	1.23
AM-9	1.46
OH-10	1.46
A-10	1.49

The major minerals in bone are Ca and P with a Ca/P ratio ranging from 1.4 to 2.1. It is known that Ca and P are present initially in bone in an amorphous phase. With age, this becomes a crystalline phase<sup>34</sup> consisting mainly of hydroxyapatite ( $\text{Ca}_{10}(\text{PO}_4)_6(\text{OH})_2$ ) which has a Ca/P ratio of 1.67. This ratio compares favorably with the data in Table 4.4 for the 4.0  $\mu\text{m}$  coated and reacted polymers. Thus the Ca-P rich film forming on the coated polymer surface is in approximately the same Ca/P ratio, independent of coating thickness.

Before reaction, polymers coated with OI 52S4.6 have a Ca/P ratio ranging from 1.9 to 4.6, and bulk OI 52S4.6 has a Ca/P ratio equal to 3.9. Thus, the aqueous reactions of bulk bioglass and the bioglass coatings results in a Ca/P ratio that is similar to that found for bone mineral. This finding is similar to related work<sup>23</sup> which also showed the change in Ca/P ratio of bioglass reaching a value similar to natural bone mineral after several hundred hours in vitro reaction.

CHAPTER 5  
SECOND REACTION SERIES OF BIOGLASS  
COATED 316L STAINLESS STEEL

Introduction

Preliminary data from Chapter 3 showed that coatings of approximately 0.5  $\mu\text{m}$  OI 52S4.6 and 1.2  $\mu\text{m}$  UF 45S5 on SS were not stable: the IRRS spectra after 100 hours of reaction returned to that of the control SS substrate. This suggested that either the coating had been removed during in vitro reaction or the depth of the coating after reaction was much less than the IRRS technique could detect (which is approximately 0.5  $\mu\text{m}$ ). Data from AES sputter profiling of SS(b) (see Figure 3.21) showed that the coating was present initially; there was evidence of silicon, calcium and oxygen which are characteristic of bioglass. As the Fe from the bulk SS was detected by sputtering, the silicon, calcium and oxygen all decreased.

Further investigation with thicker coatings was done to determine if the lack of adhesion (or loss of adhesion) was due to deficiency in the sputtering technique or in the surface analytical techniques. In this chapter data from an investigation of three different coating thicknesses, with a variety of techniques, is discussed.

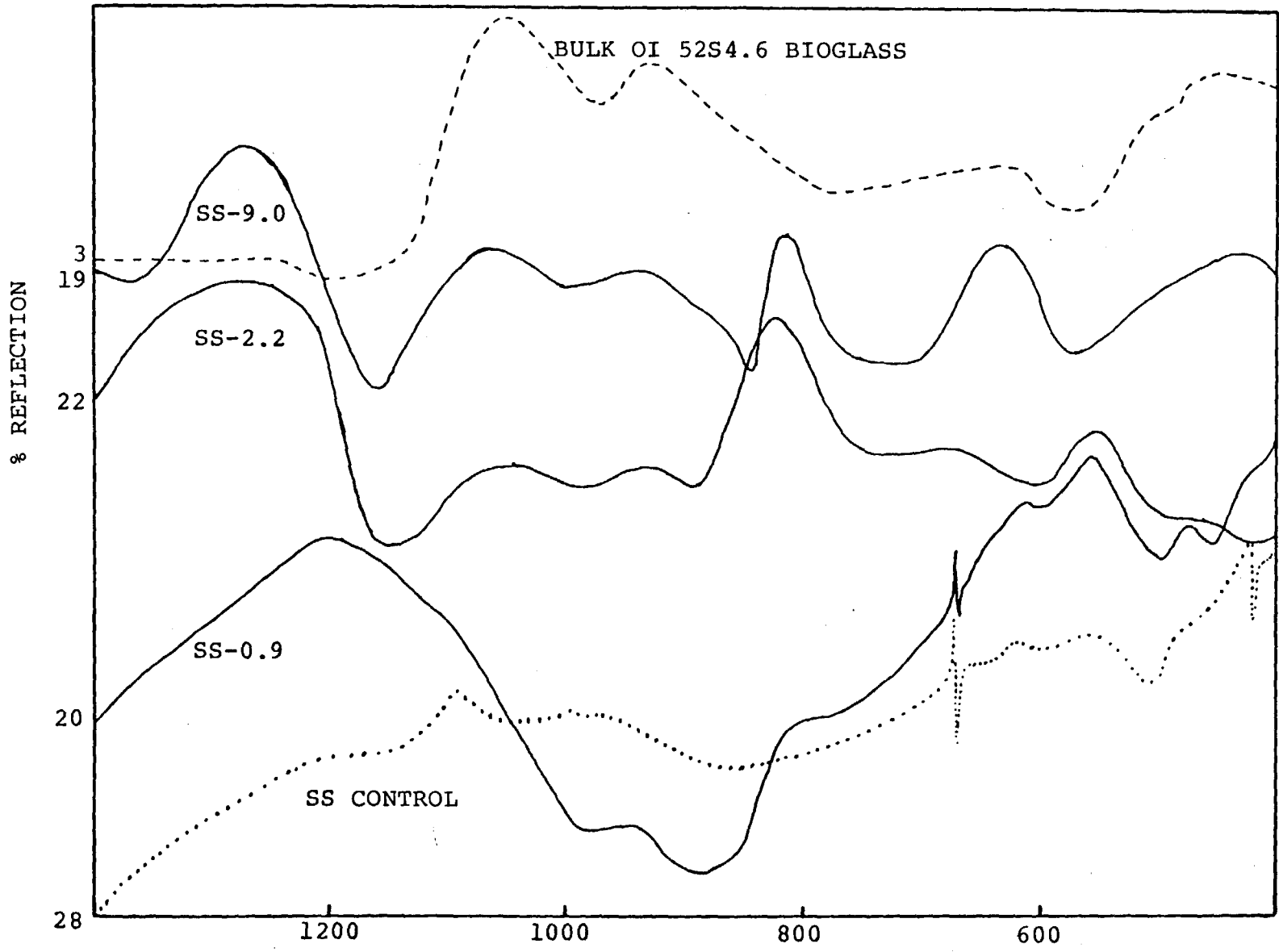
In Vitro Analysis of Bioglass Coated SS

Of the methods investigated, the first was a comparison using IRRS of coated substrates as a function of coating thickness. From Figure 5.1 we can see that there is a definite change in the IRRS spectrum when a coating thickness of 0.9  $\mu\text{m}$  OI 52S4.6 is compared with one of 9.0  $\mu\text{m}$ . A SS substrate coated with 0.9  $\mu\text{m}$  bulk OI 52S4.6 bioglass was designated as SS-0.9 with equivalent meanings for SS-2.2 and SS-9.0. For comparison purposes the dotted spectrum in Figures 5.1 to 5.4 is of the control SS while the dashed spectrum is of bulk OI 52S4.6 bioglass. Note that there is a loss of the peak at  $670\text{ cm}^{-1}$ , characteristic of the SS control spectrum, between the spectrum for SS-0.9 and SS-2.2 in Figure 5.1. By increasing the sputtering deposition time, thereby increasing the coating thickness, we observe spectra that look more like the bulk bioglass than that of the control substrate. These results indicate that as the ion beam sputtering time is increased the coating composition formed is more representative of bulk bioglass. The composition on the surface of a 9.0  $\mu\text{m}$  coated SS is similar to that of bulk, while that at the interface is less so. We assume that by increasing the coating thickness, it is less likely that the surface reaction will reach the interface, causing a breakdown of the bonds at the interface.

The next three figures (5.2 to 5.4) show the reaction sequence data of the coated samples from Figure 5.1. The SS substrates were coated and reacted in the same manner as out-

Figure 5.1 IRRS spectrum of bulk OI 52S4.6 bioglass and SS coated with 0.9  $\mu\text{m}$ , 2.2  $\mu\text{m}$  and 9.0  $\mu\text{m}$  bulk OI 52S4.6 bioglass.





lined in Chapter 2 reaction sequence 1, with an additional time period up to and including 400 hours of reaction. The first of these is of SS-0.9 (see Figure 5.2). The initial spectrum at zero hours of reaction does not resemble the bulk OI 52S4.6 bioglass and in fact shows several characteristics of the control, namely those peaks at  $670\text{ cm}^{-1}$  and between  $500\text{ cm}^{-1}$  and  $670\text{ cm}^{-1}$ . After one hour and four hours of reaction, an S peak is emerging which is shown by a peak shift to  $1100\text{ cm}^{-1}$  and an increase in overall intensity. This S peak forming is similar to that shown for fused silica.

Additionally, a peak characteristic of the control at  $670\text{ cm}^{-1}$ , and seen initially, is lost after one and four hours of reaction. This could be caused by a surface reaction masking the SS substrate. After 100 hours of reaction we see the presence of the peak at  $670\text{ cm}^{-1}$  as well as a region from  $670\text{ cm}^{-1}$  to  $500\text{ cm}^{-1}$  that is equivalent to the control spectrum. The spectrum after 400 hours of reaction shows a peak at approximately  $1110\text{ cm}^{-1}$  and a peak of low intensity at  $600\text{ cm}^{-1}$ . This suggests a Ca-P rich film is present but not in the same form as that of the bulk OI 52S4.6 bioglass (see Figure 3.2 for comparison).

The reaction sequence for SS-2.2 is shown in Figure 5.3. Comparing the initial spectrum before reaction in Figures 5.2 and 5.3, note that the thicker coated sample ( $2.2\text{ }\mu\text{m}$ ) is much more representative of a bioglass coating. After one hour of reaction a loss in the NS peak and the formation of

Figure 5.2 IRRS spectra from reaction series for SS-0.9 (0.9  $\mu\text{m}$  coating OI 52S4.6 bioglass). Sample SS-0.9 was reacted in deionized water at 37 °C according to reaction sequence 1 as outlined in Chapter 2 with an additional time period up to and including 400 hours of reaction.

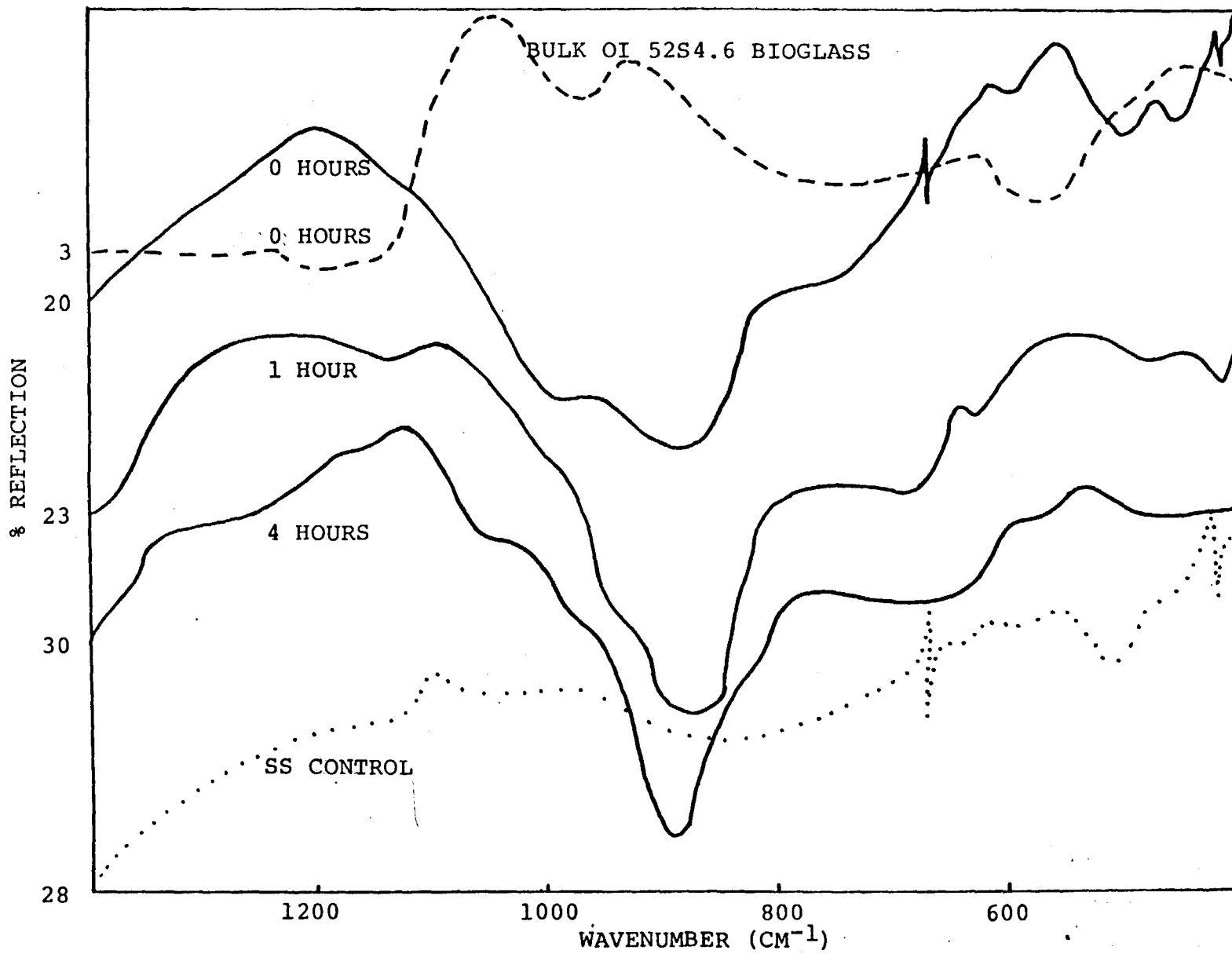


Figure 5.2 Continued

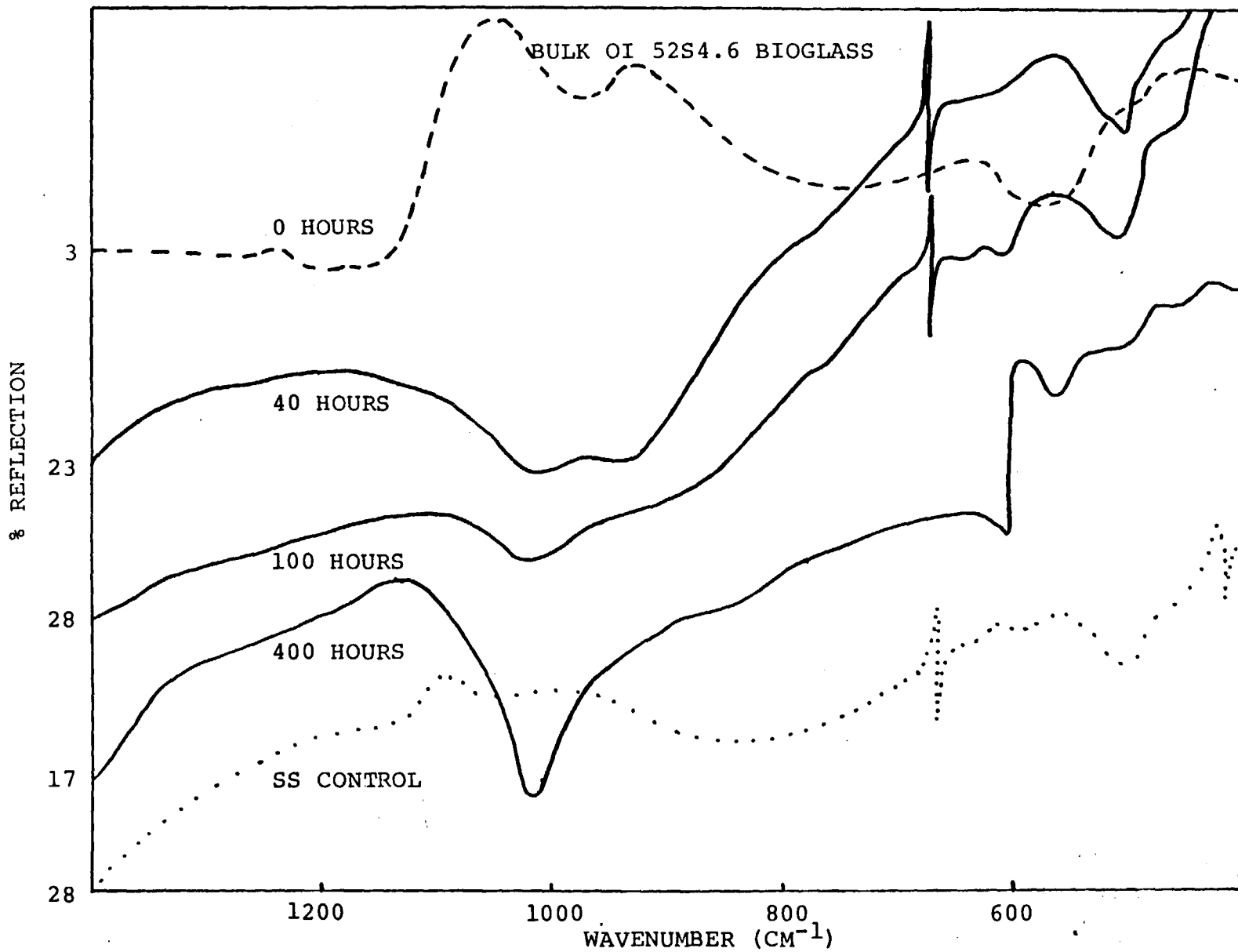


Figure 5.3 IRRS spectra from reaction series for SS-2.2 (2.2  $\mu\text{m}$  coating OI 52S4.6 bioglass). Sample SS-2.2 was reacted in deionized water at 37 °C according to reaction sequence 1 as outlined in Chapter 2 with an additional time period up to and including 400 hours of reaction.

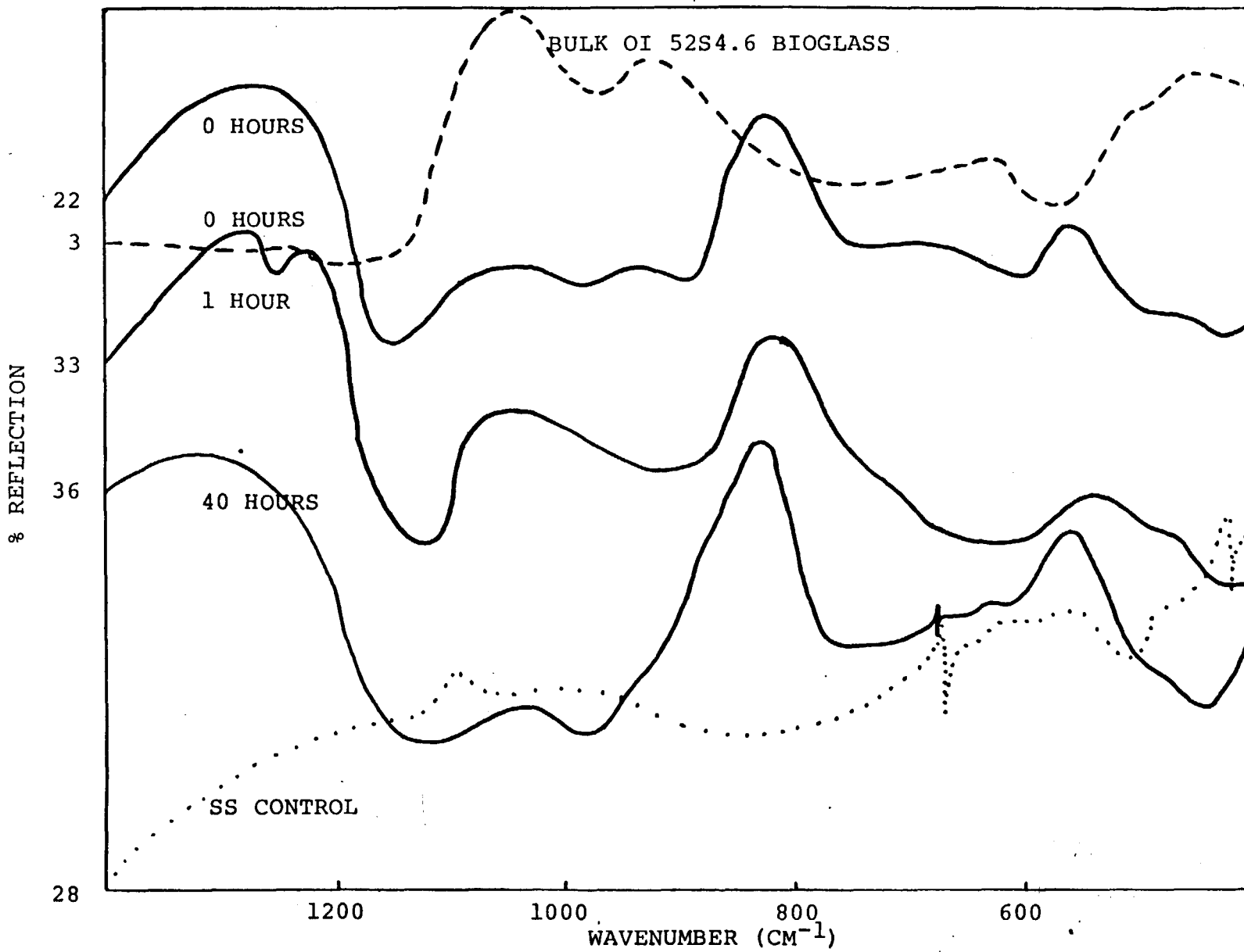
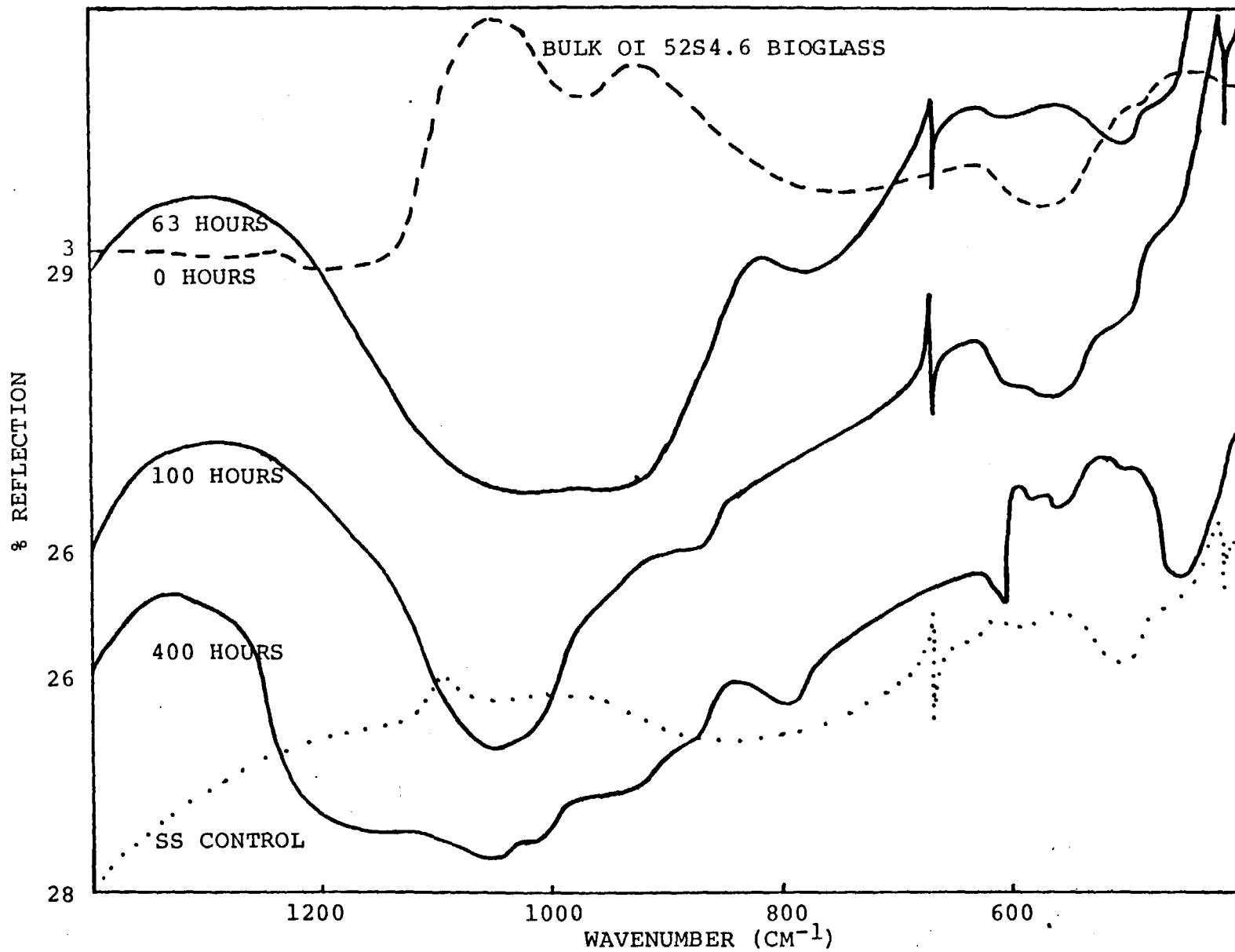




Figure 5.3 Continued



a silica rich peak at S is observed. In contrast, after 40 hours of reaction we see a decrease in the S peak and an increase in a peak designated W as well as formation of a peak at  $670\text{ cm}^{-1}$ . Additional surface compositional work would be required to assign the new peak W formed during ion beam sputtering. It is noted that the W peak survives most of the reaction. Consequently it is surmised that W comes from glass constituents that were sputtered, as W is not characteristic of either the SS control nor the bulk OI 52S4.6 bioglass.

After 63 hours of reaction there is no evidence of an S or NS peak suggesting either loss of coating, formation of a new surface composition intermediate between control and bulk OI 52S4.6 bioglass, or a coating thickness near the  $0.5\text{ }\mu\text{m}$  sensitivity depth of the IRRS. At 400 hours of reaction there is formation of a peak between  $570\text{ cm}^{-1}$  and  $600\text{ cm}^{-1}$  that is characteristic of a Ca-P rich film. Thus, some degree of coating is still present but additional analysis of the surface is required to determine the amount and type of constituents which are present.

The final sample analyzed was SS-9.0 shown in Figure 5.4. The initial spectrum at zero hours reaction has peaks at 1270, 1070, 950, 820 (W) and  $630\text{ cm}^{-1}$ . The 1070, 950 and  $630\text{ cm}^{-1}$  peaks are characteristic of the bulk OI 52S4.6 bioglass spectrum. We are mainly interested in these characteristic peaks, therefore discussion will be limited to these and compared with bulk bioglass and the S stretching

Figure 5.4 IRRS spectra from reaction series for SS-9.0 (9.0  $\mu\text{m}$  coating OI 52S4.6 bioglass). Sample SS-9.0 was reacted in deionized water at 37 °C according to reaction sequence 1 as outlined in Chapter 2 with an additional time period up to and including 400 hours of reaction.

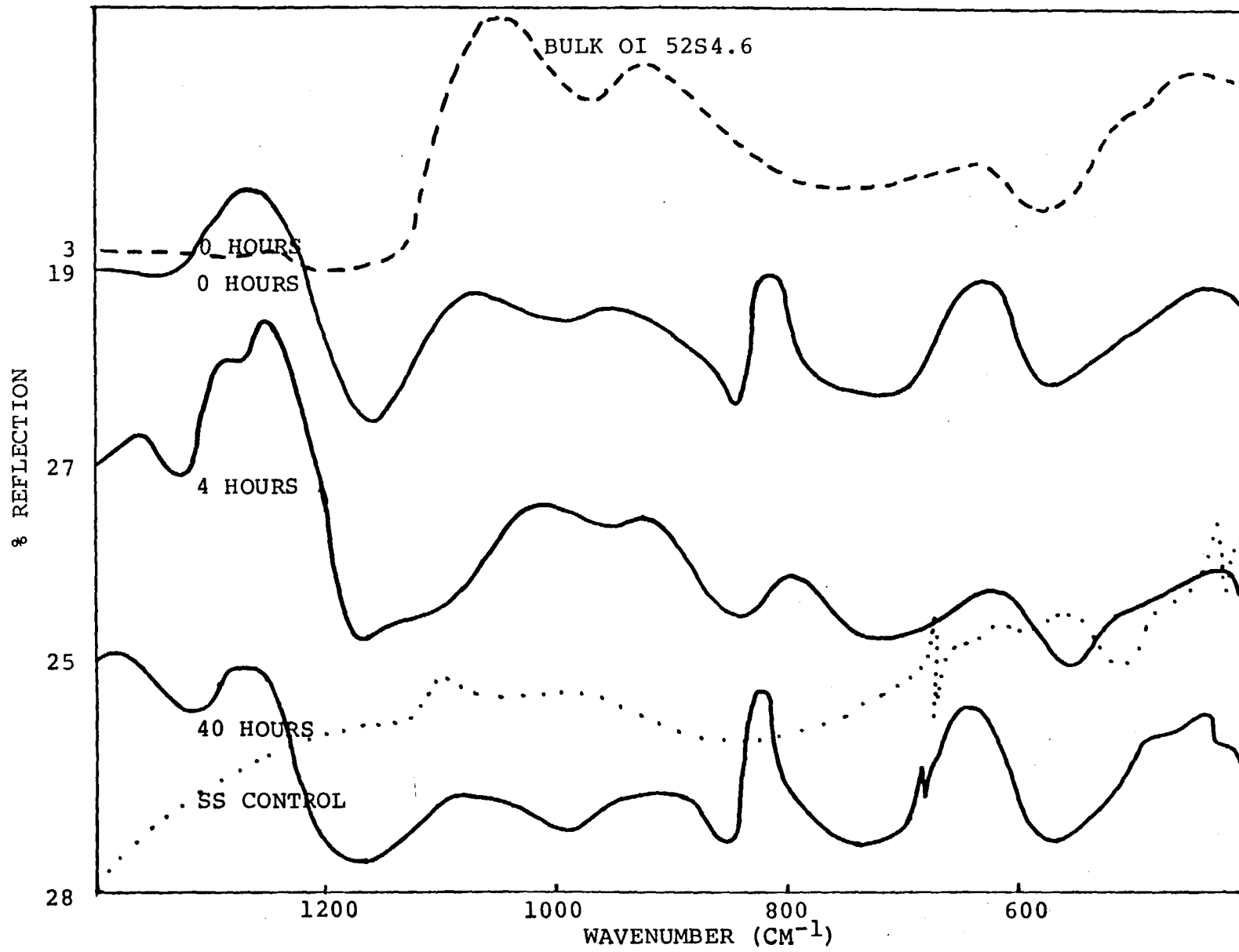
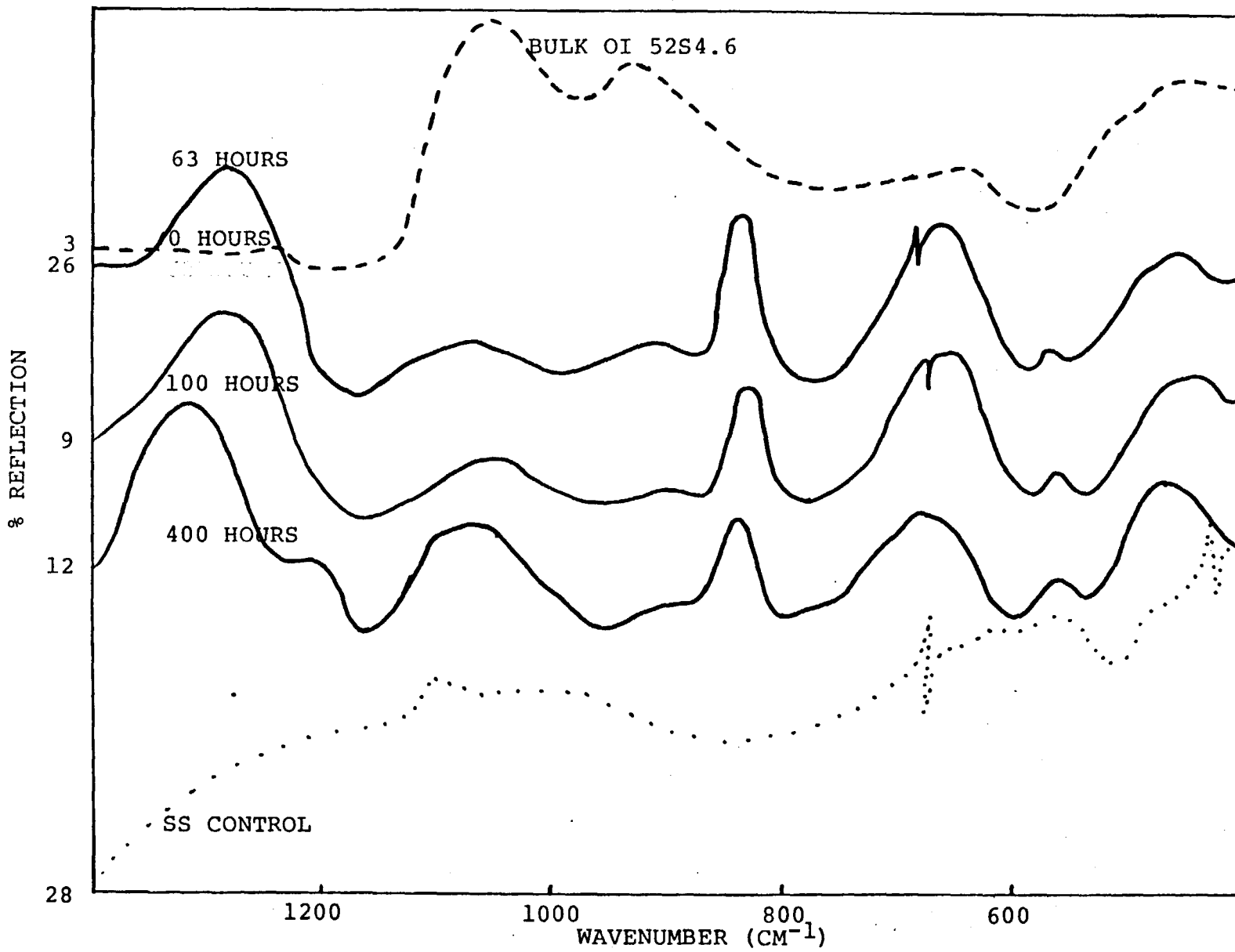


Figure 4.1 IRRS spectra from reaction sequence for SR-14 (4.0  $\mu\text{m}$  coating of OI 52S4.6 bioglass). SR-14 was reacted in deionized water at 37 °C according to reaction sequence 2 as outlined in Chapter 2.



peak for fused silica at  $1120\text{ cm}^{-1}$  (Figure 3.3). After four hours of reaction there is an increase in the intensity of the S and NS peaks. Also, the S increases in wavenumber while the NS decreases in wavenumber, suggesting total dissolution of the coating matrix rather than selective dissolution. Decoupling of peaks suggests that dealcalization is occurring. In addition the characteristic peak at  $670\text{ cm}^{-1}$  is more intense as compared to the control. Reaction after 63 hours shows an equivalent increase both in the S and NS peaks. Moreover, a small peak has formed at  $570\text{ cm}^{-1}$  which is in the same region as that in a hydroxyapatite spectrum (see Figure 3.3). An overall decrease in intensity is observed after 100 hours of reaction. The NS peak was decreased while the peak at  $565\text{ cm}^{-1}$  is increasing in intensity when compared with its counterpart at 63 hours of reaction. Finally after 400 hours of reaction there is an increase in the Si-O-Si stretching bonds suggesting the formation of a silica rich film on the surface. An increase in the peak at  $565\text{ cm}^{-1}$  was also observed. The peak characteristic of the substrate at  $670\text{ cm}^{-1}$  is not present, implying that the coating is once again masking the SS substrate. This suggests, in addition, that the coating thickness has substantially decreased at 40 hours (where the peak at  $670\text{ cm}^{-1}$  was first seen) but by 400 hours of reaction there has been reprecipitation onto the surface. The actual components involved are identified, using AES analysis later in this chapter. Note that a peak, designated W, was ob-



served in this reaction series but at this time its origin is not known.

In addition to these analyses, pH values were determined after each reaction period. Previous investigators have reported that glass corrosion (reaction) is accompanied by an increase in solution pH.<sup>19, 26, 35</sup> Ion exchange seems to be the predominant mode of reaction of alkali silicate glasses below a pH of 9.5.

Table 5.1 is a summary of the pH values from zero hours to 400 hours of reaction for each of the bioglass coated SS substrates. It is important to notice that all pH values are below 9.5 as is the bioglass pH data, thereby suggesting an ion exchange mode of reaction for the coated SS substrates. It is also seen that SS-0.9 causes an increase in pH up to 10 hours of reaction, and then a decrease for the remainder of the time sequences. Samples SS-2.2 and SS-9.0 produce an overall increase in pH up to 400 hours of reaction, when a decrease in pH is seen. As discussed earlier for the coated polymer samples, this behavior is consistent with alkali-proton exchange at intermediate times and buffering and precipitation by the hydroxyapatite layer at longer times.

#### AES Analysis

AES data were used to determine the change in surface composition before and after reaction of coated samples. In addition, the data were compared with bulk bioglass and a

Table 5.1  
pH Data for Three Coated and Reacted SS Substrates

Sample	----- Reaction time (hrs) -----							
	0	1	4	10	40	63	100	400
SS-0.9	5.7	6.8	7.2	7.6	-	7.2	7.2	7.2
SS-2.2	5.7	6.8	7.4	7.6	-	8.8	8.8	7.8
SS-9.0	5.7	6.8	7.2	7.8	-	8.6	8.6	7.6

SS control. The AES spectra of bulk OI 52S4.6 bioglass and control SS can be seen in Figure 5.5 and Figure 5.6 respectively.

The conditions under which samples were analyzed are given in each figure. Accordingly, IB Time is defined as ion beam milling time in minutes,  $E_p$  is the electron beam voltage in eV,  $T_c$  is the time constant in milliseconds, Sens. is the linear increase in output signal in  $\mu\text{V}$  and Pressure is the vacuum pressure maintained in the system in Torr.

Some characteristic ratios were obtained from Figure 5.5 for a bulk OI 52S4.6 bioglass sample. The peak-to-peak height ratios obtained were  $\text{Ca/P} = 16.1$ ,  $\text{Ca/O} = 0.52$ ,  $\text{P/O} = 0.03$  and  $\text{Si/O} = 0.25$ . These were chosen to compare a bioglass standard with the ratios of coated samples in Figures 5.6 through 5.9.

Figure 5.6 is AES data from SS(b) that has not been reacted. The ratios obtained were  $\text{Ca/O} = 0.50$  and  $\text{Si/O} = 0.40$ . There is close agreement between the  $\text{Ca/O}$  ratio for the thinly coated SS and the bulk OI 52S4.6 bioglass but not between the  $\text{Si/O}$  ratios. This could be due to an enrichment of  $\text{Si}^{+4}$  ions in the surface but not necessarily bonded as  $\text{Si-O-Si}$ , thereby not showing an S peak as was seen in Figure 3.19. Figure 5.6 can also be compared with the AES data of a SS control substrate (Figure 5.10). It is evident from these two figure that even with  $0.5 \mu\text{m}$  coating the substrate is definitely being masked by the bioglass coating.

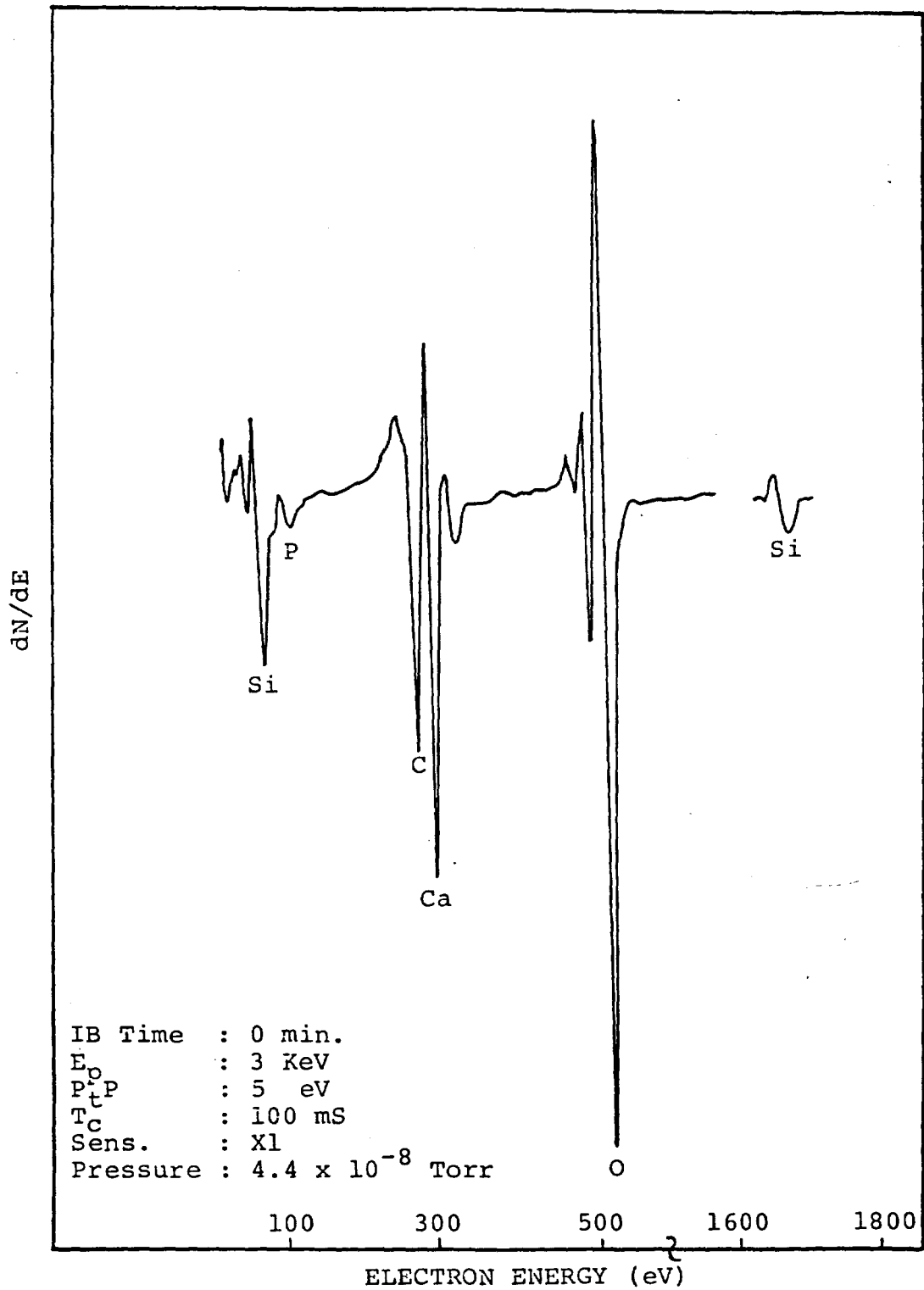


Figure 5.5 AES analysis of unreacted bulk OI 52S4.6 bioglass.

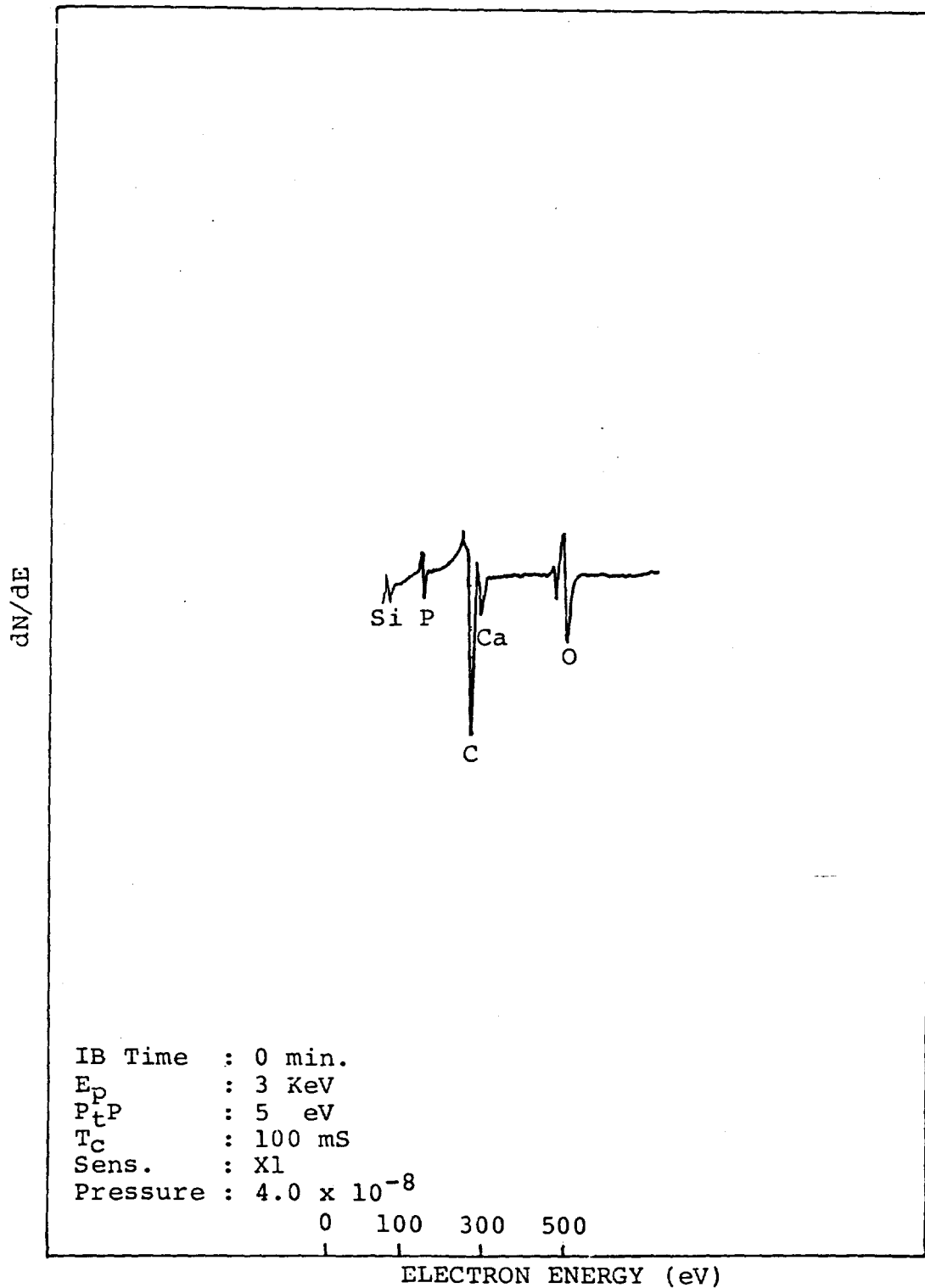


Figure 5.6 AES analysis of SS(b) unreacted and coated with 0.5  $\mu\text{m}$  OI 52S4.6 bioglass.

The AES data were also compared before and after reaction. Figures 5.7 through 5.9 show the AES data of SS-0.9, SS-2.2 and SS-9.0 samples after 400 hours of reaction. Table 5.2 is a summary of the various peak-to-peak height ratios. The three figures show evidence of surface enrichment of Ca and P after in vitro reaction. IRRS data suggest that an increase in coating thickness increases the amount of Ca-P rich film that will form; however, the AES data do not show that a thicker coating allows an increase in the amount of Ca and P formed after reaction. In fact it is seen that there is an increase in the amount of P from a SS-9.0 reacted sample, while there is a decrease in the Ca from thin to thicker coatings. The anomaly that SS-2.2 shows the least amount of Ca and P present on the surface can be due to sample variation of the sputtered surface.

It is important to note that IRRS data gives information for approximately the outer 0.5  $\mu\text{m}$  (5000 A) while AES data gives information for approximately the outer 20 A. The AES results of Figures 5.7 through 5.9 are encouraging since they show the same type of Ca-P rich film formation for the ion beam sputtered coatings as was shown by coated and reacted polymers in Chapter 4. All the AES data of reacted SS substrates that were coated in Figures 5.7 through 5.9 can be compared with AES analysis of an uncoated, unreacted SS control seen in Figure 5.10. This comparison shows that the reacted substrates do not resemble the control.

Table 5.2  
AES Data Comparison of Three Coated  
SS Substrate after 400 Hours of Reaction

Coating thickness	Ca/P	Ca/O	P/O	Si/O
0.9 um	11.9	1.5	0.13	0.05
2.2 um	11.2	0.9	0.08	0.22
9.0 um	5.7	1.1	0.19	0.12

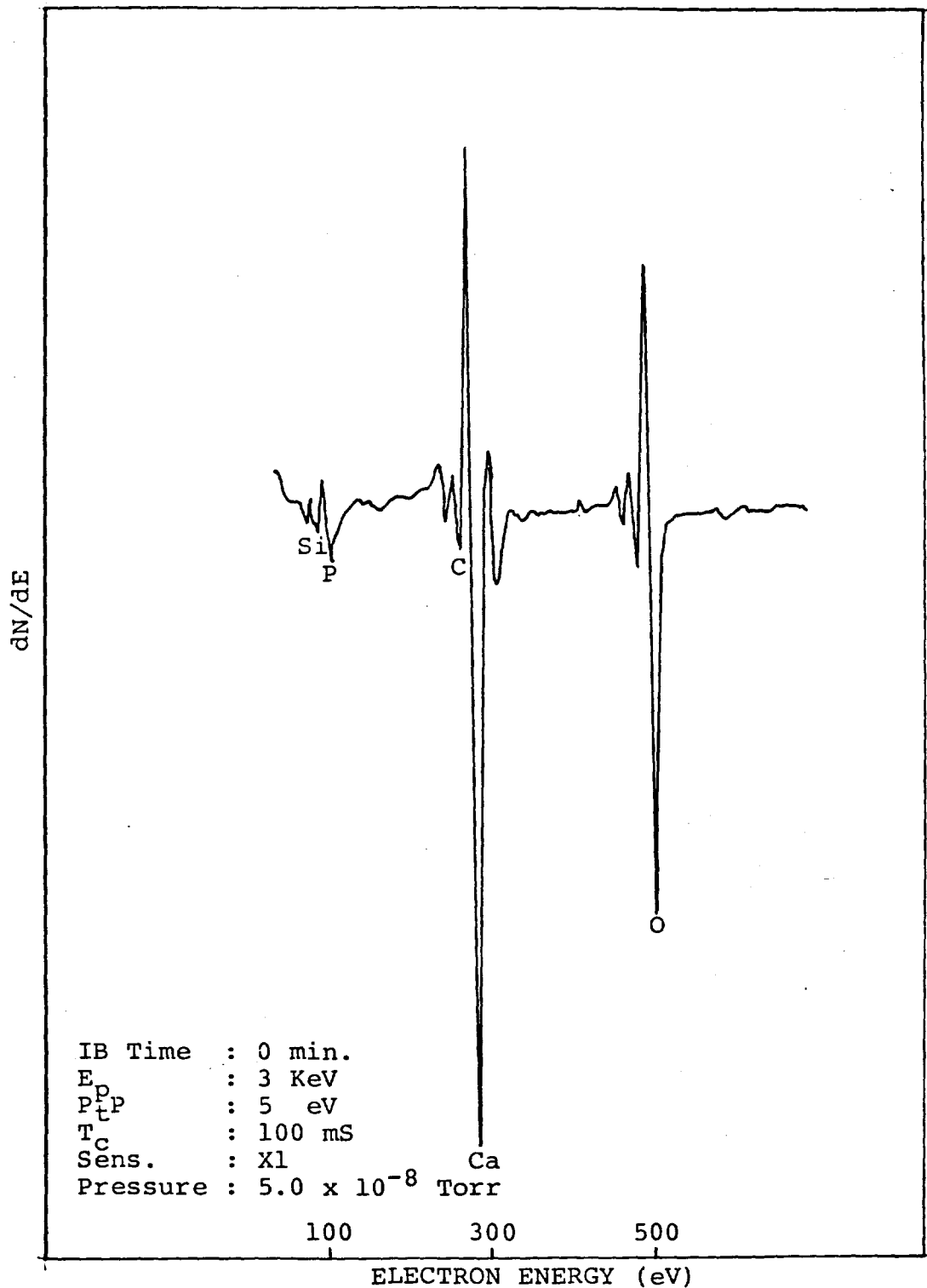


Figure 5.7 AES analysis of SS-0.9 reacted for 400 hours.



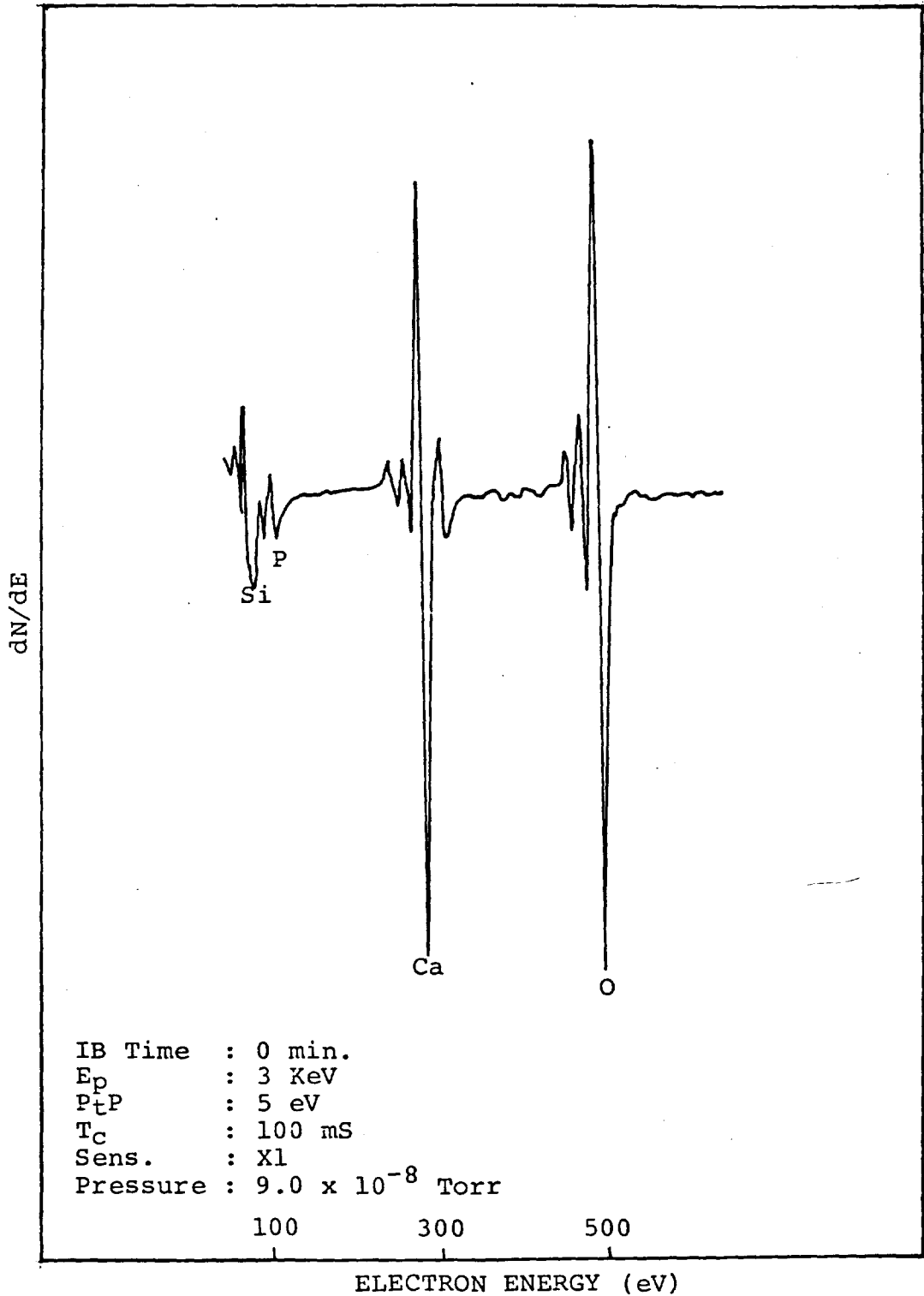


Figure 5.8 AES analysis of SS-2.2 reacted for 400 hours.

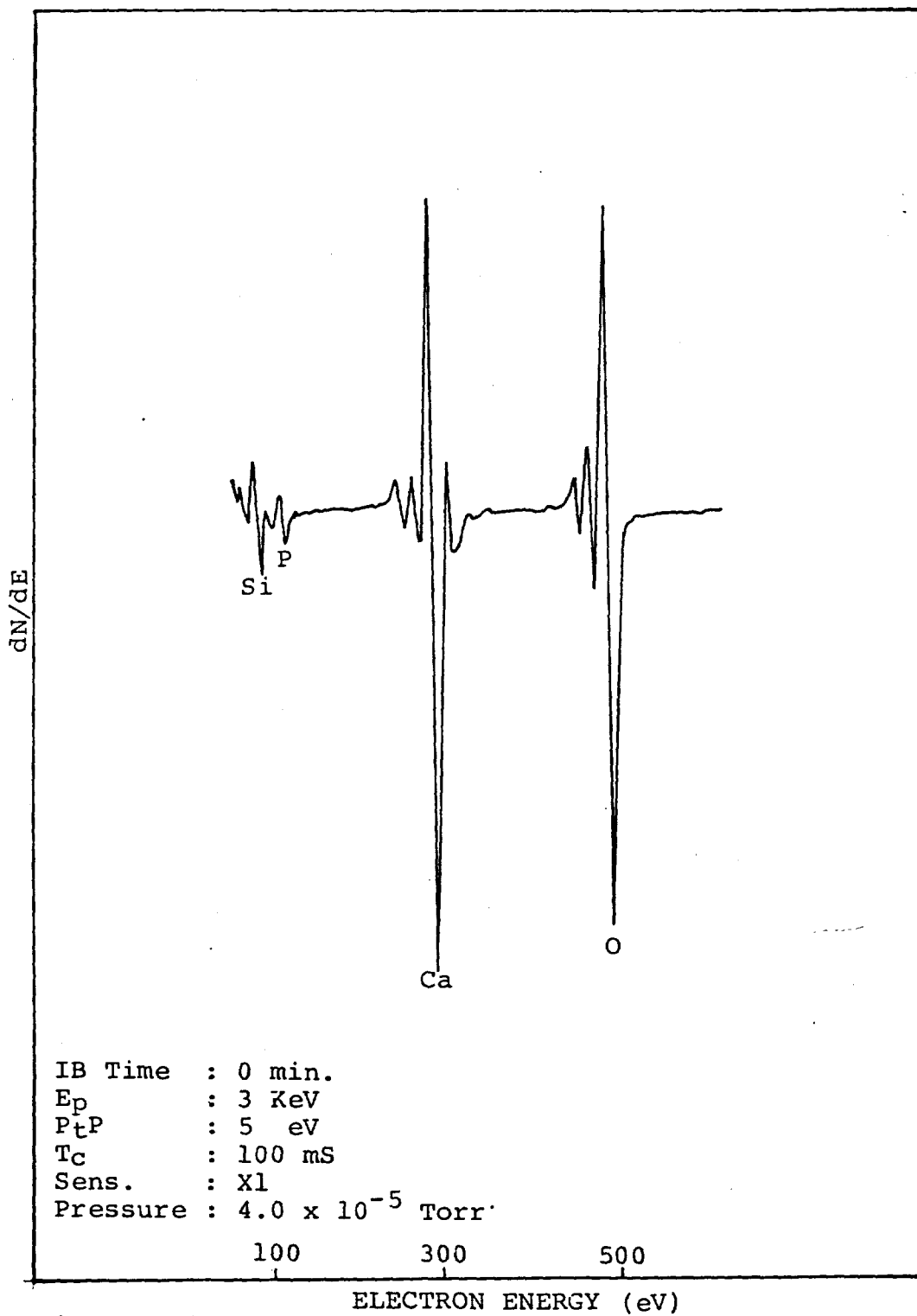


Figure 5.9 AES analysis of SS-9.0 reacted for 400 hours.

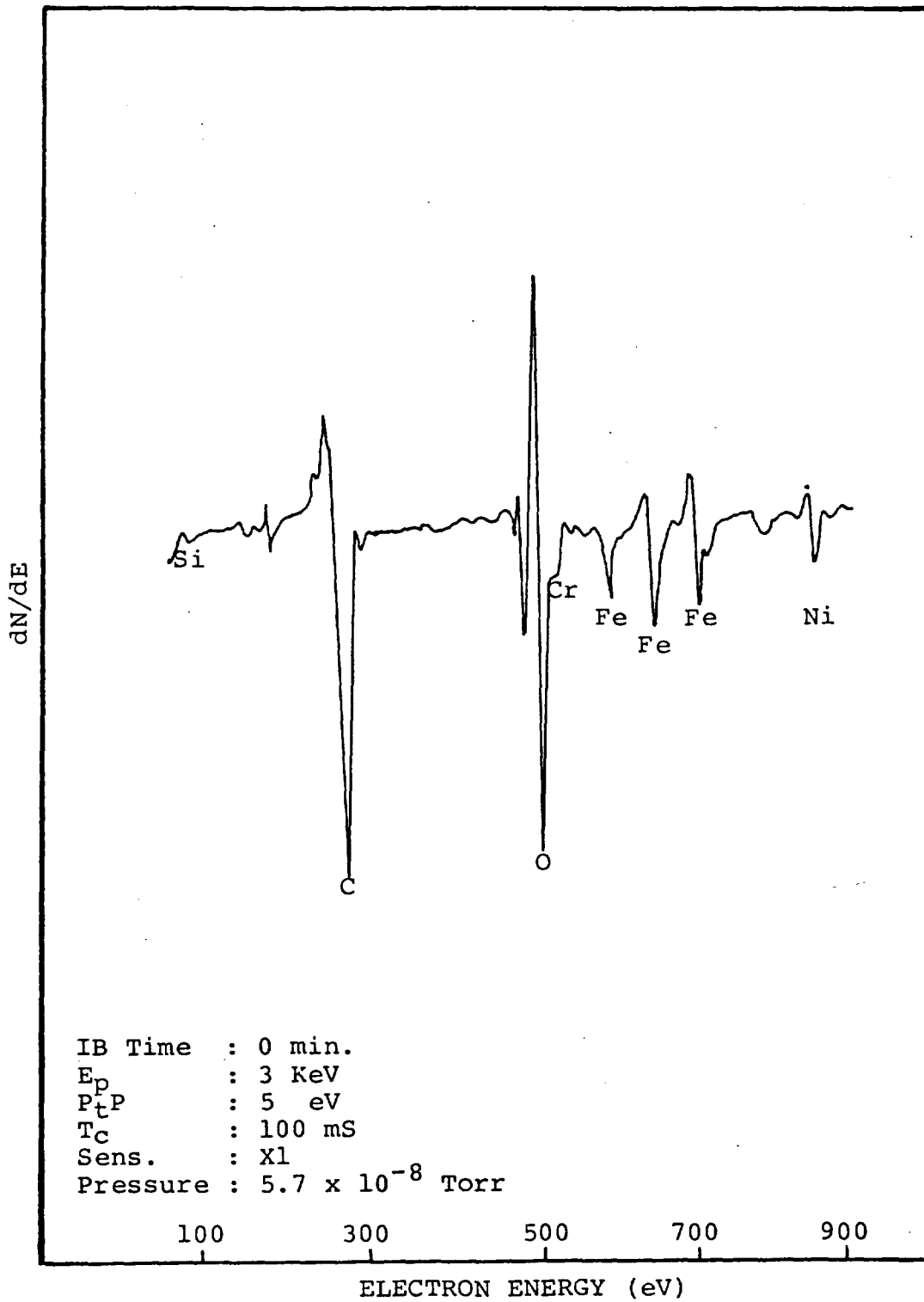
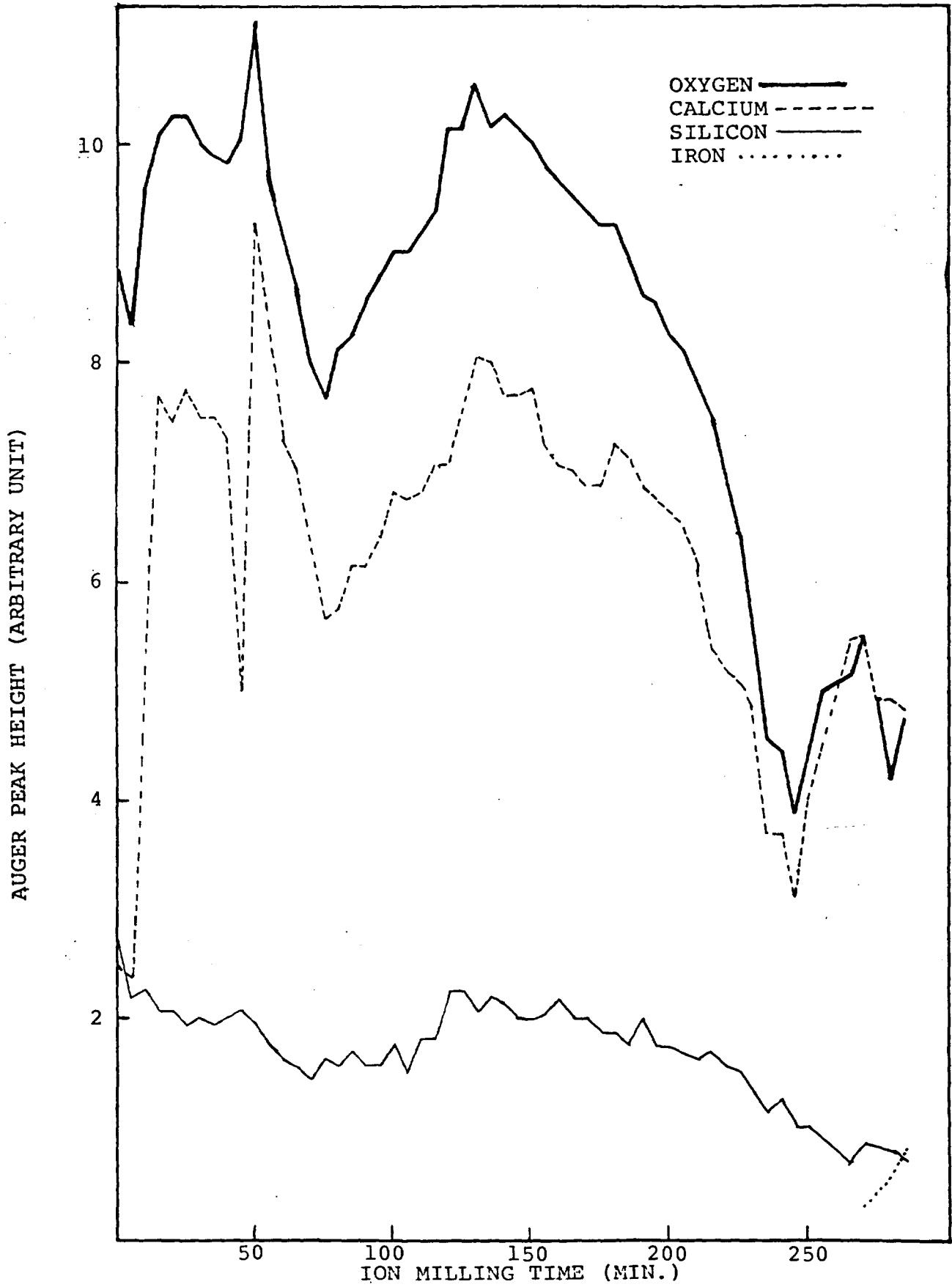


Figure 5.10 AES analysis of an SS control that was unreacted.

A final comparison needs to be made of compositional profiles before and after reaction. This can be seen in Figures 5.11 and 5.12 respectively for an approximately 0.9  $\mu\text{m}$  coating of bulk OI 52S4.6 bioglass. There are several points of interest. First, P is present in the coated and reacted SS in Figure 5.12 and is absent from that shown in Figure 5.11. Similarly, there was no silicon detected for the reacted SS while Si was detected in the unreacted SS. Second, note that unreacted, coated SS takes much more ion milling to reach the substrate material, while Fe is detected more rapidly in the reacted and coated SS. This is as expected since the surface reaction causes the coating to decrease in thickness. Third, and most important is the Ca-P rich compositional profile for Figure 5.11. Note that the Ca/O ratio is always greater than one for a reacted and coated SS while it is less than one for a coated and unreacted SS.

Figure 5.11 AES sputter profile analysis of an unreacted and coated SS (0.9  $\mu\text{m}$  coating OI 52S4.6 bioglass).



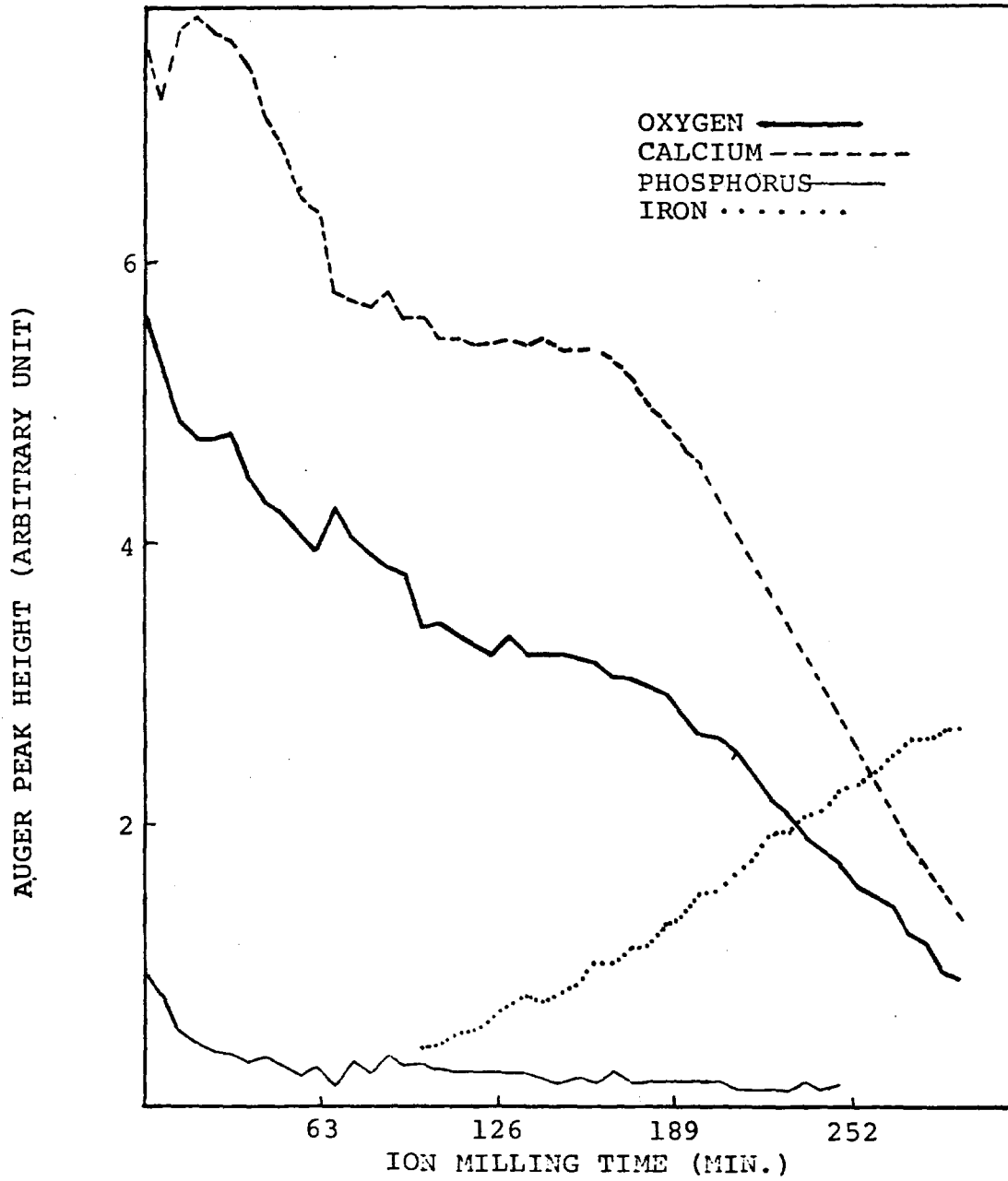


Figure 5.12 AES sputter profile analysis of SS-0.9 reacted for 400 hours.

CHAPTER 6  
SECOND REACTION SERIES OF  
BIOGLASS COATED ALUMINA

Introduction

Data reported in Chapter 3 for coated alumina substrates showed that thin coatings on the order of 0.5  $\mu\text{m}$  bulk OI 52S4.6 bioglass and 1.2  $\mu\text{m}$  bulk UF 45S5 bioglass were lost after 100 hours of in vitro reaction. Consequently, a second series of bioglass coated alumina with thicker ion beam sputtered bioglass coatings was prepared and analyzed. It was expected that by increasing sputtering time of the Ion Beam Thruster, the coating placed on the alumina substrates should be more stable, thicker and more like bulk bioglass in composition. It is suggested that there is a decrease in surface energy as the glass is initially deposited on the alumina substrate. Application of thicker coatings decreases the surface energy of the coating since the new surface formed is a glass phase bonded to a glass phase.

Topics to be discussed are the in vitro analysis of four coated alumina substrates of different thicknesses and the in vivo analysis performed. The data obtained from a variety of techniques will be presented for the four different coated alumina substrates. In addition comparisons will be made where appropriate.



In Vitro Analysis of Bioglass Coated Alumina

The alumina coated samples were reacted according to reaction sequence 2 as outlined in Chapter 2. The SA/V ratio used was  $0.7 \text{ cm}^{-1}$ . Table 6.1 is a summary of the values calculated for the coated alumina substrates in this chapter. The first three coated alumina samples were square plates (1.2 x 1.2 x 0.07 cm) coated with 0.7  $\mu\text{m}$ , 2.4  $\mu\text{m}$  and 7.0  $\mu\text{m}$  bulk OI 52S4.6 bioglass, designated as A-0.7, A-2.4 and A-7.0 respectively. The last sample analyzed was a small chip (0.4 x 0.4 x 0.06 cm) double coated with 10.0  $\mu\text{m}$  bulk UF 45S5 bioglass. The double coated samples were designated RC2 with a corresponding number for each sample analyzed. The double coated sample RC2-13 was obtained by coating with 0.5  $\mu\text{m}$  bulk UF 45S5 bioglass and then depositing a second coating of approximately 9.5  $\mu\text{m}$  in thickness of the same bulk bioglass. An IRRS reaction comparison of the RC2-13 sample with sample A-7.0 at zero hours of reaction is shown in Figure 6.1 along with respective bulk bioglass spectra. Unexpectedly the A-7.0 spectrum more closely resembles the bulk bioglass than does RC2-13 with a thicker bioglass coating. The spectra from A-2.4 and A-0.7 samples at zero hours are compared in Figure 6.2. As expected the A-7.0 sample (Figure 6.1) resembles the bulk OI 52S4.6 bioglass, more than either of the two samples with thinner coatings (Figure 6.2). Thus, increasing coating thickness produces IRRS data with both the S and NS stretching peaks in the appropriate wavenumber regions. However peaks more

Table 6.1  
Data to Calculate SA and V for Coated Alumina

Sample	A(cm)	H(cm)	SA(cm <sup>2</sup> )	V(cm <sup>3</sup> )
RC2-13	0.4	0.07	0.432	0.617
Al <sub>2</sub> O <sub>3</sub> -0.7 um coating	1.2	0.06	3.17	4.52
Al <sub>2</sub> O <sub>3</sub> -2.2 um coating	1.2	0.06	3.17	4.52
Al <sub>2</sub> O <sub>3</sub> -7.0 um coating	1.2	0.06	3.17	4.52

Figure 6.1 IRRS spectrum of bulk OI 52S4.6 bioglass and bulk UF 45S5 bioglass compared with A-7.0 and RC2-13.

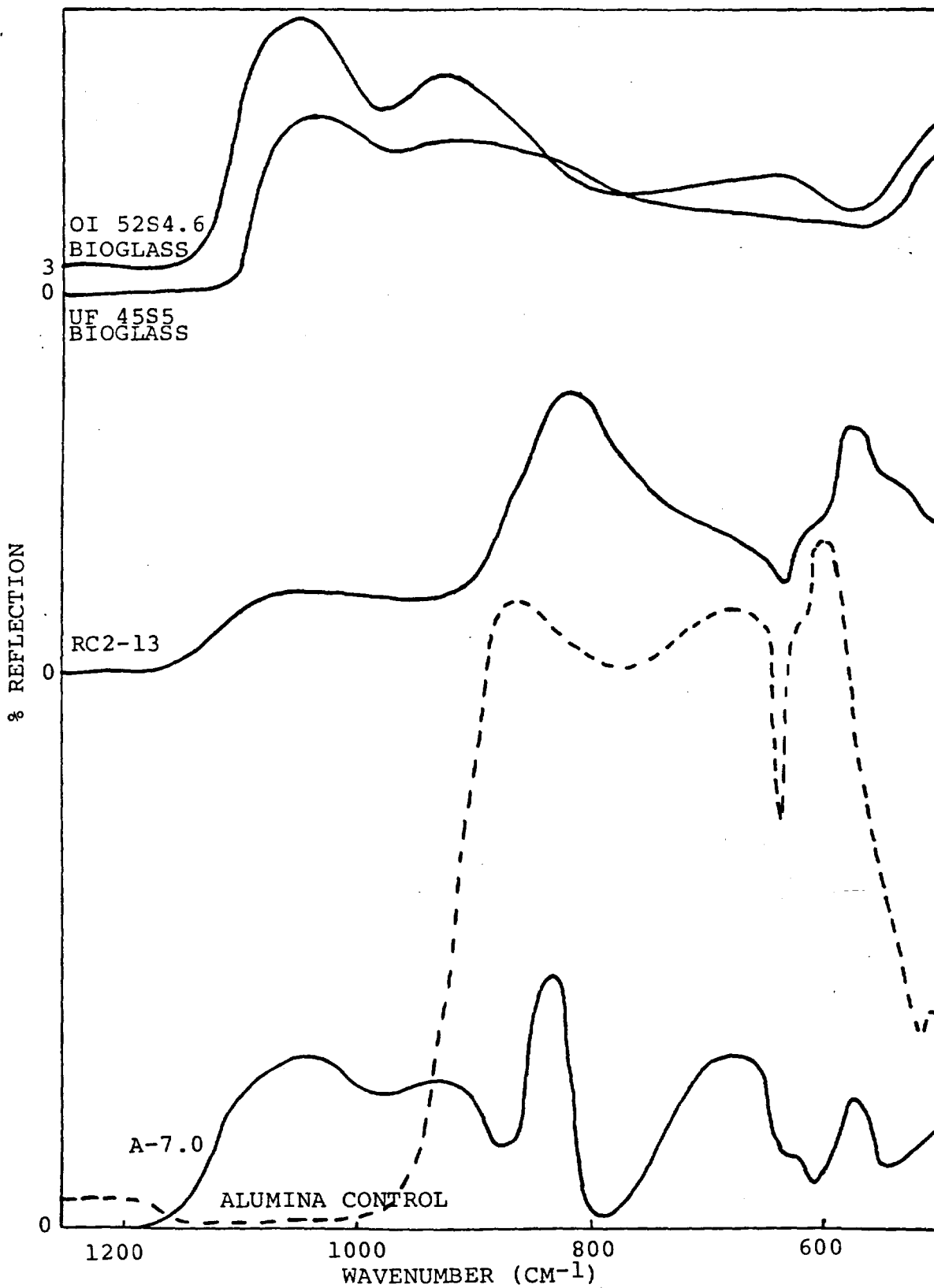
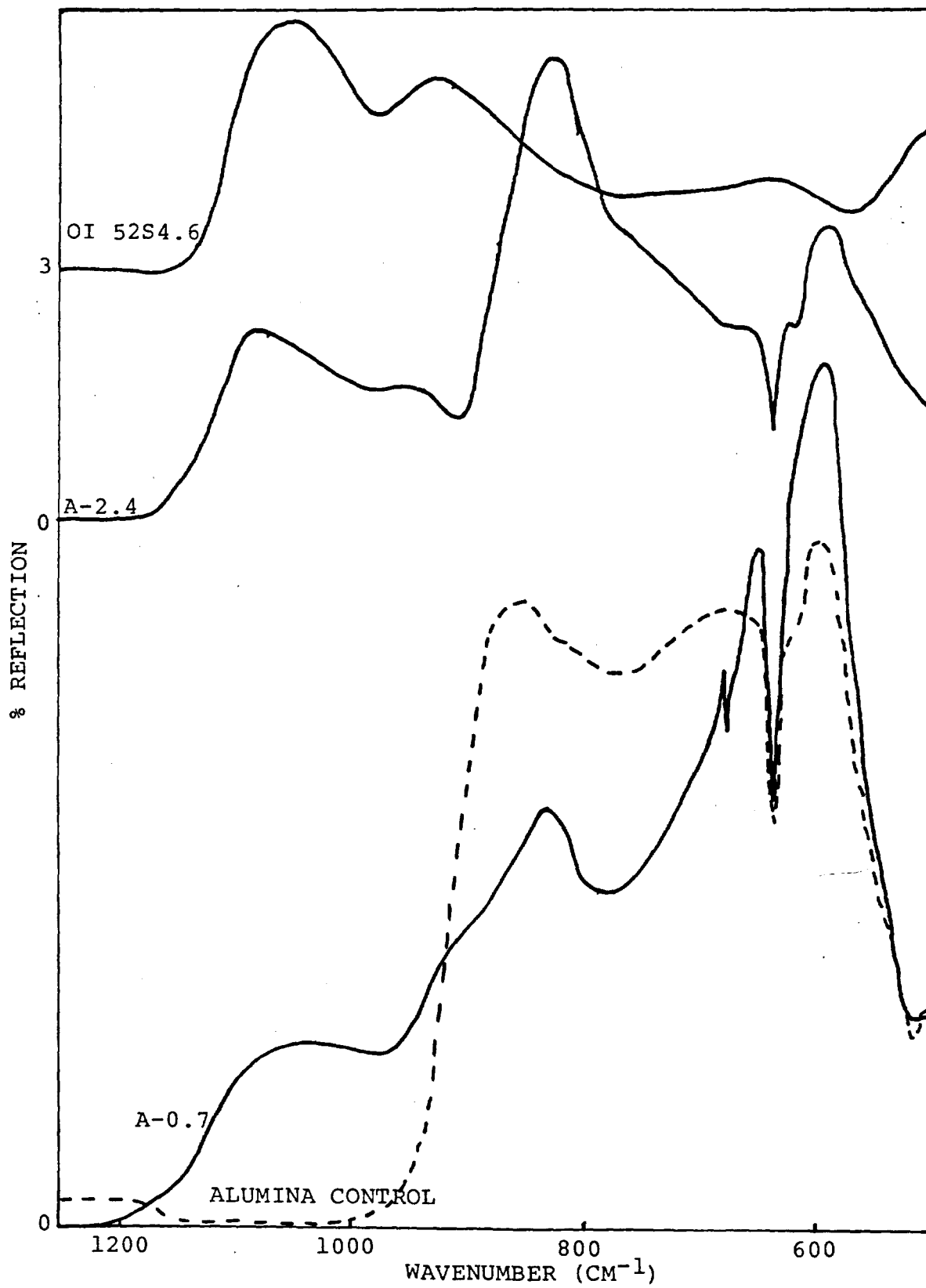


Figure 6.2 IRRS spectrum of bulk OI 52S4.6 compared with A-0.7 and A-2.4.



characteristic of the substrate than the coating are present regardless of the coating thickness. This indicates that the coating is patchy in nature rather than uniform.

The next step was to look at the IRRS data after various reaction times, for each sample. Figure 6.3 shows the in vitro reaction sequence of A-0.7. After one hour of reaction there is an overall decrease in peak intensities, possibly due to surface roughening and the formation of a shoulder in the region of NS. The NS peak seen at one hour of reaction is gone at four hours of reaction. Not until 100 hours of reaction do we see a loss in the S peak with a simultaneous reoccurrence of a shoulder shifted to a higher wavenumber. At 100 hours of reaction there is still a peak in the S region. The origin of this peak could be either a shift of the shoulder to higher wavenumbers or the loss of the NS peak with the formation of a silica rich film. After 1000 hours of reaction some evidence of a glass phase is suspected. However, the predominant analytical feature is the alumina substrate spectrum. Thus it appears that a 0.7  $\mu\text{m}$  coating is too thin or too non-uniform to sustain surface reactions necessary to form a Ca-P rich layer without dissolving away.

The next sample analyzed was A-2.4 whose reaction sequence can be seen in Figure 6.4. The initial spectrum at zero hours is more characteristic of the bulk bioglass than was A-0.7. After one hour of reaction the spectrum seems to enrich in NS peak intensity while the peak at  $820\text{ cm}^{-1}$  is

Figure 6.3 IRRS spectra of reaction sequence for A-0.7 (0.7  $\mu\text{m}$  coating OI 52S4.6). Sample A-0.7 was reacted in deionized water at 37  $^{\circ}\text{C}$  according to reaction sequence 2 as outlined in Chapter 2.



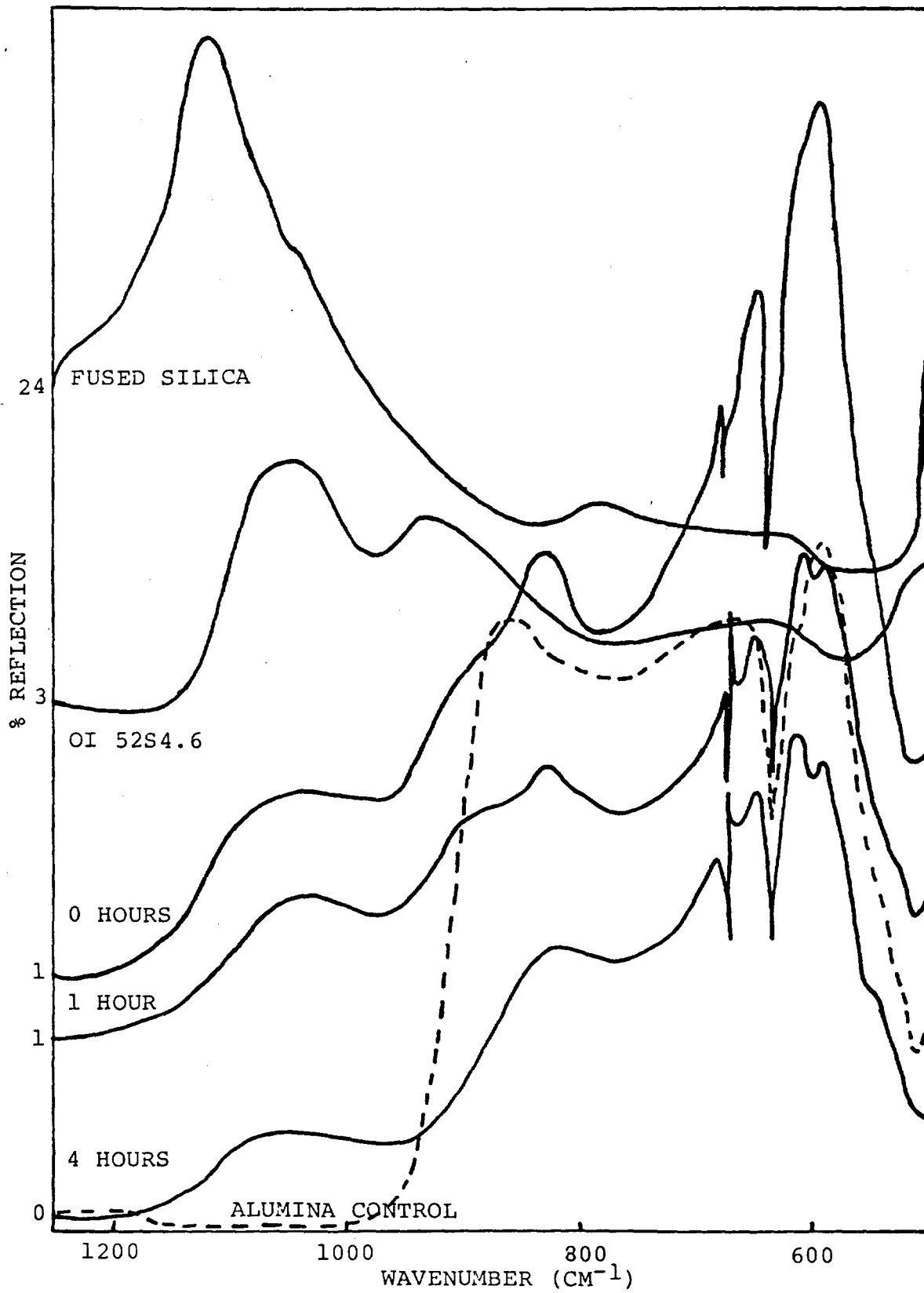


Figure 6.3 Continued

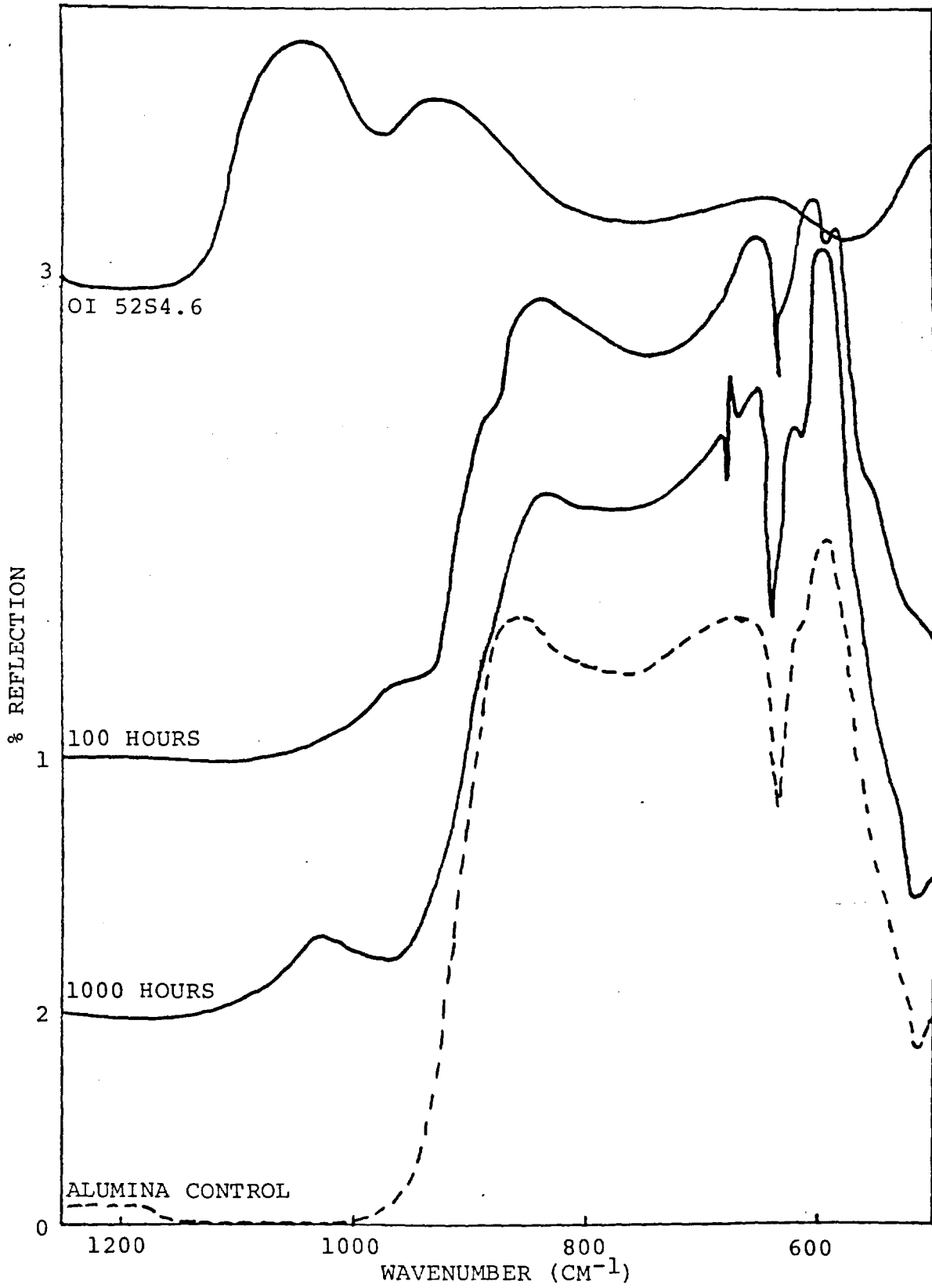


Figure 6.4 IRRS spectra of reaction sequence for A-2.4 (2.4  $\mu\text{m}$  coating OI 52S4.6). Sample A-2.4 was reacted in deionized water at 37 °C according to reaction sequence 2 as outlined in Chapter 2.

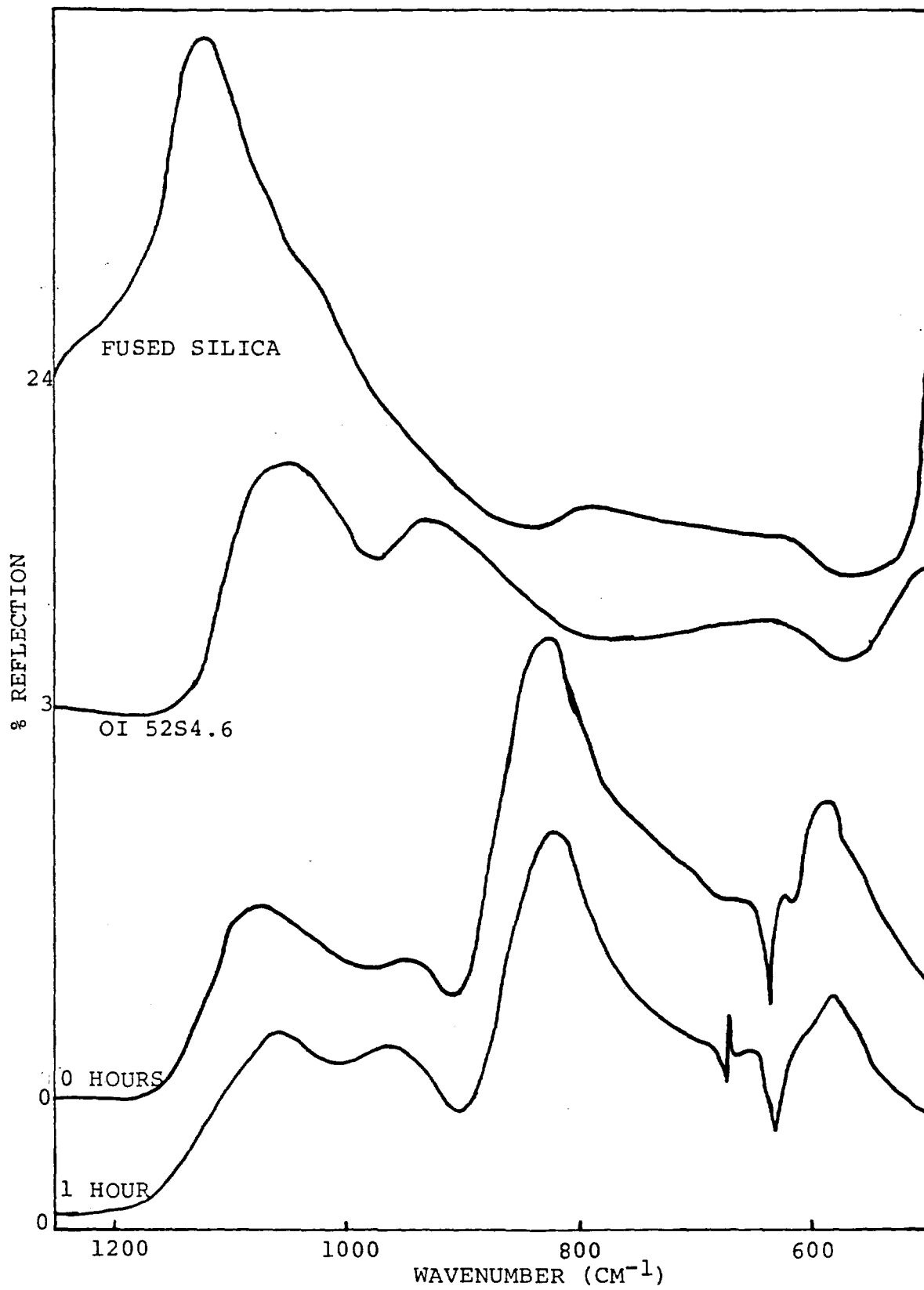
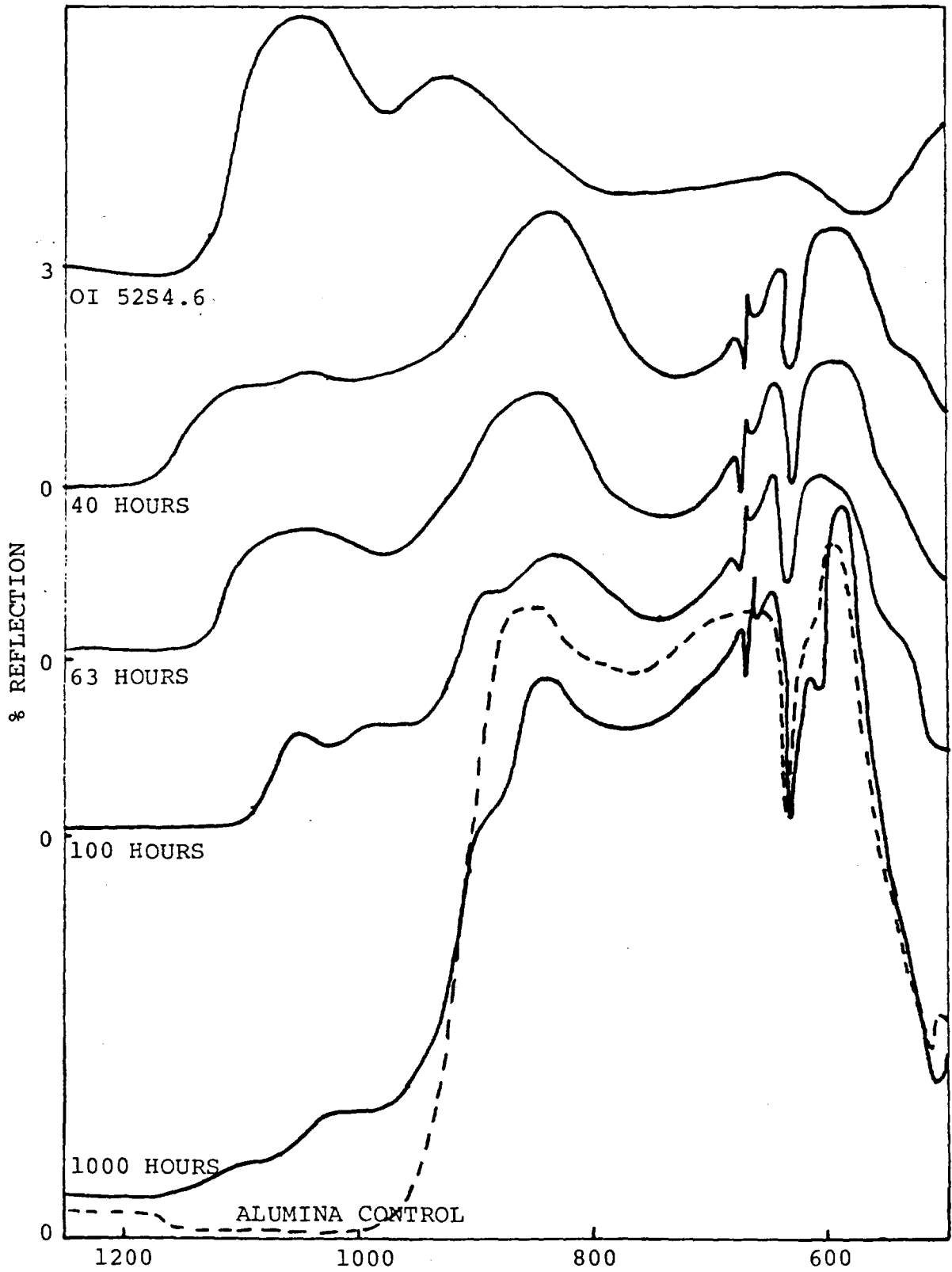


Figure 6.4 Continued



decreasing in intensity. Loss of the NS peak is seen after 40 hours of reaction, while the peak at  $870\text{ cm}^{-1}$  (one hour) has broadened and shifted to  $890\text{ cm}^{-1}$ . The spectrum at 1000 hours of reaction resembles the spectrum at 100 hours of reaction in an expanded version with peaks characteristic of hydroxapatite (see Figure 3.3). Thus the  $2.4\text{ }\mu\text{m}$  coating appears to be stable but there is insufficient information to know whether or not a HA layer is forming.

The final spectra from a sample in this series, A-7.0, are seen in Figure 6.5. It was mentioned earlier that A-7.0 was more like the bulk bioglass than any other coated alumina sample based on IRRS data. After one hour of reaction we see the formation of a sharp peak at  $670\text{ cm}^{-1}$  with the continued presence of the S and NS peaks. There is an overall decrease in intensity at 40 hours and the peak at  $580\text{ cm}^{-1}$  has sharpened, resembling its counterpart in the alumina control. The spectrum for 63 hours of reaction shows decoupling, that is, a shifting away from each other of two sets of peaks. The first being in the S and NS stretching peaks which occurs during dealkalization. The second is the broad peak and shoulder between NS and  $580\text{ cm}^{-1}$ . There is a partial loss in the NS peak after 400 hours of reaction and an additional loss after 1000 hours of reaction. Even after 100 hours of reaction the peak at  $855\text{ cm}^{-1}$  on the alumina control spectrum is not detected. It is not clear what the peaks at  $810\text{ cm}^{-1}$



Figure 6.5 IRRS spectra of reaction sequence for A-7.0 (7.0  $\mu\text{m}$  coating OI 52S4.6). Sample A-7.0 was reacted in deionized water at 37 °C according to reaction sequence 2 as outlined in Chapter 2.

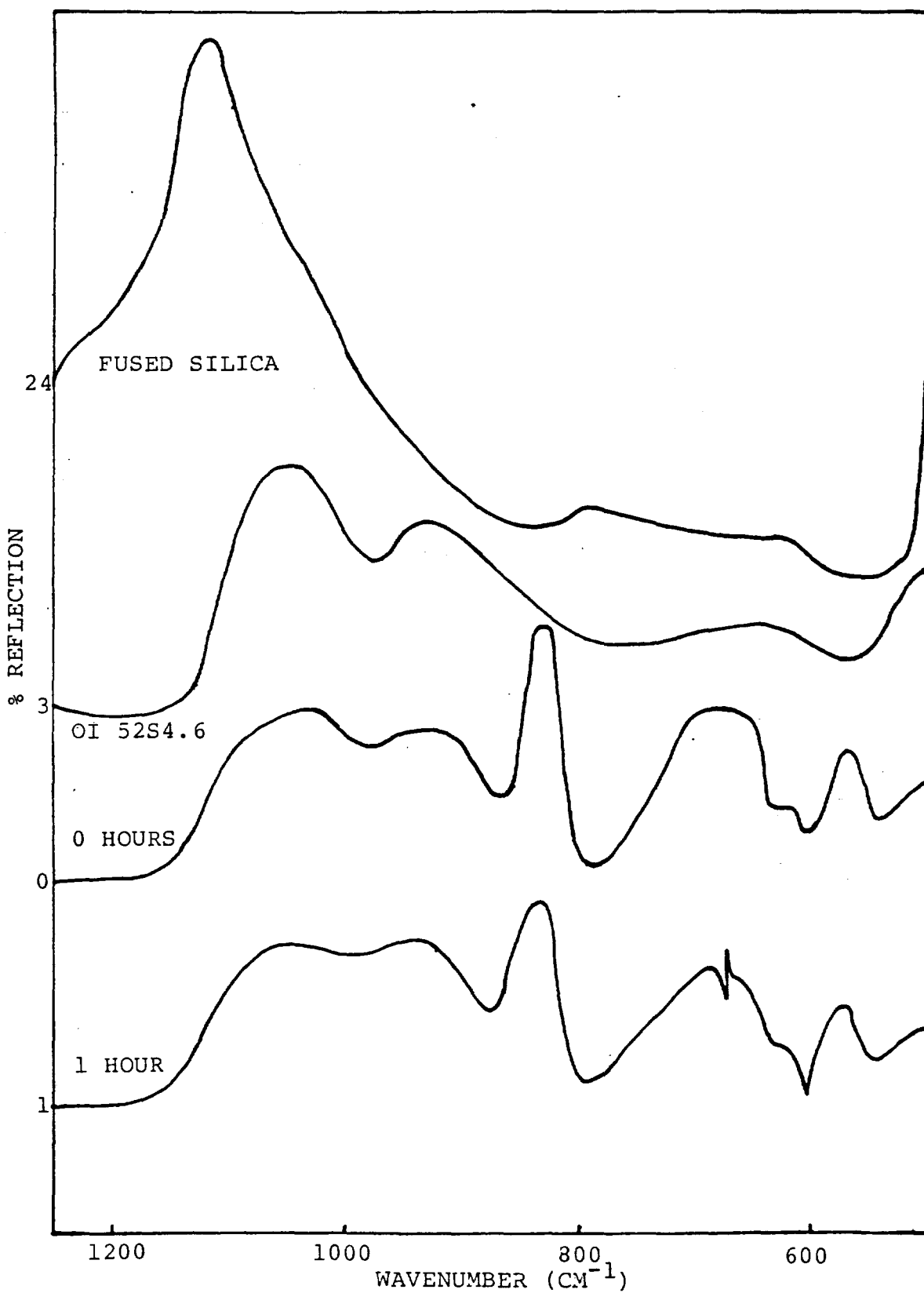
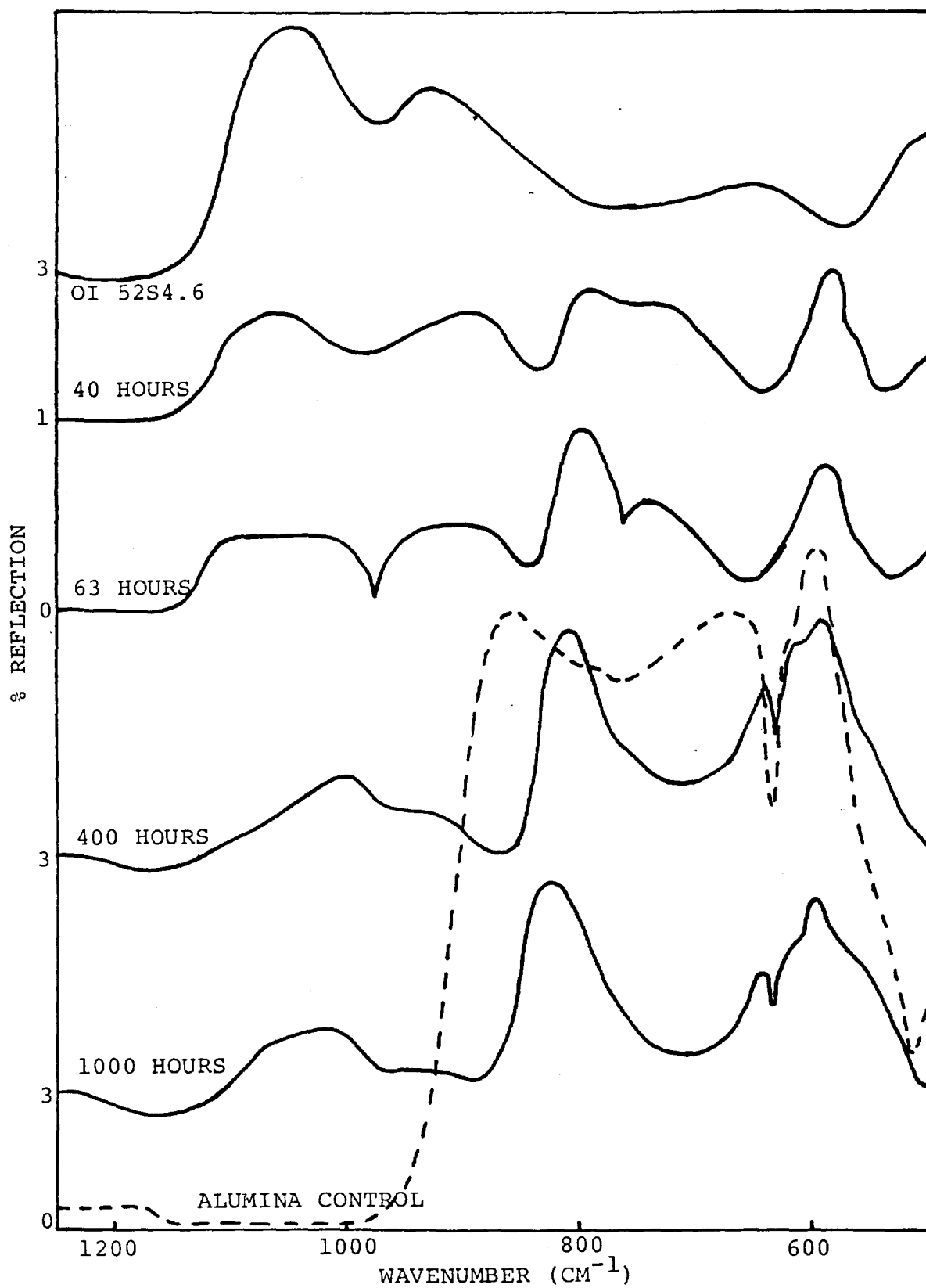


Figure 6.5 Continued



and  $825\text{ cm}^{-1}$  represent. It is interesting to note that these peaks are similar to the W peak formed on the coated SS substrates (see Chapter 5).

During the in vitro analysis the pH was monitored (see Table 6.2) to determine if ion exchange or total network dissolution was occurring. It was concluded that ion exchange was occurring as the pH did not exceed 9.5 in any reaction time, which is the limit for bulk bioglasses.<sup>26</sup> It is also noted that after 400 hours of reaction, the thicker the coating, the higher pH value obtained. Previous work has shown that an alkaline pH is necessary at the surface of the implant in order to form a chemical bond between bone and bioglass.<sup>26</sup> Thus, the 7.0  $\mu\text{m}$  bulk OI 52S4.6 bioglass coating shows IRRS evidence of masking, AES evidence of a Ca-P rich film forming (discussed at the end of this chapter) and the development of an alkaline pH with reaction time. All of these suggest a reliable bioglass coating.

#### AES Analysis

AES analysis of three different coating thicknesses of bulk OI 52S4.6 bioglass on alumina substrates are shown in Figures 6.6 to 6.8. By comparing these figures with Figure 5.5 it is noted that surface structure is similar to bulk bioglass in terms of constituents. Data from AES analysis showed that only the outer 20 Å contained those constituents representative of a bulk bioglass further supporting the

Table 6.2  
pH Data for Three Coated and Reacted Alumina Substrates

Sample	-----Reaction time (hrs.)-----								
	0	1	4	10	40	63	100	400	1000
A-0.7	5.7	6.5	7.0	8.9	8.1	7.6	7.2	6.4	6.5
A-2.4	5.7	6.5	7.0	7.4	8.9	9.5	9.5	8.7	7.4
A-7.0	5.7	6.5	6.5	8.1	8.9	8.9	8.9	9.2	9.2

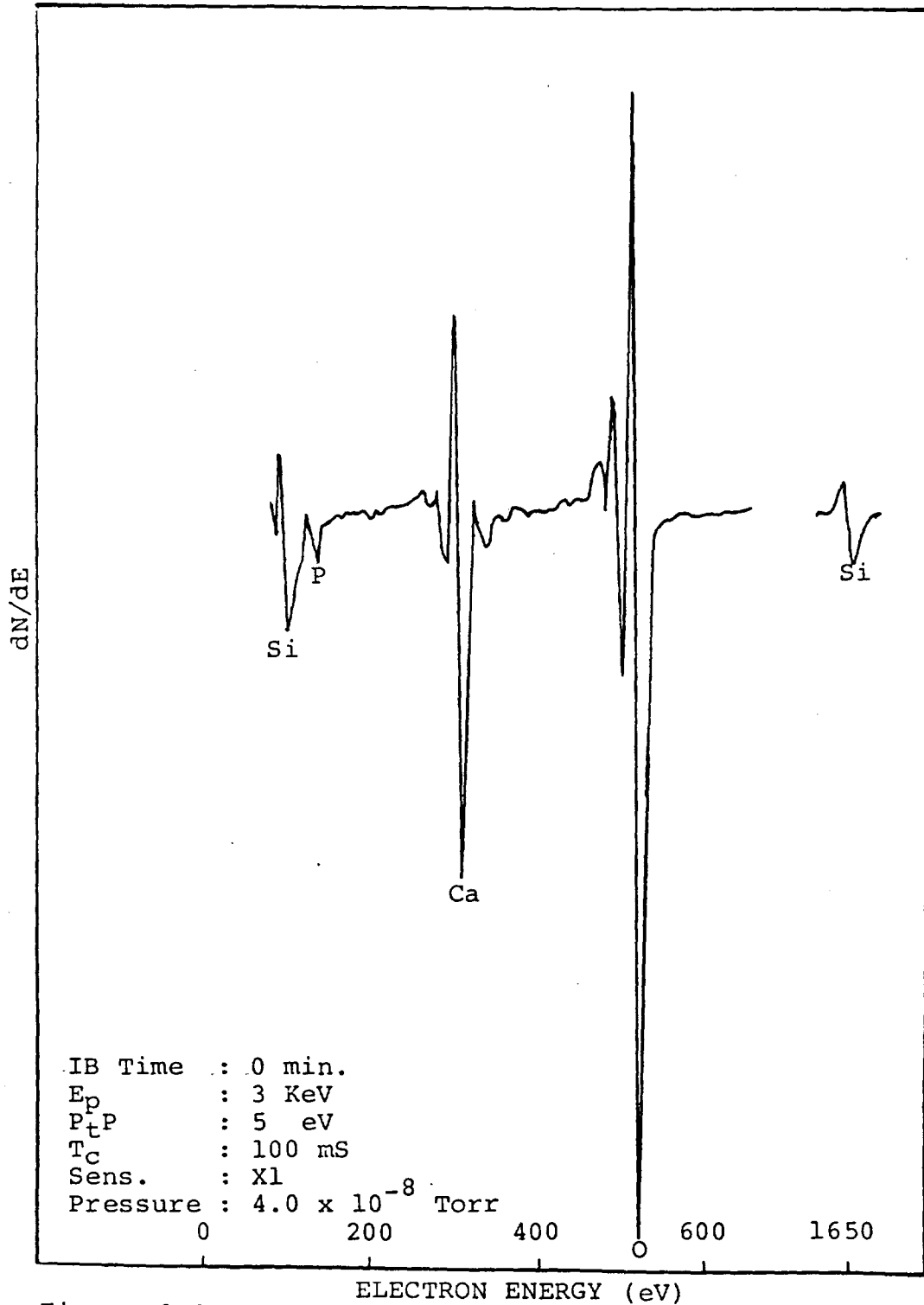


Figure 6.6 AES elemental analysis of unreacted coated alumina (0.7  $\mu\text{m}$  OI 52S4.6).

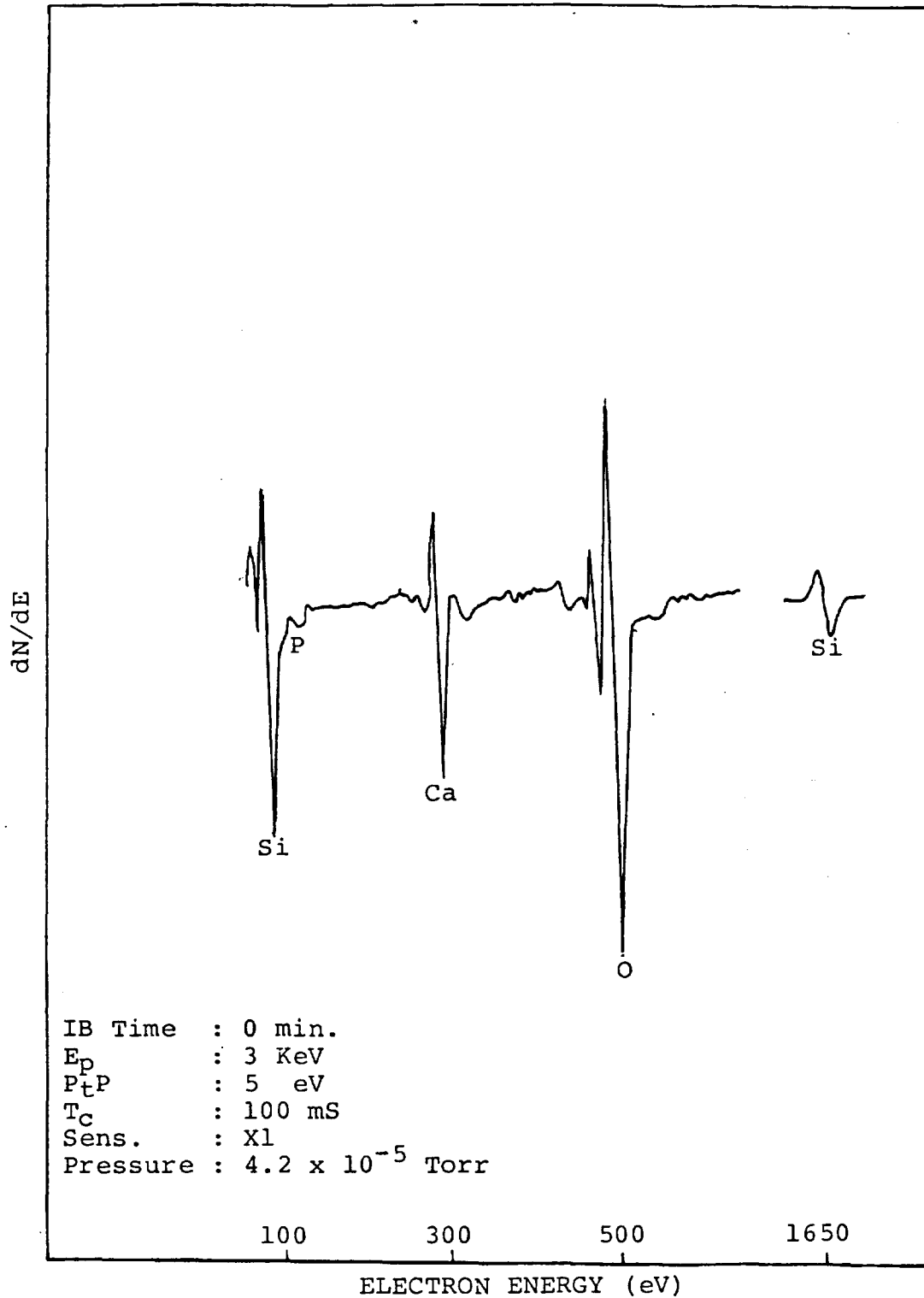


Figure 6.7 AES elemental analysis of unreacted coated alumina (2.4  $\mu\text{m}$  OI 52S4.6).



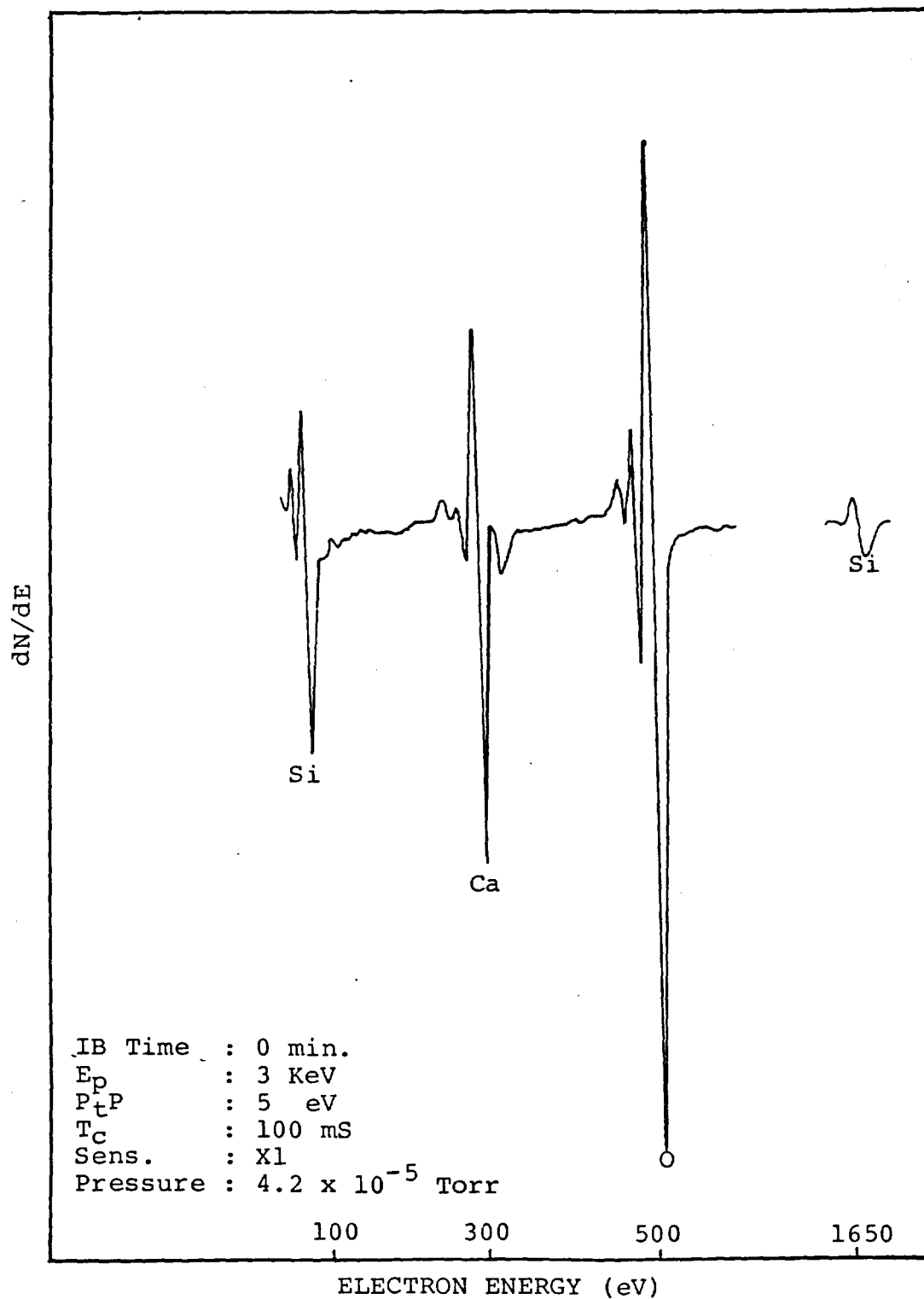


Figure 6.8 AES elemental analysis of unreacted and coated alumina (7.0  $\mu$ m OI 52S4.6).

IRRS data which showed that approximately  $0.5 \mu\text{m}$  (5000 Å) of the surface was masked by the coating. Table 6.3 is a summary of the peak-to-peak height ratios compared to a coated, unreacted SS substrate ( $0.5 \mu\text{m}$  coating OI 52S4.6) and bulk OI 52S4.6 bioglass. Likewise, these ratios are used in this chapter to compare coated and unreacted alumina substrates with unreacted bulk bioglass. It was observed that all the ratios for the coated alumina substrates were in the range of 0.4 to 1.7 times those of the bulk bioglass. Thus, the surface composition of coated alumina substrates is similar in nature to the surface composition of the bulk bioglass.

The next area under investigation was the compositional profile of the bioglass coating before and after reaction and the composition of the bioglass deposited. Of interest was a comparison of the composition of bulk OI 52S4.6 bioglass with the Ca/O ratio obtained for the coated samples (Table 6.3). The Ca/O ratio in the Auger sputter profiling analysis (Figure 6.9) ranged from approximately 0.3 to 0.7. Similarly the Ca/O ratio in Table 6.3 varied from 0.25 to 0.53, that is the Ca/O ratio is less than one in the unreacted coated metals, specifically those in Figure 5.6 and Figure 5.11. Thus the IBST is depositing Ca and O in ratios close to that of the target material. In addition the Ca/O ratio is less than one in all cases.

AES analysis of samples after 1000 hours of reaction was used to determine compositional profiles of the coatings.

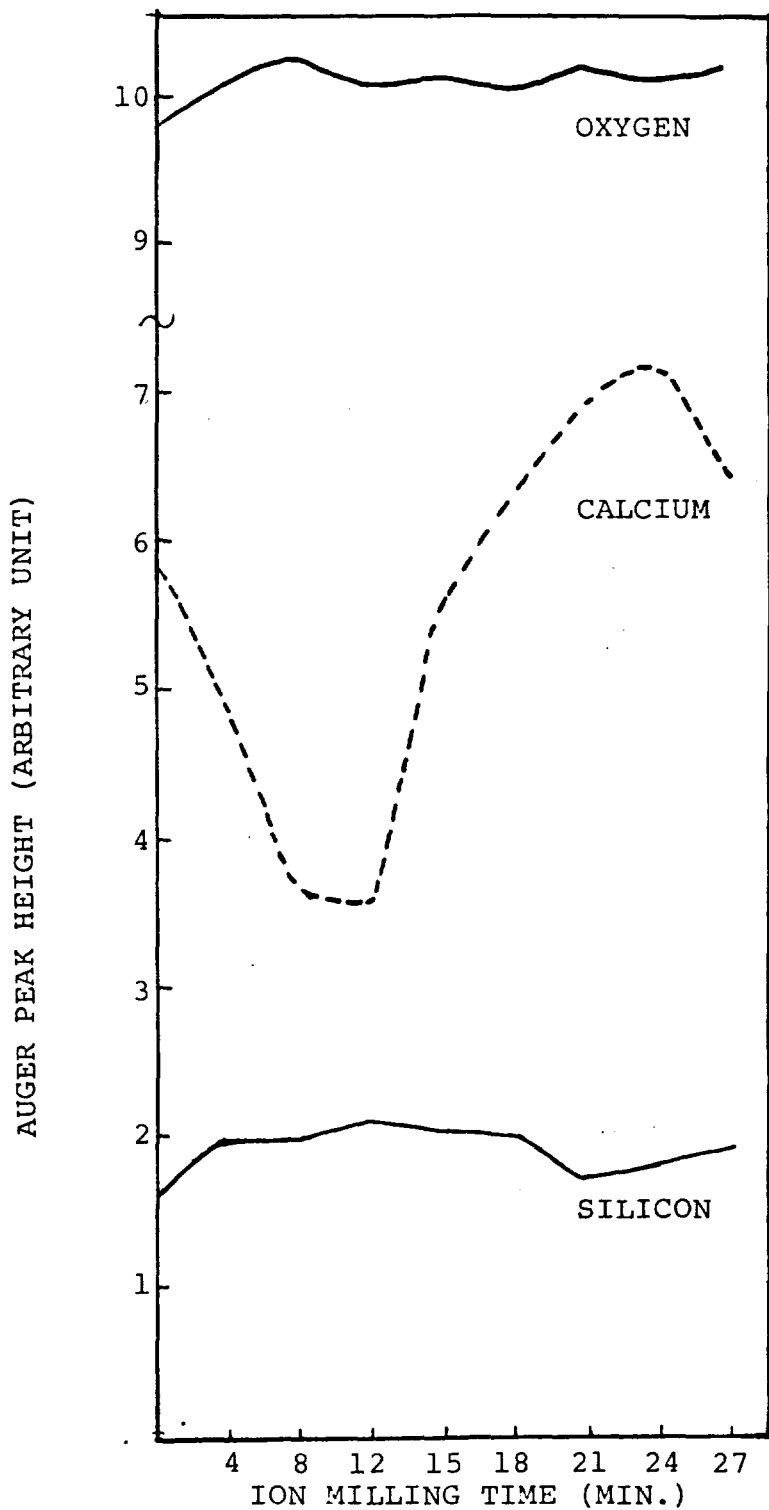


Figure 6.9 AES sputter profile of Bulk OI 52S4.6 Bioglass.

Table 6.3  
 AES Ratio Data for Bioglass Coated Alumina before Reaction  
 at Zero Minutes Ion Milling

Sample	Ca/P	Ca/O	P/O	Si/O *	Si/O **
0.7 um OI 52S4.6	10.18	0.49	0.048	0.312	0.057
2.4 um OI 52S4.6	18.67	0.25	0.013	0.312	0.062
7.0 um OI 52S4.6	27.00	0.53	0.019	0.330	0.064
OI 52S4.6	16.13	0.52	0.032	0.250	0.059

\* LOW ENERGY END

\*\* HIGH ENERGY END

Figure 6.10 and Figure 6.11 show AES sputter profiles during approximately 30 minutes of sputtering of the surface of A-2.4 and A-7.0. In both cases it is seen that the Ca/O is greater than one. Moreover, it can be seen that P was detected after 1000 hours of reaction whereas it was not detected before reaction. This suggests that a Ca-P rich film has formed. Similarly, this was observed for A-0.7 as can be seen in Figure 6.13, with between approximately zero to 30 minutes of sputter profiling.

The compositional profile of a 0.7  $\mu\text{m}$  coated alumina was measured to determine the nature of the constituents from the surface through to the bulk alumina. The ion milling time is proportional to the depth sputtered. The sample sputter rate was approximately 30 A per minute. The first sample investigated was a 0.7  $\mu\text{m}$  bulk OI 52S4.6 bioglass coated and unreacted alumina shown in Figure 6.12. Three regions can be seen. The first is representative of a glass surface which then reaches an interfacial region where aluminum is detected. At this point the calcium and silicon contents decrease while the aluminum and oxygen increase as the bulk alumina is eventually reached. Thus, a coating of 0.7  $\mu\text{m}$  bulk OI 52S4.6 bioglass shows a glass phase, an interfacial region, then bulk alumina implying that the A-2.4 and A-7.0 samples should have similar profiles but with progressively thicker glass layers.

It was also of interest to examine the compositional profile of a 0.7  $\mu\text{m}$  bulk OI 52S4.6 bioglass coated sample

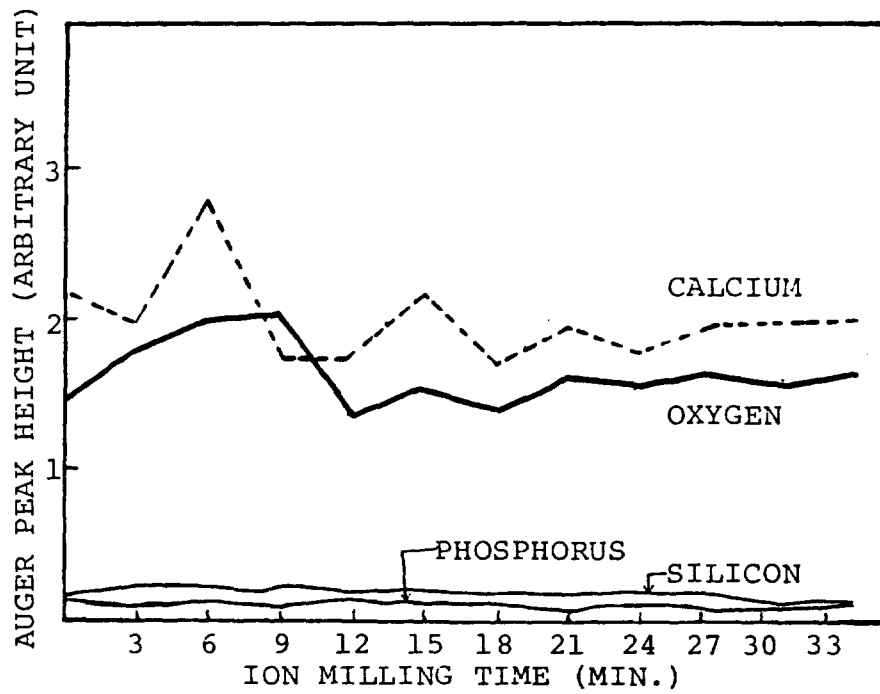


Figure 6.10 AES sputter profile of A-2.4 reacted for 1000 hours.

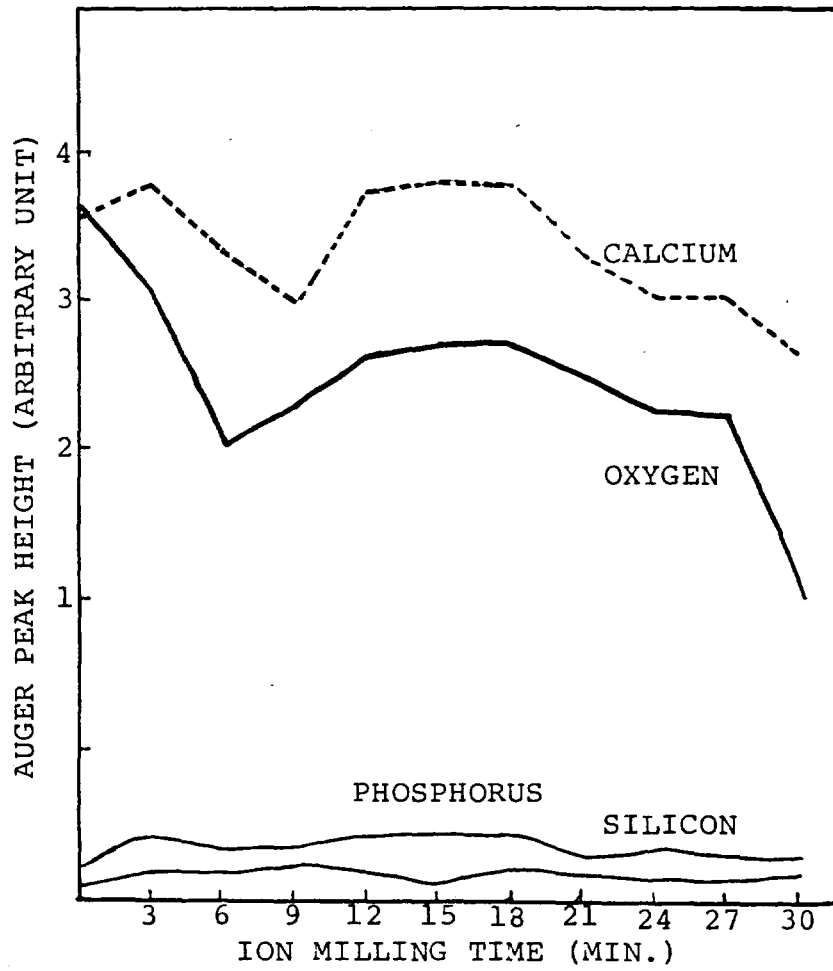


Figure 6.11 AES sputter profile of A-7.0 reacted for 1000 hours.

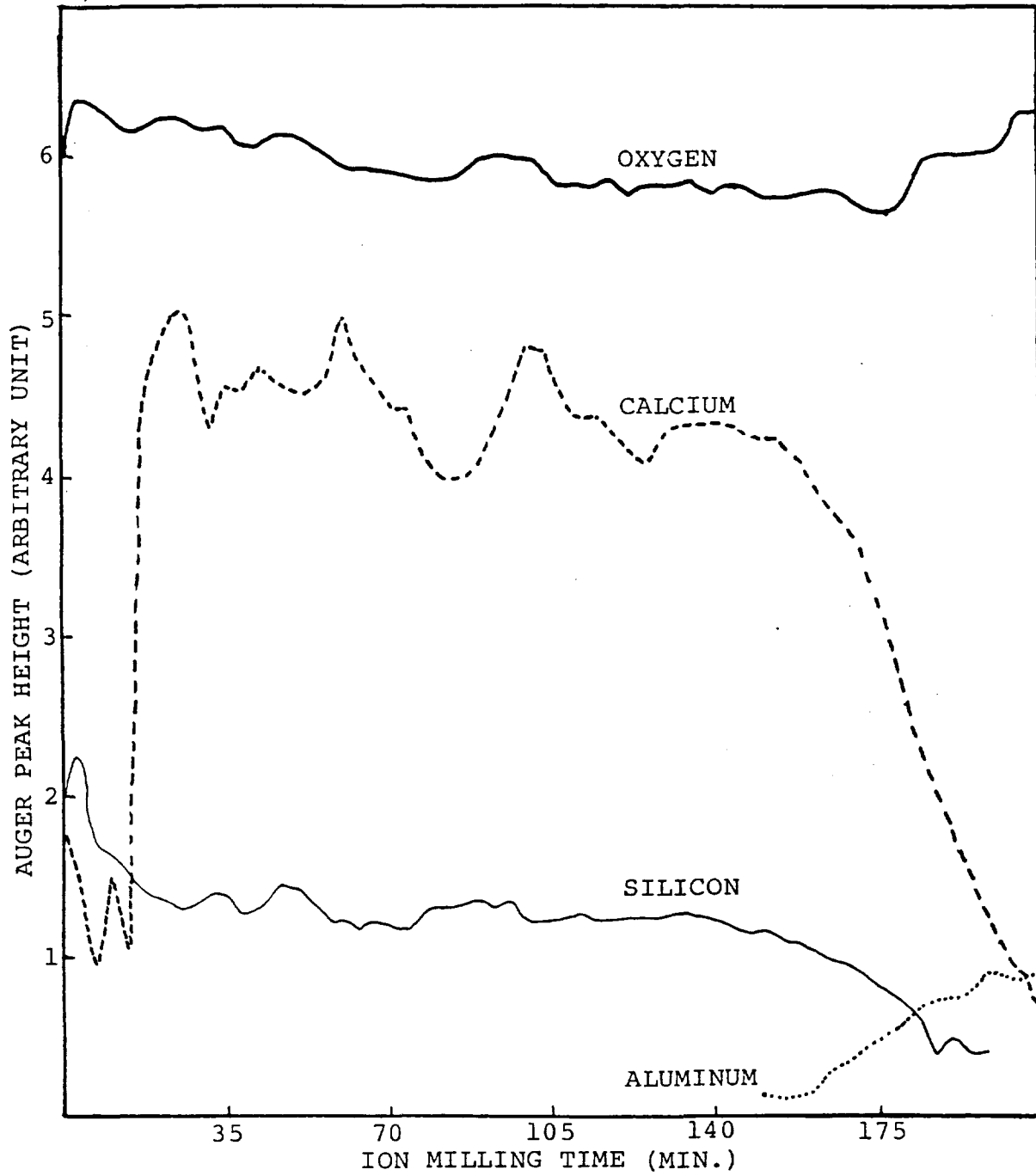


Figure 6.12 AES sputter profile of an unreacted alumina substrate coated with 0.7  $\mu\text{m}$  bulk OI 52S4.6 Bioglass.



after 1000 hours of reaction and compare it with that of an unreacted, coated sample. This analysis is shown in Figure 6.13. From zero to 110 minutes of sputter profiling a Ca/O ratio greater than one is observed for the surface reacted region of the glass coating. The next region (observed from 110 minutes to 142 minutes) is a region representing the bulk bioglass (Ca/O 1). At 142 minutes Al is detected, although this is still considered the bulk bioglass region since there is no increase in both aluminum and oxygen. There is a continued decrease in calcium suggesting the approach of the bulk alumina region. Thus for sample A-0.7 after reaction there is strong evidence that a Ca-P rich film has formed on top of bulk OI 52S4.6 bioglass which is connected to an interfacial region leading to the bulk alumina. It can be inferred that the same is true of the thicker coated alumina samples (A-2.4 and A-7.0) with the added increase of each region beyond the Ca-P rich region.

#### SEM Data

Morphological examination of the surface texture of uncoated and coated alumina samples was performed. An SEM micrograph of an uncoated alumina is shown in Figure 6.14. This is compared to coated and unreacted alumina as well as coated and reacted alumina in Figures 6.15 to 6.17. The alumina control in Figure 6.14 has a sharper grain texture free of precipitates as compared to Figures 6.15, 6.16 and

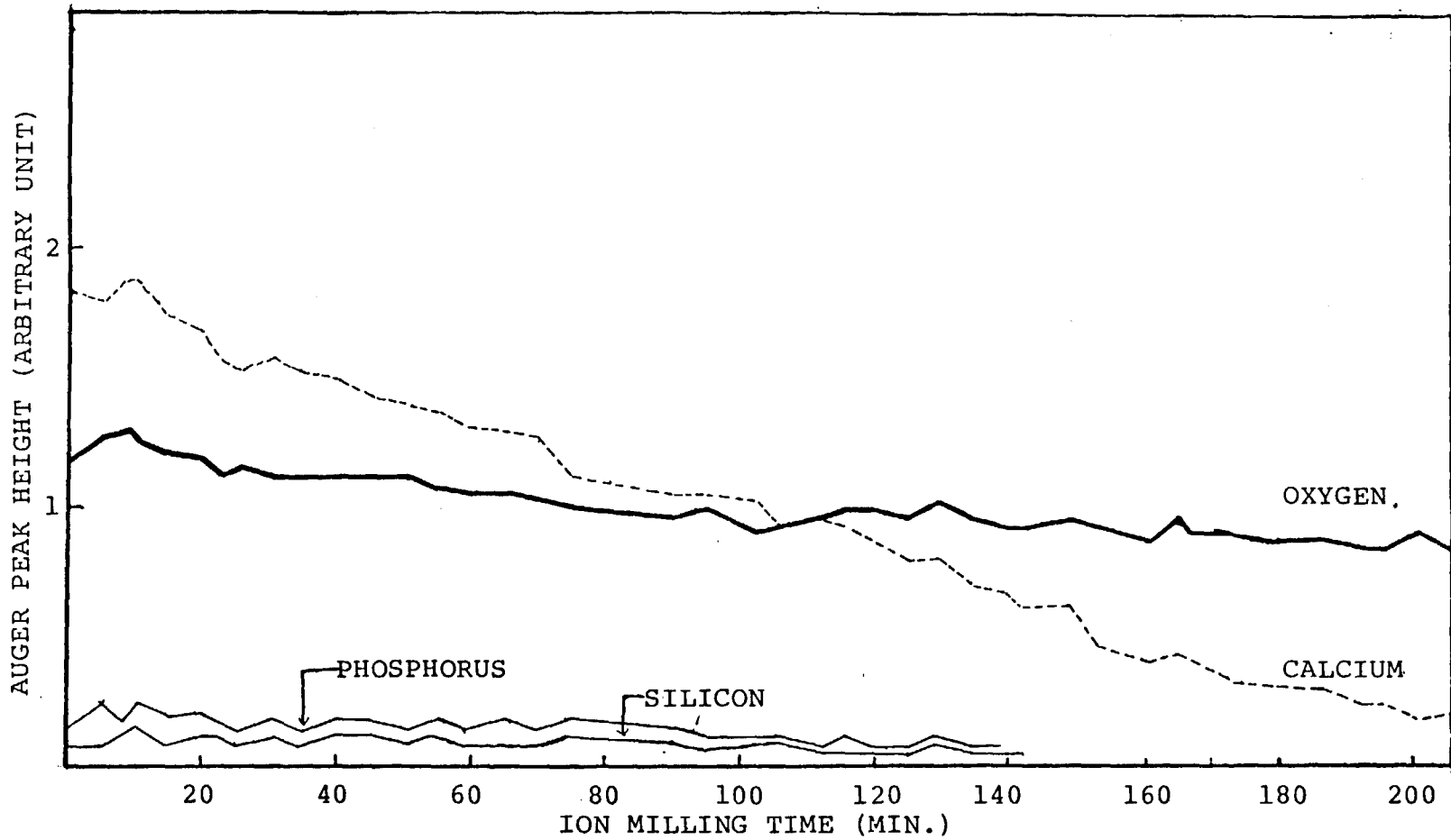


Figure 6.13 AES sputter profile of A-0.7 reacted for 1000 hours.



Figure 6.14 SEM photograph of an alumina control at an original magnification of 4800X.

C-3

ORIGINAL PAGE IS  
OF POOR QUALITY

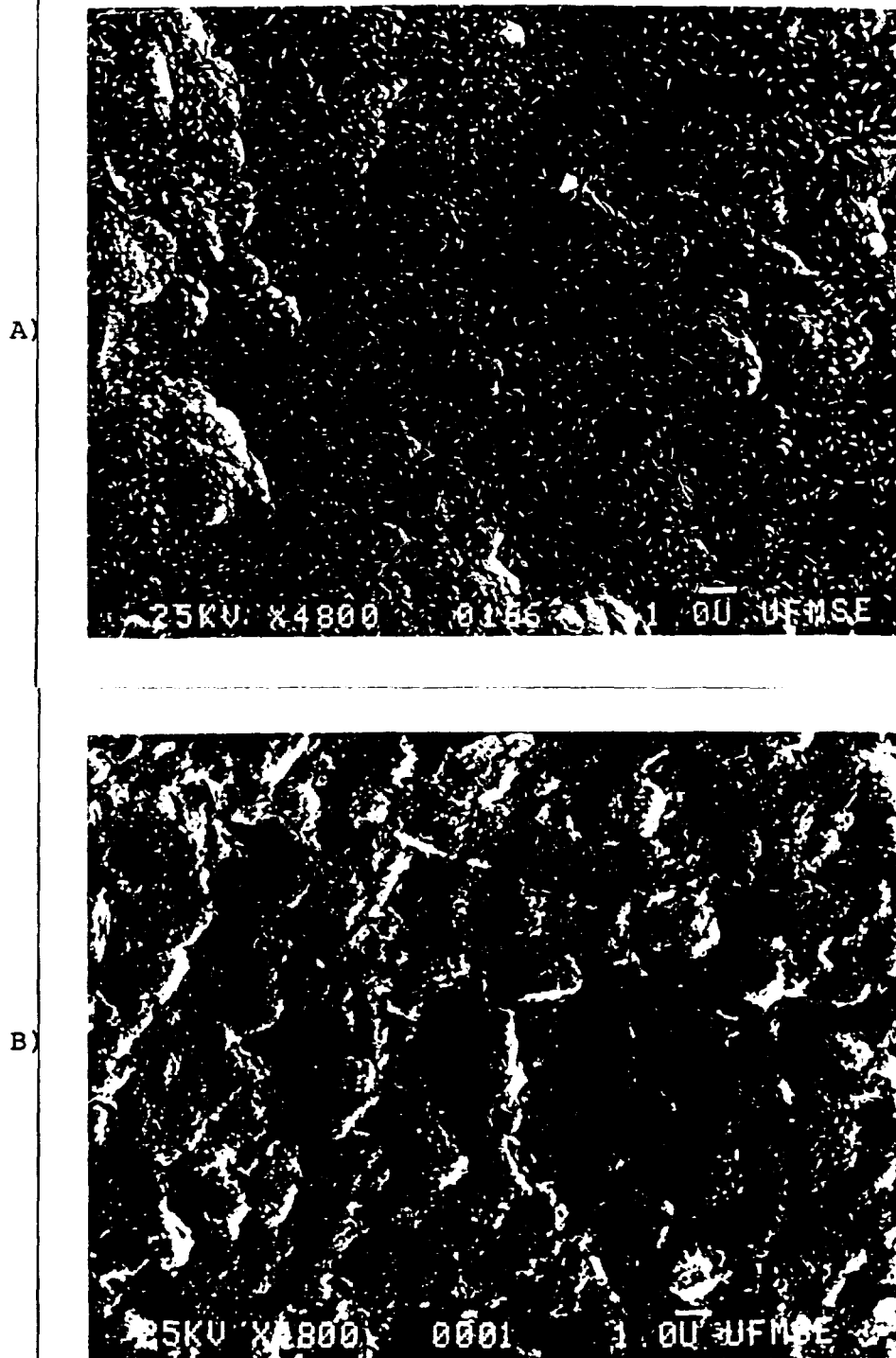


Figure 6.15 SEM photograph comparison: A) A sample coated with  $0.7 \mu\text{m}$  OI 52S4.6 bioglass before reaction and B) Sample A-0.7 after 1000 hours of reaction. Both at an original magnification of 4800X.

A)



B)

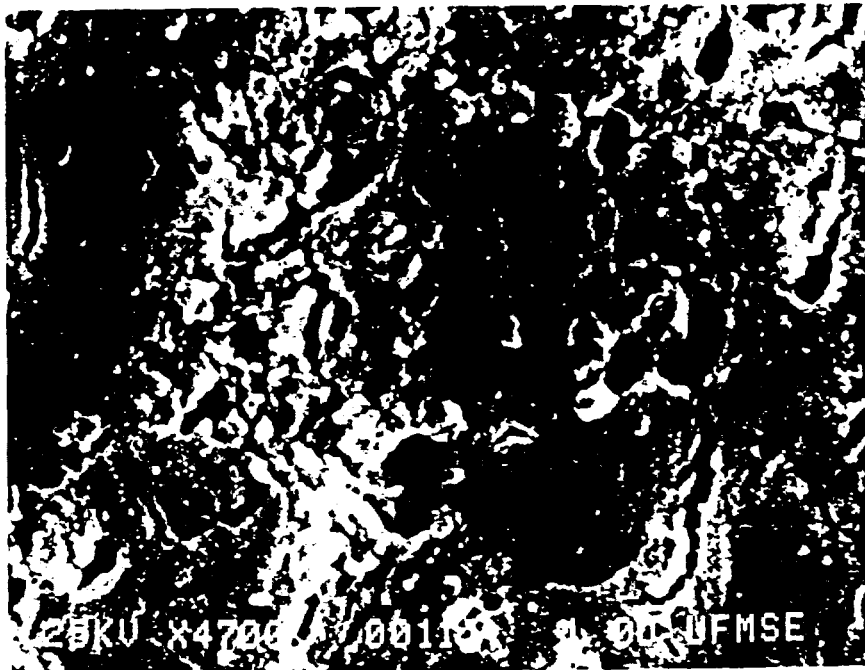


Figure 6.16 SEM photograph comparison: A) A sample coated with  $2.4 \mu\text{m}$  OI 52S4.6 bioglass before reaction and B) Sample A-2.4 after 1000 hours of reaction. Both at an original magnification of 4800X.

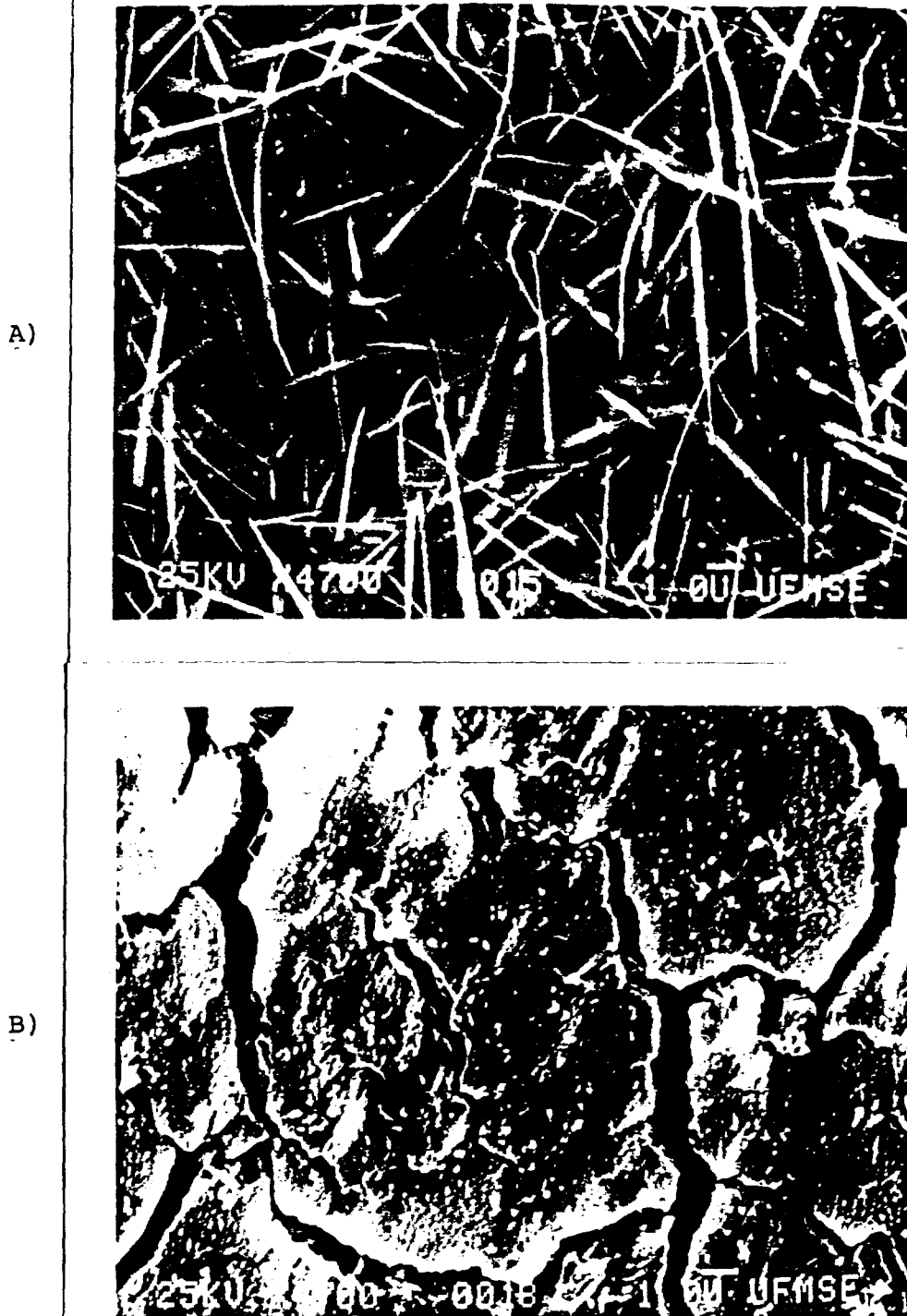


Figure 6.17 SEM photograph comparison: A) A sample coated with 7.0  $\mu\text{m}$  OI 52S4.6 bioglass before reaction and B) Sample A-7.0 after 1000 hours of reaction. Both at an original magnification of 4800X.

6.17 both before and after 1000 hours of reaction. Figure 6.15 A before reaction has a uniform amount of precipitates (small whiskers) approximately  $0.25\ \mu\text{m}$  in size. As coating thickness is increased a fibrous morphology is developed which increases in both size and density of precipitates (compare Figures 6.15 A, 6.16 A and 6.17 A).

Morphological examination of samples before and after reaction can be made. In general it is seen that as coating thickness is increased the reacted samples show a surface morphology that initially has grains similar in size to the control alumina then shows a roughened surface with pores and some cracks and finally a surface having many cracks that may be due to stresses in the coating generated by in vitro reaction.

#### In Vitro Analysis of a Double Coated Alumina Substrate

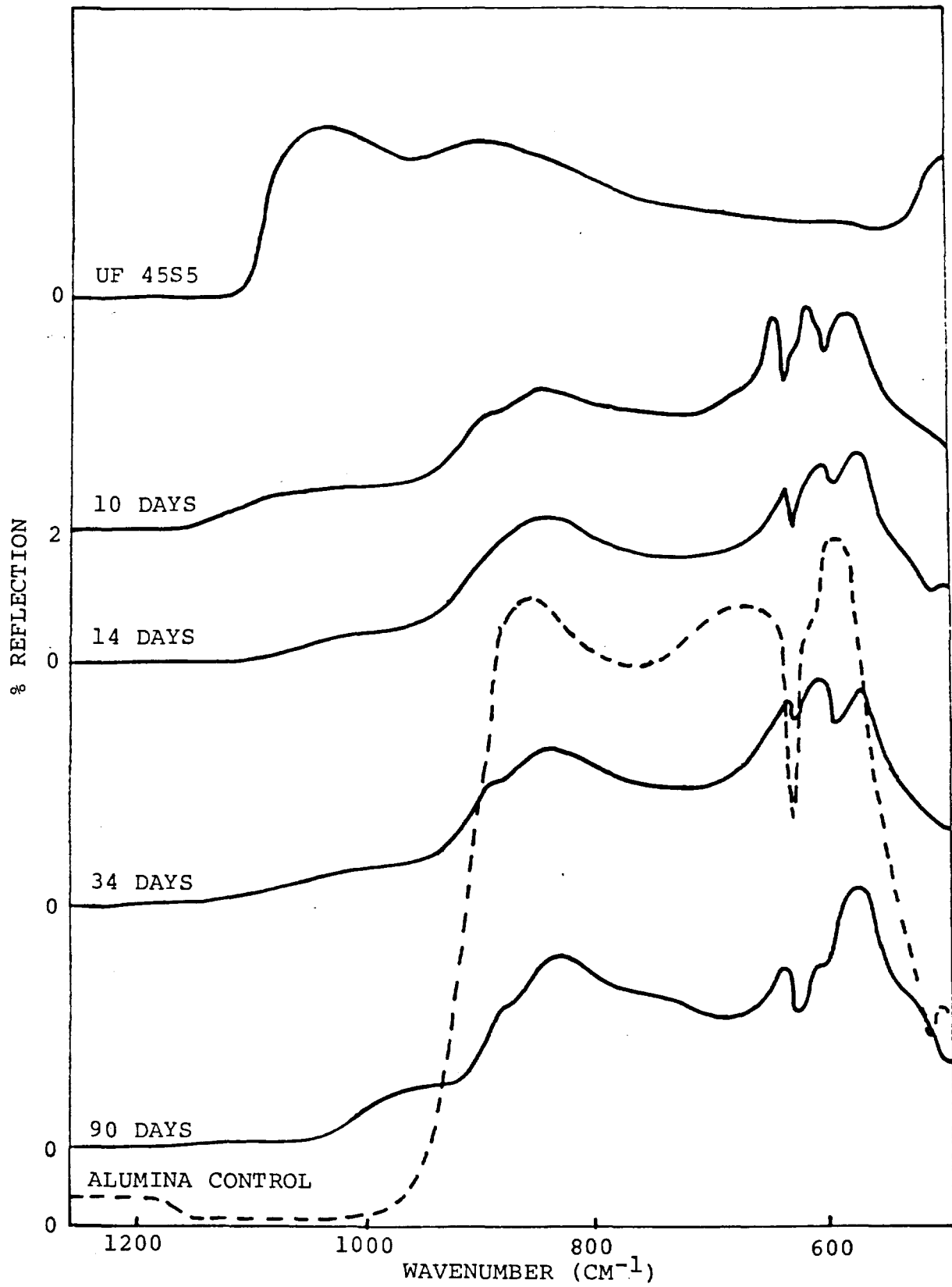
A double coating of  $10.0\ \mu\text{m}$  was placed on RC2-13 (alumina substrate) in two stages. The first stage deposited an approximately  $0.5\ \mu\text{m}$  bulk UF 45S5 bioglass coating through the IBST. The sample was then removed and the second stage placed an approximately  $9.5\ \mu\text{m}$  bulk UF 45S5 bioglass coating onto the first coating. The double coated sample was reacted in vitro. IRRS data is shown in Figure 6.18 for RC2-13. The initial spectrum at zero hours of reaction shows the presence of a glass coating but also resembles the spectrum of A-0.5 (see Figure 3.22). As the coating was twenty times the thickness of that on A-0.5 the similarity

Figure 6.18 IRRS spectra of reaction sequence for RC2-13 (double coated with bulk UF 45S5 bioglass up to 10.0  $\mu\text{m}$  thickness). Sample RC2-13 was reacted in deionized water at 37 °C according to reaction sequence 3 as outlined in Chapter 2 for up to 90 days (2160 hours).





Figure 6.18 Continued



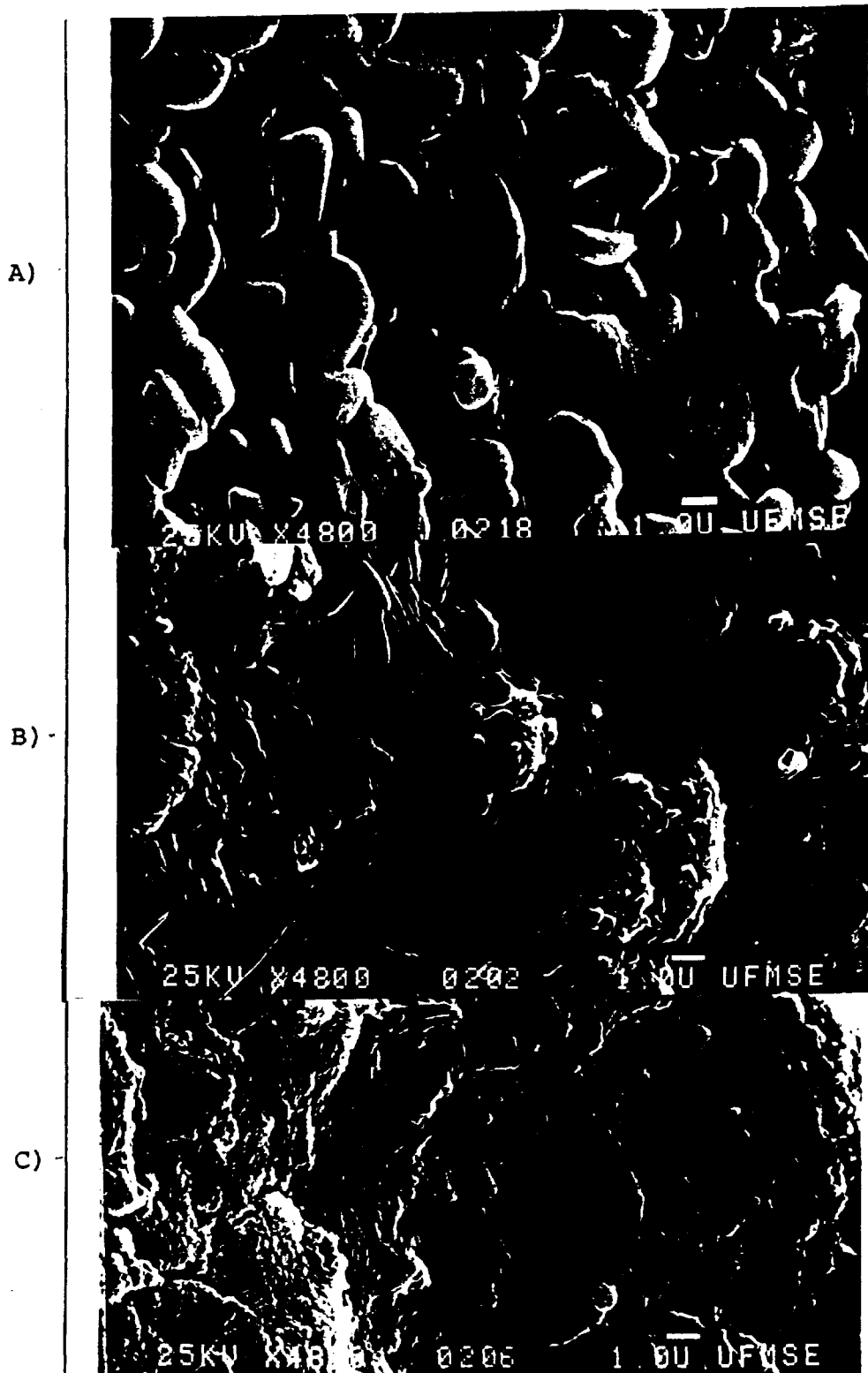


Figure 6.19 SEM photograph comparison: A) Alumina control, B) RC2-12 (10.0  $\mu\text{m}$  UF 45S5) and C) RC2-13 (coated with 10.0  $\mu\text{m}$  UF 45S5 and reacted for 90 days). Original magnification is 4800X.

to A-0.5 was unexpected. Moreover RC2-13 was more like A-0.5 than A-1.2 (coated with UF 45S5) before reaction. This suggests that the sputtering process may be less dependent on the composition of target than expected or that the thickness was not truly linear in sputter time. It also reinforces the conclusion that the coatings on alumina and stainless steel substrates are non-uniform. Increasing the amount deposited does increase extent of surface covered but only partially.

The IRRS reaction analysis of RC2-13 shows a decrease in the peak at  $580\text{ cm}^{-1}$  between zero and 72 hours of reaction. After seven days of reaction three peaks are formed in the region from  $580\text{ cm}^{-1}$  to  $620\text{ cm}^{-1}$ . These three peaks persist up to 34 days of reaction. After 90 days of reaction the spectrum formed shows evidence of a glass coating from the shoulder seen at  $980\text{ cm}^{-1}$ .

SEM micrographs were taken of the samples after 90 days of reaction and compared to a control alumina and a  $10.0\text{ }\mu\text{m}$  bulk UF 45S5 bioglass coated alumina. These micrographs are shown in Figure 6.19. A change in surface texture is observed as a result of sputter coating. The sharper grains seen in the control are rounded and spaces are less predominant, being filled in by coating. After 90 days of reaction a rough surface with cracks is observed which is in contrast to the surface structure of the control. A com-

parison of RC2-13 with A-7.0 shows that these coatings are different in morphology (compare Figure 6.11 with Figure 6.19 B). Thus, a double coated alumina coated with UF 45S5 does not seem to react in a manner either analagous to bulk UF 45S5 or OI 52S4.6 coated alumina.

#### In Vivo Analysis

Preliminary in vivo studies on coated alumina substrates was done to determine if bone bonding was possible. This was justified by the IRRS and AES data for 7.0  $\mu\text{m}$  bulk OI 52S4.6 bioglass coated alumina both of which showed the presence of a Ca-P rich film needed for bone bonding. Implants were either bulk OI 52S4.6 bioglass or coated alumina (7.0  $\mu\text{m}$  OI 52S4.6) in the form of 4.0 mm x 4.0 mm x 1.0 mm squares.

Sprague-Dawley albino rats were used for bone bonding tests in the weight range of 200 to 300 grams. They were housed individually and fed laboratory cube diet and given water ad lib. The animal rooms were temperature and humidity controlled. The animals were inspected daily.

The detailed surgical procedures used for bone bonding experiments are described elsewhere.<sup>26</sup> After eight weeks animals were killed and implants were removed and tested for bone bonding.

Six out of seven animals with bulk OI 52S4.6 bioglass implants showed complete bonding. In six animals in which alumina coated with 7.0  $\mu\text{m}$  bulk OI 52S4.6 bioglass was im-

planted, partial bonding was suspected in two animals. No bonding had occurred in four. The implants, when recovered, were shiny and appeared unchanged.

The 7.0  $\mu\text{m}$  coating on these implants may be too thin despite the encouraging in vitro results, to allow bonding to occur. Previous work has shown a minimum of a 500  $\mu\text{m}$  thickness of coating to be needed for bonding. In the cases in which bonding was suspected the pushout test could not be applied but the bond resisted pulling with forceps.

Clearly the failure of these implants to bond suggests that the coating was insufficient in vivo despite its behavior in vitro.

## CHAPTER 7 SUMMARY

This study has shown that thin coatings of bioglass can be deposited on to a variety of materials by an ion beam sputtering technique. Some degree of substrate masking was obtained in all samples although stability and reactivity equivalent to bulk bioglass was not observed in all coated samples. Some degree of stability was seen in all coated samples that were reacted in vitro.

For thinly coated polymers (1.2  $\mu\text{m}$ ) the spectra observed after 1000 hours of reaction showed that the coating stability and reactivity persisted. This was determined from the characteristic IRRS peaks observed and identified at  $1080\text{ cm}^{-1}$  and  $560\text{ cm}^{-1}$ , both representative of a Ca-P rich film. SEM and IRRS data suggested the reacted coatings were patchy in nature.

Preliminary in vivo tissue adhesion of coated polymers (0.5  $\mu\text{m}$  OI 52S4.6 bioglass) showed signs of partial masking of a normal tissue response to the silicone rubber sample. The implant showed signs of tearing from tissue which is not characteristic of an uncoated silicone rubber subcutaneous implant. Other thinly coated polymer implants showed signs of inflammation with increased cellularity at the implant-tissue interface. This reactivity is characteristic of



these polymers. In these cases the coating evidently did not completely mask the polymeric substrates.

Thus, the use of the ion beam sputtering technique to coat polymeric substrates is most effective even for thin coatings where there was evidence of tissue adhesion. The ability to control coating thickness is also very useful with far reaching applications biomedically.

Data from a second series of thicker (4.0  $\mu\text{m}$  OI 52S4.6) coated polymers generally showed improvement in the degree of masking, coating stability and coating reactivity. However, the degree of masking did not improve in all cases for the thicker coatings. This was observed by comparing IRRS data. Samples coated and reacted showing improvement as a result of thicker coatings were PMMA-7 (4.0  $\mu\text{m}$  OI 52S4.6, polymethyl methacrylate), AM-9 (4.0  $\mu\text{m}$  OI 52S4.6, 20 DMAEMA/ 80 MMA) and A-10 (4.0  $\mu\text{m}$  OI 52S4.6, 10 AA/ 90 MMA) as compared to SR-14 (4.0  $\mu\text{m}$  OI 52S4.6, silicone rubber) and OH-10 (4.0  $\mu\text{m}$  OI 52S4.6, 10 HEMA/ 90 MMA). ESCA analysis after reaction showed that a higher atomic % of Ca and P was found in the surface of samples PMMA-7, AM-9 and A-10 further supporting the IRRS data.

Thinly coated stainless steel (0.5  $\mu\text{m}$  OI 52S4.6) showed evidence of a coating through both IRRS analysis and AES sputter profile analysis before reaction. IRRS spectra for reaction of a coated stainless steel showed a return to the stainless steel control spectrum after reaction, consequently a Ca-P rich film was not detected.

In a second series of coated SS substrates three different coating thicknesses were studied; 0.9  $\mu\text{m}$ , 2.2  $\mu\text{m}$  and 9.0  $\mu\text{m}$  OI 52S4.6 bioglass. The degree of masking improved as a function of increased coating thickness. Sample SS-9.0 showed an IRRS spectrum after 400 hours of reaction that was partially representative of a Ca-P rich film. The spectrum shown was a complicated one as other peaks observed were neither characteristic of the substrated nor of an unreacted bioglass. AES data showed the presence of both Ca and P with a Ca/O ratio greater than unity after reaction which is characteristic of hydroxyapatite. Thus, some of the thicker coatings after reaction showed a Ca/O ratio that potentially could result in bone bonding. Data obtained from pH measurements showed the 9.0  $\mu\text{m}$  coated SS to be reacting in an ion exchange mode similar to bulk bioglass reaction.

Thinly coated alumina substrates (0.5  $\mu\text{m}$  OI 52S4.6) showed evidence of loss of coating after four and 10 hours of reaction with no indication of a Ca-P rich film formation based on IRRS analysis. A second series of coated alumina with three different coating thicknesses; 0.7  $\mu\text{m}$ , 2.2  $\mu\text{m}$  and 7.0  $\mu\text{m}$  OI 52S4.6 bioglass showed that the degree of masking improved as a function of increased coating thickness. Sample A-7.0 (alumina coated with 7.0  $\mu\text{m}$  OI 52S4.6 bioglass) showed a spectrum after 1000 hours of reaction with partial signs of a Ca-P rich film. Evidence of formation of the critical Ca-P surface film was present in AES analysis after reaction as well as changes in solution pH data.

SEM analysis of unreacted and reacted bulk OI 52S4.6 bioglass coated onto alumina indicated that the coating had a fibrous character. Further work is necessary to establish growth mechanism and details of the complicated coating structure observed. A difference in surface morphology of UF 45S5 coatings and OI 52S4.6 coatings on alumina substrates was observed through SEM analysis but the origin of the differences could not be established. Consequently no final conclusions could be made on the difference bioglass compositions had with respect to effectiveness of coating or reactivity at this time.

In vivo bonding studies on coated alumina showed that in most cases bonding did not occur, occasionally partial bonding was suspected. Complete bonding occurred with a bioglass control, this suggests that even thicker coatings will be required to ensure bone bonding.

As a consequence of this study it was found that polymers coated with the Ion Beam Sputtering Technique have far reaching applications. Not only can polymers be coated with a glass but it is also possible to vary the coating thickness. Preliminary in vivo studies showed signs of tissue adhesion with coatings 0.5  $\mu\text{m}$  in thickness.

Although metals have been coated with the Ion Beam Sputtering Technique, it was not found to be a more effective coating technique than previous techniques used. The use of the Ion Beam Sputtering Technique in coating alumina similarly was not found to be a better coating technique through IRRS analysis and the partial bonding observed.

## REFERENCES

1. G. W. Hastings and D. F. Williams, Mechanical Properties of Biomaterials, John Wiley and Sons Ltd., New York, Ch. 41 (1980).
2. A. J. Weigand and B. A. Banks, "Ion-Beam-Sputter Modification of the Surface Morphology of Biological Implants," J. Vac. Sci. Technol., 14 (1), 326-331 (1977).
3. J. B. Park, Biomaterials-An Introduction, Plenum Press, New York (1979).
4. G. F. Green, "Hydrogels for Biomedical Use: Synthesis, Characterisation and In Vivo Evaluation," Ph. D. Thesis, University of Liverpool (1978).
5. W. Lacefield, "The Bonding of Bioglass to a Cobalt-Chromium Medical and Dental Alloy," Ph. D. Dissertation, University of Florida (1981).
6. D. Greenspan, "The Chemical and Mechanical and Implant Properties of Glass Coated Alumina," Ph. D. Dissertation, University of Florida (1977).
7. A. E. Clark, "Solubility and Biocompatibility of Glass," Ph. D. Dissertation, University of Florida (1974).
8. G. Piotrowski, L. L. Hench, W. C. Allen and G. J. Miller, "Mechanical Studies of the Bone-Bioglass Interfacial Bond," J. Biomed. Mats. Res., 9 (6), 47-61 (1975).
9. L. L. Hench, "The Processing of Bioceramics," Ceramurgica International, 7 (5), 252-266 (1977).
10. L. I. Maissel, An Introduction to Thin Films, Gordon and Breach Science Publishers, New York (1973).
11. A. J. Weigand, personal communication.
12. J. P. Sweer and W. B. White, "Study of Na Silicate Glass and Liquids by Infrared Reflection Spectroscopy," Physics and Chemistry of Glasses, 10 (6), 246-251 (1969).

13. D. M. Sanders, W. B. Person and L. L. Hench, "Quantitative Analysis of Glass Structure with the use of Infrared Reflection Spectra," Applied Spectroscopy, 28, 247-255 (1974).
14. P. E. Jellyman and J. P. Proctor, "Infrared Reflection Spectra of Glasses," J. Soc. Glass Technol., 39, 173-192 (1955).
15. S. Anderson, "Investigation of Structure of Glasses by their Infrared Reflection Spectra," J. Amer. Ceram. Soc., 33 (2), 45-51 (1950).
16. I. Simon and K. O. McMahon, "Study of Some Binary Silicate Glasses by means of Reflection in the Infrared," J. Amer. Ceram. Soc., 36 (5), 160-164 (1953).
17. T. M. El-Shamy, J. Lewina and R. W. Douglas, "Dependence of pH of Decomposition of Glasses by Aqueous Solution," Glass Technol., 13 (3), 81-87 (1972).
18. E. J. Jenkins, personal communication.
19. R. A. Abdel-Fattah, "An Investigation into the bonding mechanisms of Bioglass," Masters Thesis, University of Florida (1978).
20. E. C. Ethridge, D. E. Clark and L. L. Hench, "Effect of Glass SA to V ratio in Glass Corrosion," Physics and Chemistry of Glasses, 20 (2), 35-40 (1979).
21. L. L. Hench, M. Prassas and J. Phalliapon, "Surface Behavior of Gel Derived Glasses," in Proceedings of 1982 American Ceramic Society Conference on Composites and Advanced Materials, Cocoa Beach, Fl., Jan 18-21 (1982).
22. C. D. Wagner, W. M. Riggs, C. E. Davis, J. F. Moulder and G. E. Mullenberg eds., Handbook of X-Ray Photoelectron Spectroscopy, Perkin Elmer Corporation, Eden Prairie (1979).
23. M. Ogino, F. Ohuchi and L. L. Hench, "Compositional Dependence on the Formation of Calcium Phosphate Films on Bioglass," J. Biomed. Mats. Res., 14, 55-64 (1980).
24. A. E. Clark Jr., H. A. Paschall, L. L. Hench and M. S. Harrell, "Compositional Analysis of the Formation of Bone-Implant Bond," J. Biomed. Mats. Res. Symp. "Materials for Reconstruction Surgery," Clemson University, Clemson, S. C. (1975).

25. C. G. Pantano, A. E. Clark Jr. and L. L. Hench, "Multilayer Corrosion Films in Bioglass Surfaces," J. Amer. Ceram. Soc., 57 (9), 412 (1974).
26. L. L. Hench, T. K. Petty and G. Piotrowski, Report #9, 1970-1978, U. S. Army Medical Research and Development Command, Contract # DADA-17-70-c-0001.
27. C. D. Batich, personal communication.
28. R. Holms and S. Storp, "ESCA Studies on changes in Surface Composition under Ion Bombardment," Appl. Phys., 12, 101-112 (1977).
29. J. S. Sovey, "Ion Beam Sputtering of Fluoropolymers," J. Vac. Sci. Technol., 16 (2) (1979).
30. D. W. Dwight and B. R. Beck, "Ion Beam POLYMER Surface Modification: Characterization by ESCA and SEM," Org. Coat. and Plast. Chem., 40, 494-499 (1979).
31. D. T. Clark and W. J. Feast, Polymer Surfaces, John Wiley and Sons, New York (1970).
32. P. W. Palmberg, G. E. Reach, R. E. Weber and N. C. McDonald, Handbook of Auger Electron Spectroscopy, Physical Electronics Ind., Inc., Chicago (1972).
33. I. N. Askill, D. Annes, J. Wilson, G. H. Pigott and D. K. Gilding, "A Comparative Study of Parameters affecting the Synthetic Material/Tissue Interface Part III," Biological Response 10<sup>th</sup> Annual International Biomaterials Symposium, San Antonio, Texas (1978).
34. A. W. Ham and D. H. Cormack, Histology, J. B. Lippincott Co., Philadelphia (1979).
35. R. W. Douglas and T. M. El-Shamy, "Reaction of Glasses with Aqueous Solubility," J. Amer. Ceram. Soc., 50 (1) 1-8 (1967).
36. June Wilson, G. H. Pigott, F. J. Schoen, L. L. Hench, "Toxicology and Biocompatibility of Bioglasses," J. Biomed. Mat. Res., 15, 805-817 (1981).

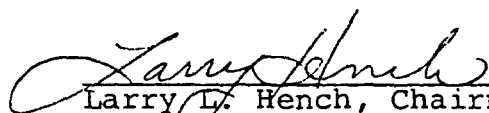
## BIOGRAPHICAL SKETCH

Patricia Henrietta Anne Ruzakowski was born in [REDACTED], on [REDACTED] [REDACTED]. Living in Miami, Florida, since 1959 the author completed her education through high school in Miami. Graduating from South Miami Senior High School in June of 1975 she immediately started at the University of Florida receiving a Bachelor of Science degree in mathematics in June of 1978.

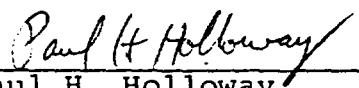
In September of 1978 the author started graduate school in the Department of Chemical Engineering. In March of 1980 the author started on a research project in the Department of Materials Science and Engineering intending to prepare a thesis in this department and to obtain a Master of Science degree in the Department of Chemical Engineering. After some time and thought, the decision to change to the Department of Materials Science and Engineering was made.

Officially entering the Department of Materials Science and Engineering in June of 1980 the author has pursued the degree of Master of Science in materials science and engineering with a minor in chemical engineering. The author is a member of the American Ceramic Society, Society of Plastics Engineers and Pi Mu Epsilon.


I certify that I have read this study and that in my opinion it conforms to acceptable standards of scholarly presentation and is fully adequate, in scope and quality, as a thesis for the degree of Master of Science.

  
Larry L. Hench, Chairman  
Professor of Materials  
Science and Engineering

I certify that I have read this study and that in my opinion it conforms to acceptable standards of scholarly presentation and is fully adequate, in scope and quality, as a thesis for the degree of Master of Science.

  
Paul H. Holloway  
Professor of Materials  
Science and Engineering

I certify that I have read this study and that in my opinion it conforms to acceptable standards of scholarly presentation and is fully adequate, in scope and quality, as a thesis for the degree of Master of Science.

  
Tim J. Anderson  
Professor of Chemical  
Engineering



This thesis was submitted to the Graduate Faculty of the College of Engineering and to the Graduate Council, and was accepted as partial fulfillment of the requirements for the degree Master of Science.

May 1982

Herbert A. Bewis  
Dean, College of Engineering

Dean for Graduate Studies and  
Research